University of Southern Queensland

Renewable Energy in the Australian Red Meat Processing Industry
&
The Viability of Paunch as a Biofuel

A Dissertation submitted by

Jennifer E Spence, BSc

In fulfilment of the requirements of

Master of Science

2012

Abstract

This thesis has investigated the feasibility of using renewable energy sources at Churchill Abattoir in South-east Queensland. Three widely utilised renewable energy sources (algae for biodiesel production, solar photovoltaics and wind turbines) were assessed, and found to be not cost-effective at current electricity prices. However, the use of solar thermal energy to dry paunch (a waste product cumulated at the abattoir) seems a promising way to produce useful biomass to replace boiler coal for water heating and for pyrolysis to generate electricity.

The payback periods for photovoltaics were found to be 24 – 56 years depending on the capital cost of the photovoltaic system and the competing electricity price currently makes photovoltaics uneconomic. Photovoltaic research and development however, suggests the use of solar panels will become viable in the future. Wind turbines were found to have a payback period of 67 years, and due to the low wind speed at Churchill Abattoir wind power is unlikely to become feasible in the future. Algae photobioreactors were investigated, but the technology does not appear to be a feasible preposition for Churchill Abattoir at the present time. On the other hand, the drying properties of paunch waste produced at the abattoir were investigated, and average drying rates of 1.2 – 6.1 % reduction per hour in moisture content was measured. The drying rate of this paunch demonstrates that paunch waste from the abattoir can be dried to a useful moisture content thus, making it a viable biofuel. The drying rates also demonstrate that increased air temperature can significantly increase drying rates.

Certification of Dissertation

I certify that the ideas, experimental work, results, analyses, software and conclusions reported in this dissertation are entirely my own effort, except where otherwise acknowledged. I also certify that the work is original and has not been previously submitted for any other award, except where otherwise acknowledged.

_____ _____

Signature of Candidate Date

ENDORSEMENT

_____ _____

Signature of Supervisor Date

_____ _____

Signature of Supervisor Date

Acknowledgements

I would like to thank Researchers in Business and Churchill Abattoir for funding part 1 of this study. I would also like to thank my supervisors for their support and belief in this project. A most heartfelt thank you goes to my family; Mum, Dad, Glenda, and most especially to the most beautiful girl in the world my daughter Alysha. Thank you also to my friends and the employees at Churchill Abattoir.

Contents

Abstract i
Certification of Dissertation ii
Acknowledgements iii
Contents iv
List of figures vi
List of tables x
Abbreviations xii
Chapter 1: Introduction 1
1.1.0 Renewable energy technologies 2
1.1.1 Photovoltaics 3
1.1.2 Wind 6
1.1.3 Algae for biodiesel production 9
1.1.4 Organic waste 12
1.2 Project objectives 15
Chapter 2: Part 1 – Renewable Energy in the Australian Red Meat Processing Industry 18
2.1.0 Part 1: Renewable Energy Methods 18
2.1.1 CA energy consumption 18
2.1.2 Expected electricity increases 2011 to 2014 22
2.1.3 Australian incentives for renewable energy use 24
2.1.4 PV user information 27
2.1.4.1 Types of PV 31
2.1.5 Wind turbines 33
2.1.5.1 Types of wind turbines 35
2.1.6 Algae for biodiesel 37
2.1.6.1 Photobioreactor designs for the production of biofuel 40
2.1.6.2 Flat plate photobioreactors 41
2.1.6.3 Tubular photobioreactors 43
Chapter 3: Part 1 Renewable Energy Results 48
3.1.0PV 48
3.1.1 Wind Turbines 52
3.1.2 Algae 57
Chapter 4: Part 1 Renewable Energy Discussion 58
4.1.0 PV 58
4.1.1 Wind 59
4.1.2 Algae 60

Chapter 5: Part 2 – The viability of paunch for use as a Biofuel 64
5.1.0 Paunch literature review 64
5.1.1 Concluding remarks regarding this review of literature 77
5.2.0 Paunch Methods 77
5.2.1 The Meteorological conditions at CA 78
5.2.2 Solar drying 85
5.2.3 Churchill Abattoir 87
5.2.4 Factors that affect drying 89
5.2.5 Moisture content 94
5.2.6 Experimental equipment 96
5.2.7 Experimental procedure 100
Chapter 6: Part 2 – Paunch Results 102
6.1.0 Operating temperature inside tunnel dryer 102
6.1.1 Average drying rates 104
6.1.2 Equilibrium moisture content 108
6.1.3 Drying constant 109
6.1.4 Optimal drying temperature and RH 112
Chapter 7: Part 2 – Paunch Discussion 113
7.1.0 Effect of temperature 113
7.1.1 Viability of paunch for use in boilers 114
7.1.2 Comparison of results with previous research 117
7.1.3 Limitations of the present research 122
7.1.4 Active dryers as an effective design 123
Chapter 8: Conclusions and future work 124
8.1 Conclusions 124
8.2 Future work 125
5.3 Paunch 128
References 130
APPENDIX 1 - ADR graphs for 55°C and 41°C entry air. 138
APPENDIX 2 – Example data for tunnel dryer monitoring 140
APPENDIX 3 – PV theory 141
APPENDIX 4 – Wind theory 145
APPENDIX 5 - Algae 154
APPENDIX 6- Glossary 159

List of figures

Figure 1 - The projected 210 year industrial life cycle for wind turbines (Dismukes, Miller and Bers 2009). 8

Figure 2 - Schematic of the water circulation from the boiler at CA to the cooker, heat exchangers, and bio-filter. 19

Figure 3 - EnergyAustralia's (2010) graph of expected yearly average electricity price increases for the period 2010 to 2014. 23

Figure 4 – The predicted electricity price increases from 2010 to 2014 (EnergyAustralia 2010). The non-linearity of the graph does not allow for price predictions beyond 2014. The starting point is CA's current (2010) electricity price of between $0.05 and $0.11 per kWh (Spence, M 2010, pers. Comm., 6 January). 23

Figure 5 - I-V and P-V characteristic of a PV. The graph gives the maximum power point (MPP) which is the ideal operating point for maximum power delivery from the PV (Quaschning 2007). 27

Figure 6- Electrical power output vs wind speed for a 5.5m HUSH wind turbine. A theoretical speed-power graph using the rated output and speed information available from the manufacturer for a HUSH wind turbine. 34

Figure 7 – Electrical power output vs wind speed for a Proven 9m wind turbine. A theoretical speed-power graph using the rated output and speed information available from the manufacturer for a Proven wind turbine. 34

Figure 8 - The diagram shows horizontal and vertical axis wind turbine design (Scottish government 2010). 36

Figure 9- A longitudinal section through a Conwy vessel. Note the fluorescent lamp placed in the centre of the reactor. The outer walls are white to help reflect light back into the reactor (Helm, Laing & Jones 1979). 38

Figure 10 -"Big bag" vessel diagram. The outer frame supports polythene bags, which are replaceable in this type of reactor (Baynes, Emerson & Scott 1979). 40

Figure 11 -'Schematic diagram of the flat inclined modular photobioreactor (FIMP) showing the first (1F) and last (1L) units in the cascade, (2) perforated tubes for bubbling compressed air, (3) thermosensor, (4) cooling water

line and sprinklers, (5) thermostat, (6) solenoid valve, (7) culture medium reservoir, (8) pump, (9) airlift pipe, (10) recycling tubing, connecting the first with the end reactor in the row, (11) harvesting outlet, (12) harvesting reservoir, (13) compressed air supply, (14) line supply 2% CO_2 enriched air, (15) compressed air port for the airlift, and (16) sampling port.' (Hu, Guterman & Richmond 1996) 42

Figure 12 - The plexiglass tubular photobioreactor. The tube loops are placed on a white sheet to help reflect light back into the reactor (Tredici & Materassi 1992). 44

Figure 13 - Tubular photobioreactor with Compound Parabolic solar Concentrator (34) incorporated into the design. The parabolic reflector concentrates light back into the tube (2) of the reactor (Amnon Yogev & Dan Yakir 1999).....45

Figure 14 - Diagrams of the photobioreactors used in the comparison study. (A) is the coiled tubular reactor, (B) are the near horizontal flat and tubular reactors, and (C) are the flat and curved chamber reactors (Tredici & Zitelli 1997).....47

Figure 15 - A histogram demonstrating the frequency of wind speeds for Amberley air base using data obtained from the Bureau of Meteorology spanning from June 1952 to March 2010. The majority of wind speed falls within the 1 -10 km/h range.....52

Figure 16- Speed-power graph for a Proven brand (9m) wind turbine with wind speeds and output for Amberley air base shown in pink and yellow. Note the 9am wind speed is below the cut-in speed and therefore is not producing power.....56

Figure 17 -The concentrating solar air collector was 1.10 m × 1.75 m, adjusted to remain perpendicular to incoming solar radiation and produced energy equivalent to a 1.5 times larger flat plate collector (Farmer, Farouk, and Brusewitz 1980) 73

Figure 18 – Shows the annual average daily solar exposure for Australia in MJ/m^2. Ipswich, Australia has on average 18 – 21 $MJ/ m^2/d$ (BOM 2011). 82

Figure 19 - Shows the Australian annual daily sunshine hours average. Ipswich annually has between 7 to 8 hours of sunshine daily (BOM 2011). 82

Figure 20- Clear/ cloudy day, and cloud cover data for Amberley. The months of June to October each year show greater than 10 clear days per month (BOM 2011). 83

Figure 21– Average maximum and minimum monthly relative humidities, 9am & 3pm, for the greater Brisbane area, Australia (BOM 2011)..... 84

Figure 22 - Paunch on site at CA passes from the screw press to fall into a pile in the cement holding area. 88

Figure 23 - Tunnel dryer; hot air passes from the entry at left, over the paunch and out the air vent at the end on the right..... 98

Figure 24- Paunch inside the tunnel dryer. 99

Figure 25 –The Ohaus MB45 moisture balance. 100

Figure 26 - The variation of entry (i) and exit (x) temperature (Tp) and relative humidity (RH) in the tunnel dryer averaged for all 3 hr runs at 72°C entry air. 103

Figure 27 - The variation of entry (i) and exit (x) temperature (Tp) and relative humidity (RH) in the tunnel dryer for one run at 72°C entry air for 4 hr. The run on this particular day had a period of rain which increased the RH inside the box at two and a half hours into the measurement sequence. 103

Figure 28- Change in moisture content (wet basis) versus time for 72 °C entry air temperature, paunch depth 2.5cm, time up to 5hrs. The data points have been fitted with a linear trend line. 105

Figure 29 - Change in moisture content (wet basis) versus time for 55 °C entry air temperature, paunch depth 2.5cm, time over 5hrs. The data points have been fitted with a linear trend line. 106

Figure 30 - Change in moisture content (wet basis) versus time for 41 °C entry air temperature, paunch depth 2.5cm, time over 5hrs. The data points have been fitted with a linear trend line. 107

Figure 31 - Change in moisture content (wet basis) versus time for 72 °C entry air temperature, paunch depth 2.5cm, time over 5hrs. The data points have been fitted with a linear trend line. 107

Figure 32 - Drying constant ,k, for 71°C entry air for up to 12 hours. Data have been fitted with a linear trend line. 110

Figure 33 - Drying constant, k, for 55°C entry air for up to 14 hours. Data have been fitted with a linear trend line. 111

Figure 34 - Drying constant, k, for 41°C entry air for up to 16 hours. Data have been fitted with a linear trend line. 111

Figure 35 – Initial and final total % total solids versus time for 72°C entry air. All final total solids are >30% and were achievable in under 24hr. 116

Figure 36 - Griffith and Brusewitz's (1980) and present experiment k values. The A series (-1.17) is the believed typographical error in Griffith and Brusewitz's (1980) paper and series B (-0.0117) is the corrected value. Series C, D, and E are the present experiment values for 41, 72, and 55°C respectively. 121

Figure 37 - Change in moisture content (wet basis) versus time for 55°C entry air temperature, paunch depth 2.5cm, time up to 5hrs. The data points have been fitted with a linear trend line.....138

Figure 38 – Change in moisture content (wet basis) versus time for 41°C entry air temperature, paunch depth 2.5cm, time up to 5hrs.The data points have been fitted with a linear trend line.....138

Figure 39 - Change in moisture content (dry basis) versus time for 55 °C entry air temperature, paunch depth 2.5cm, time over 5hrs. The data points have been fitted with a linear trend line.....139

Figure 40 - Change in moisture content (dry basis) versus time for 41 °C entry air temperature, paunch depth 2.5cm, time over 5hrs. The data points have been fitted with a linear trend line.....139

Figure 41 - Conductor, semiconductor and insulator energy bands. Insulators have a full valence band and high band gap energy which makes them have high electrical resistance. Semiconductors have a full valence band but a low band gap energy which allows them to behave as a conductor in the presence of radiation. Conductors have a full valence band and partially filled conduction band which makes them have low electrical resistance. (Quaschning 2007). 142

Figure 42 - P-n junction (Quaschning 2007).....144

Figure 43 - The diagram shows air circulation and global wind patterns. Wind is formed due to the rising of hot air (heated by the sun) and the sinking of cool air (Simmons 2006). 145

Figure 44 - The maximum theoretical output for a wind turbine based on wind speed and blade diameter using the equation: $P = 2.83 \times 10^{-4} D^2 v^3$ 150

Figure 45 - The diagram demonstrates the lift and drag forces acting perpendicular to each other (First flight n.d). 151

Figure 46 - The diagram shows the chord length for an object which gives the area of an object when multiplied by the span (NASA 2009). 153

Figure 47 - The major factors available for manipulation in both closed and open systems (Grobbelaar 2000) 156

List of tables

Table 1 - Energy contents for paunch, switch grass, coal, and wood. Paunch (17 GJ/Mg) energy content is comparable to that of switch grass (18 GJ/Mg). 14

Table 2 –Some of the characteristics of dry and wet paunch. 15

Table 3- Energy consumption, emission, and production reportable under NGER. The amount values have been rounded to retain some confidentiality for CA. 21

Table 4 – Information provided by the Australian government (2011) on the requirements of small generation units. The relevant information for CA is the requirements for solar PV units installed after November 2005. 26

Table 6 - Demonstrates the payback calculations for Ekoenergy using a competing energy price of $0.05 and $0.11 per kWh, giving payback periods of 53 and 24 years respectively. 49

Table 7 - Demonstrates the payback calculations for Solar Guys using differing competing energy prices and a calculation based on a $1 per Watt PV system. The viable payback periods belonging to the $0.50 competing electricity price and the $1.00 per Watt PV system. 51

Table 8 - Demonstrates using Hinrichs and Kleinbach's (2006) method for calculating energy output for specific wind turbines. As shown by the figures below the wind turbine will be operating at far below the rated output capacity and thus will be ineffective. 54

Table 5 - Factors that affect the two stages of drying 92

Table 9- Paunch average drying rates (ADR) for wet and dry basis up to 5 hrs. 104

Table 10 - Paunch average drying rates (ADR) for wet and dry basis for over 5 hrs. 106

Table 11 - Equilibrium moisture contents for yellow dent corn (wet and dry basis). 109

Table 12 – Summary of drying constants, K, (dry basis) for present experiment...110

Table 13 – Example table of data collected for each run of the present experiment. T1 and T2 are the thermocouple reading for temperature, Rhi is the entry relative humidity, Rhx is exit relative humidity, Tpi is entry psychrometer temperature reading, and Tpx is exit psychrometer temperature reading. 140

Abbreviations

ADR	Average drying rate
BOD	Biochemical oxygen demand
CA	Churchill Abattoir
COD	Chemical oxygen demand
DAF	Dissolved air floatation
d.b	Dry basis
G	Giga (10^9)
GHG	Greenhouse gas
GJ	Giga Joule
GW	Giga Watt
kWh	Kilo Watt hour
L	Litre
M	Mega (10^6)
MC	Moisture content
Mg	Mega gram
MW	Mega Watt
MWh	Mega Watt hour
PV	Photovoltaic
RH	Relative humidity
t	Tonne
TS	Total solids
w.b	Wet basis

Chapter 1: Introduction

Globally and locally there is a need for renewable energy to cope with rising energy demands and finite non-renewable resources. According to Varela (2006) for example, projected oil reserves should reach their peak around 2014, and humanity appears to be using three times the amount of oil that is discovered, and has consumed half of the world's available oil reserves. According to this source natural gas supply is also predicted to peak around 2030, with uranium supplies for nuclear power lasting roughly 60 years, and with 40% of the world's coal consumed by 2050. Such resource use means that rising fossil fuel prices are inevitable, and that renewable energy technologies need to be integrated into energy markets.

In addition to rising costs, Australia is one of the biggest per capita greenhouse gas (GHG) emitters in the world (Diesendorf 2003, Bradshaw, Giam & Sodhi 2010, Saidur et al. 2010). This is largely because coal-powered electricity generation provides 84% of Australian electricity, and is responsible for 170 million tonnes of carbon dioxide (a GHG that contributes to global warming). As well as carbon dioxide, coal burning also emits sulphur dioxide, nitrogen oxides, fluoride, hydrochloric acid, boron, and particulates containing sulphuric acid and mercury (Diesendorf 2003). Further environmental damage is caused by burning large volumes of coal with its subsequent pollution of fresh water, land degradation, and loss of biodiversity (Diesendorf 2003, Boyle, Everett & Ramage 2003). For example, the sulphur content of coal can vary from 0.5 – 5 %. This is released into the atmosphere as sulphur dioxide, a precursor to acid rain (Boyle, Everett & Ramage 2003). In addition to financial cost and dwindling supply, human health problems, such as respiratory disease, are caused by living close to power plants, and mining is

the third most dangerous job in Australia (Diesendorf 2003). The hidden costs of coal powered electricity generation and other fossil fuels demonstrate the need to find clean renewable energy sources. Global climate change (rising temperatures) has been predicted to have catastrophic effects on mankind (e.g. Arrow 2007). These effects may include increases in heat-related deaths in both humans and livestock, the retreating of glaciers, increases in extreme weather conditions, peak river flow shifts, and a decline in water quality (Boyle, Everett & Ramage 2003). Thus, there is a growing interest in renewable energy technologies as a means of reducing GHG emissions.

1.1.0 Renewable energy technologies

Renewable energy technologies have been integrated into industry in varying degrees. This implementation of renewables has been limited mainly by the cost of the renewable energy source compared to the cost of the competing fossil fuel derived energy. Photovoltaics, wind turbines, and algae for use as biodiesel appear to be three of the most commonly accepted renewable technologies for industry. Large amounts of research have gone into these fields which are showing rapid acceptance into global markets. The following pages will briefly review these technologies and their applicability into industry.

1.1.1 Photovoltaics

Solar photovoltaics (PV) are one of the fastest growing renewable energy technologies. Its production worldwide has almost doubled every two years since 2002, with the price since the 1950s dropping by a factor of 1000 (Kropp 2009, Hinrichs & Kleinbach 2006). The use of PV's produces almost no air emissions or waste products, thus reducing damaging GHG emissions which are produced by traditional fossil fuel energy production, such as coal, crude oil and natural gas, which together make up 85% of the world primary energy demand (Tsoutos, Frantzeskaki & Gekas 2005, Quaschning 2007). The goal of solar PV technology is to efficiently convert the radiant energy from the sun (light quanta) into electrical energy using doped semi-conductor material. The Sun, in human terms, will produce an almost limitless supply of radiant energy to the Earth. This radiant energy excites electrons in the semi-conductor material and the p-n junction, with a gradient of electrical potential, creates a force that drives the electrons and holes to move in opposite directions. When these reach the edges of the semiconductor material it is possible for the device to deliver electrical energy to an external circuit (Sorensen 2004) (Appendix 3). This ability to create electrical energy from a 'free' energy source (the sun) has made PV a popular choice as a renewable technology.

Traditionally PV have high capital cost which has limited them being integrated into industry. They are highly successful in remote areas as standalone systems where they are the only viable source of energy. In addition, they are also showing widespread success as large scale utility power plants, in the domestic market (due to extra government incentives), and for use in consumer products such as solar

powered calculators (Hinrichs & Kleinbach 2006). In the words of Oliver and Jackson:

> Photovoltaics present a difficult tradeoff to policy makers: on the one hand, they offer clear resource and environmental advantages over fossil-fuel-based electricity generation; on the other hand, they remain more expensive than conventional technology in most grid-connected applications. However, the dynamics of this tradeoff are changing as the technology develops (Oliver & Jackson 2000).

The total global installed capacity for PV has increased from 5.4 GW in 2005 (Braun et al. 2011), 5.95 GW in 2008 (Dincer 2011), to 40 GW in 2010 (Braun et al. 2011, Cucchiella & D'Adamo 2012). The installed growth in 2010 was 16.6 GW and was mainly due to the German and Italian markets in conjunction with decreases in PV price and well developed support schemes (Cucchiella & D'Adamo 2012). It is interesting to note that Germany has a lower level of solar insolation than Australia but due to government policy and incentives they have the most installed PV capacity in the world.

The full cost of PV systems still appears to be the biggest drawback to replacing fossil fuel derived energy. The full cost of PV systems comprises the module cost and all other system components, such as installation and inverters (Van der Zwaan & Rabl 2004). There are a number of areas where improvements will lead to lower costs for PV systems. These include:

1. *Increased plant size.*

   Increased demand of PV systems will allow manufacturers to increase their plant size which means lower costs due to their ability to exploit economies

of scale (Nemet 2006). Economies of scale being that it is assumed that the cost per unit produced falls as the scale of production is increased. This is due to things such as: bulk buying materials, specialized managers, and lower interest rates.

2. *Increased efficiency/ technological advances.*

   Technological advances will reduce costs due to increased module efficiency and increased efficiency in cell and module production (Nemet 2006). Van der Zwaan and Rabl (2004) predict that cell efficiencies could reach 20% by 2020 and 30% after 2020 due to technological improvements compared to today's 15%.

3. *Reduced silicon cost.*

   As technologies like thin film panels improve less silicon is used to produce the panel. This will reduce the amount of silicon needed and also reduce the amount of silicon wasted in cutting wafers for mono and polycrystalline panels.

4. *Incorporation of policy measures.*

   Van der Zwaan and Rabl (2004) state that there are a number of policy measures that could help reduce the cost of PV systems. These include government subsidies, requirements for utility companies to install minimum percentage of PV in their generating mix, and internalised damage costs such as an energy or pollution tax. Damage costs are external costs such as pollution caused by the use of fossil fuels. If there was a tax placed on the use

of environmentally damaging energy sources this would help to equalize the cost difference between clean energy production and fossil fuels.

PV cost has been dramatically decreasing over recent years and with help from incentives, rising fossil fuel costs, and possible carbon taxing they appear to be becoming an attractive choice for industry as a renewable energy. However, it is unclear whether the rate with which PVs have been decreasing in cost will continue or how soon they will become truly cost competitive against fossil fuel derived energy.

1.1.2 Wind

Wind turbines convert the kinetic energy contained in the wind into electrical energy by the rotation of their blades. Diesendorf (2003, p. 43) states that 'a wind farm, when installed on agricultural land, has one of the lowest environmental impacts of all energy sources'. Wind turbines are emission-free and repay their manufacture debt between 3-6 months (Diesendorf 2003). Wind is an indirect form of solar energy and the Earth's wind contains roughly 10 million MW of continuous energy (Joselin Herbert et al. 2007). Wind energy has been in use for thousands of years, mostly for milling grain and pumping water. Recent designs have been created to produce electrical energy that is pollution free. These are called wind turbines to distinguish them from their wind*mill* predecessors (Boyle 2004).

Wind turbine technology is a mature renewable energy market that produces emissions free 'clean' energy. Recent turbine design use aerodynamics to increase the turbine efficiency. Economically, turbines are comparable to fossil fuels based on

their energy return on investment. This is calculated by the energy produced by the turbines divided by the primary energy used to find, extract and convert the energy into a useful form (Kubiszewski, Cleveland & Endres 2010). However, in low-wind areas wind turbines are not yet economically viable due to their cost compared to output. Before wind turbines can be economical for low wind speed areas the industry in Australia will need better government incentives and further research and development (especially into lower minimum cut-in speeds).

Joselin Herbert et al. (2007) state that wind energy has an edge over other renewable energies due to its 'technical maturity, good infrastructure and relative cost competitiveness'. Turbine size (output) has increased from 100 kW in the early 1980's to up to 3500 kW in 2007. It is estimated that wind power development could be expected to reach 1.9×10^9 kW by 2030-35 (Joselin Herbert et al. 2007). Dismukes, Miller and Bers (2009) show that wind power is in an industrial technological cycle for which they have done a life cycle spanning 210 years (Figure 1). This cycle shows the initial exploration stage, the current acceleration stage, and the third maturation stage. These technological stages show that through research and development, economies of scale, and increased political incentives energy from wind turbines will become cheaper and therefore, further integrated into society for energy generation.

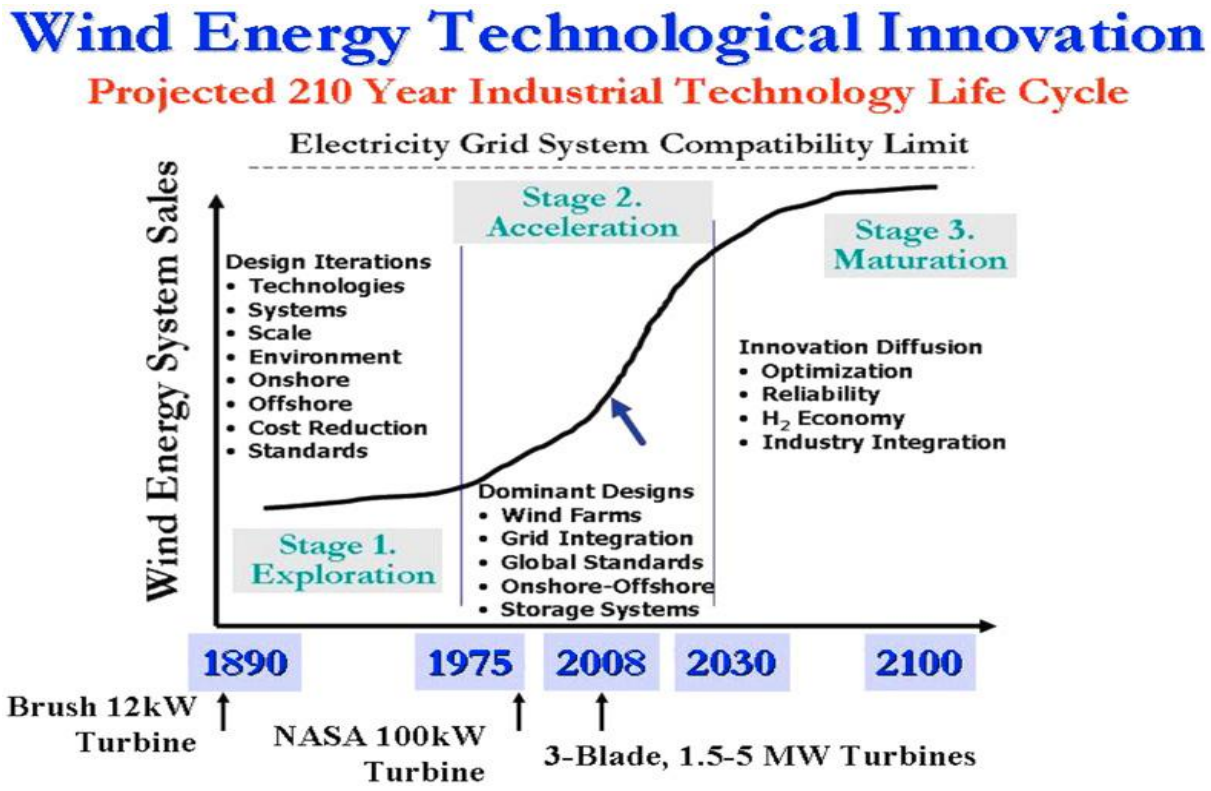

Figure 1 - The projected 210 year industrial life cycle for wind turbines (Dismukes, Miller and Bers 2009).

Although wind turbines are currently one of the most cost effective renewable energy sources available (in high wind areas) most are still not competitive compared to fossil fuel due to their high initial cost (especially for large scale turbines) and long pay back periods. Energy return on investment can be used to compare wind turbine power to other types of power generation. Kubiszewski, Cleveland and Endres (2010) state that this comes down to a simple ratio. As stated on page 6, where the energy return on investment is the cumulative electricity generated divided by the cumulative primary energy required to find, extract, and produce useful energy. These calculations demonstrate that wind power is on par in

regards to energy return on investment with current energy generation systems such as fossil fuels, nuclear, and solar. However, Kubiszewski, Cleveland and Endres (2010) state that wind power still has a number of issues, such as social, economic, environmental, and regulatory issues to resolve before it can be truly competitive to other power generation systems. For example, community groups in Crows Nest, Australia tried to stop a plan for wind turbines which they believed would be a noise pollutant and ruin the natural beauty of the area (ABC 2006).

1.1.3 Algae for biodiesel production

Algae are shown to be of great promise as a renewable energy source due to their ability to produce lipids for biodiesel. Of particular importance is the high lipid content of some species (Sheehan et al. 1998). This lipid can be extracted and in turn processed to produce biodiesel. A key challenge, however, is the reduction of production costs to produce viable and sustainable algal biofuels (Christi 2007). Photobioreactors have been designed with this limitation in mind and offer potential as a new renewable energy source.

A photobioreactor is a closed system designed to optimise light availability and other environmental factors such as nutrients and carbon dioxide that affect the growth of the algae. In contrast, ponds containing algae are typically large open systems which can be affected by external factors, such as the weather and contamination by unwanted algal strains. Most systems are either completely closed or open, though hybrid systems do exist in which a bioreactor is used to produce the starter culture

for a pond. Modern photobioreactors for biodiesel designs are closed systems based on tubular and flat plate reactors that allow for continuous culture production.

Photobioreactors using algae to produce biodiesel offer promise as a renewable energy source, because:

- Bioreactors allow the selection of those algae that are rich in the lipids used to make biodiesel while excluding unproductive competitor strains.
- Algae can reproduce rapidly under the controlled conditions of a bioreactor.
- Algae absorb significant amounts of carbon dioxide when used to make biodiesel and so can be utilised as part as of an overall strategy to use plant photosynthesis to remove excess atmospheric carbon dioxide (Huntley & Redalje 2007).
- The leftover biomass from the algal production of biodiesel provides high-protein feed for livestock.
- The water usage involved in the algal production of biodiesel can be employed as a wastewater treatment process.
- As a variant of diesel fuel, biodiesel can be readily stored, transported and used.

Economic factors appear to have held back the implementation of photobioreactors for the production of biodiesel due to the traditionally higher cost of biofuel compared to fossil fuel. However, with global climate change and limited reserves of fossil fuel there are now increased economic and environmental drivers for the use of photobioreactors or ponds in the production of biodiesel. For example, Christchurch

Waste Water Treatment in New Zealand installed a waste water algae system and aim to produce 150 – 300 tonnes of algae per year from 5 hectares of high rate algal ponds, which has the potential to produce 45 000 -90 000 L of biocrude oil (NIWA 2010).

The cost of biodiesel from algae is still comparatively high compared to crude oil and palm oil. Christi (2007) suggests that for biodiesel produced from algae to replace petroleum the cost of production needs to be related to the price of crude oil as shown in the equation:

$$C_{algal\ oil} = 6.9 \times 10^{-3} C_{petroleum};$$

Where $C_{algal\ oil}$ is the price of algal oil in dollars per litre ($\$L^{-1}$) and $C_{petroleum}$ is the price of crude oil in dollars per barrel. In 2006 the price of petrodiesel (without tax) was $0.49 per litre, biodiesel from palm oil was approximately $0.66 per litre, and biodiesel from algae estimates the cost at $1.40 per litre assuming biomass production of 10 000 t per year and 30% oil content (Christi 2007). The economic viability of biodiesel production from algae will increase with molecular engineering, increased photobioreactor efficiency, rising crude oil prices, and emerging environmental policy.

Christi (2007) identifies seven potential benefits of molecular level engineering:

1. increased biomass yield due to increased photosynthetic efficiency
2. enhanced biomass growth rates
3. higher oil content

4. better temperature tolerance
5. removal of the light saturation phenomenon
6. reduced photoinhibition
7. reduced susceptibility to photooxidation

Further research and genetic modification of algae will add to the productivity of photobioreactors and thus, increase the economic viability of these reactors.

1.1.4 Organic waste

Organic waste material can be used as a renewable energy source. The British meat industry have had success with co-combustion units using meat and bone meal as a secondary fuel in coal-fired stations or as standalone units/fluidised beds (PDM Group 2010, Ravelli, Perdichizzi & Barigozzi 2008, Gulyurtlu et. al n.d). Fluidised beds burn particles by suspending the particles in the air in conjunction with high temperatures (Bell 1980). These systems work well as a renewable energy source using biomass comprised of meat and bone meal in countries containing the Bovine Spongiform Encephalopathy (BSE) pathogen (mad cow disease). It benefits doubly, by providing energy generation as well as a way of disposing of a pathogen that cannot be dumped in landfill. However, in Australia where there is no pathogen the market for meat and bone meal is worth more to the meat industry as a resalable by-product than as a secondary fuel.

Beef tallow is a possible renewable energy source for use as biodiesel (Nelson & Schrock 2006). Beef tallow is a by-product of the meat industry. However, as with

meat and bone meal it is of greater resale value to the Australian meat industry than as a fuel source, retailing at between $600 - $1000 per tonne (Spence, M 2010, pers. comm., 19 April). Other organic waste in the form of waste water is being used and tested in anaerobic digestion ponds (MLA 2010). Anaerobic digestion takes place through specialized bacteria operating in the absence of oxygen (Johns 1995). They are a widespread secondary treatment process for abattoir waste water before releasing into aerobic ponds. They have low operating costs and high BOD and COD removal rates however, they produce large amounts of methane (a GHG) (MLA 2010) and therefore new studies on pond covers to capture this gas are a current area of research and are not included in the scope of this project.

Paunch appears to be the only other organic waste energy source worth investigation for Australian abattoirs. Paunch is the partially digested feed from the first stomach of ruminant animals such as, sheep, pigs, and cows and may be a viable fuel source for use in co-combustion units, as a coal substitute, or pyrolysis (eds Witherow & Scaief 1976, Bridle 2011).

Paunch has a substantial energy content. Early energy measurements done with a Parr Oxygen Bomb Calorimeter showed that paunch has an average energy content of 4 000 cal/g (Ricci 1977) or 16.7 GJ/Mg. This energy content is comparable to switch grass (a renewable biomass crop) which has an energy content of 18.4 GJ/Mg (Table 1) (McLaughlin et al. 1999). However, the energy content for paunch is variable due to the different feed rations fed to the livestock. Some of the characteristics of paunch both dried and wet have been tabulated below (Table 2). Table 2 shows that there are slight discrepancies between values for dehydrated

paunch. However, the biggest problem regarding paunch for use as a biomass is its moisture content. The high moisture content (around 80 -85% when dewatered of surface water (Ricci 1977, eds Witherow & Scaief 1976)) of undried paunch makes it a non-viable biomass, instead the paunch needs to be dried to below 70% moisture content to become useful. A study funded by Meat and Livestock Australia found that for use in pyrolysis the paunch needs to be further reduced to 20% moisture content (Bridle 2011). The report also identified a beneficial outcome for using paunch as a biomass for gasification or pyrolysis; each tonne of paunch used as a feedstock would generate GHG credits of up to 1 tonne CO_{2e} and gain energy credits up to 3.2 GJ (Bridle 2011). These energy credit benefits combined with its high energy content make paunch a suitable biomass candidate.

Table 1 - Energy contents for paunch, switch grass, coal, and wood. Paunch (17 GJ/Mg) energy content is comparable to that of switch grass (18 GJ/Mg).

Type	**Energy Content GJ/Mg**
Paunch	16.7
Switch grass	18.4
Coal	27.4
Wood	19.6

*Values for switch grass, coal, and wood obtained from (McLaughlin et al. 1999).

Table 2 –Some of the characteristics of dry and wet paunch.

Composition of dehydrated paunch				
Reference				
	Witherow & Scaief (eds) 1976, Baumann 1971	Ricci 1977	Bridle 2010	Bridle 2011
	% average	% average	%TS wet	%TS dry
Moisture	6.8	15.3		
Protein	12.7	10.3	8.1	
Fat	3.1	4.4		
Crude fibre	26.2	21.2		
Calcium	0.6	0.5		
Ash	7.2	6.7	13.5	7.02
P2O5	1.5	1.4		
Carbohydrate	40.8	42	72.9	

1.2 Project objectives

The meat industry in Australia faces the likelihood of rising energy costs and now has a carbon tax. To safeguard its future, the Australia meat industry should thus look towards renewable energy sources to combat these rising costs. Australia currently is well behind other developed nations in the implementation of renewable energy technologies into industry in general, and specifically the meat processing industry. For example, anaerobic waste water ponds capturing methane (CH_4) are gaining momentum in the United States, yet the uptake of this technology has been

much smaller in Australia, due to various problems including solids build up under covers and inappropriate cover materials (Spence, M 2010, pers. comm., 8 May). A question thus arises as to what other renewable energy technologies are most feasible for the Australian meat processing industry to adopt in the near future? To address this question, a renewable energy feasibility study was done on the implementation of renewable energy into a meat processing plant – specifically Churchill Abattoir (CA), Ipswich, Australia. CA is a medium sized, energy intensive facility and representative of the larger Australian meat industry. The main energy consumptions at the abattoir are in the form of electricity for refrigeration as well as coal to produce hot water.

In the first part of what became a two-part study, three of the most widely available renewable technologies available commercially (solar photovoltaics, wind turbines and algae for biodiesel production) were investigated for possible adoption by CA to replace current sources of energy. However, the results of this investigation showed that none are currently viable in an economic sense. This study thus moved into a second part in which organic waste streams produced at CA were investigated in a search for a viable source of biofuel. Of the various abattoir waste streams paunch is an industry specific absolute waste product left over from the slaughter process, and is currently the only unusable part of the animal. If paunch is dried however it has the potential to be a viable fuel source for co-combustion, both as a coal replacement for water heating, and for pyrolysis to generate electricity.

This study focuses on characterising the properties of paunch produced through the production of beef as a step towards the use of paunch as a biofuel at CA and other

abattoirs. Paunch is generally made up of partially digested grass and grain with a pH ranging from 5.6 to 7.0 and 85% moisture content when dewatered (eds Witherow & Scaief 1976). As indicated above it is a waste product with little value at present, and its minimal value has led to its use in just producing compost or as worm food. In addition, it is a problematic waste stream for abattoirs as it has a number of unusual characteristics that prevent it from being treated using conventional methods such as sewage treatment plants (Ricci 1977, Train et al. 1974, eds Witherow & Scaief 1976). These include its high biochemical oxygen demand (BOD) and its tendency to clog bar screens, hopper bottoms, pits, and suction pumps. In conventional septic type tanks paunch settles out and hardens into a low-density rock-like substance. This concrete-like behaviour clogs pipelines which then require augering, and paunch does not decompose in digesters and will eventually clog them. Paunch also cannot be dewatered by vacuum filters, nor dried in a flash drier or burned in suspension, and has a highly objectionable odour (Ricci 1977). Current best practice for paunch handling includes dry dumping instead of wet dumping (Doyle & Lant 2001, MIRINZ 1996), the separation of the solids from the liquid followed by land disposal of the solids for uses such as composting or worm feed. In contrast, given its intrinsic energy content, successfully drying paunch can enable a problematic waste to instead become a useful energy source for abattoirs.

The second part of this thesis aims to determine some of the drying properties of paunch to enable conclusions to be drawn as to the potential of solar dried paunch to become a viable biofuel source for CA.

Chapter 2: Part 1 – Renewable Energy in the Australian Red Meat Processing Industry

2.1.0 Part 1: Renewable Energy Methods

The feasibility study was broken into two parts. The first study was done on the viability of the top three renewable technologies PV, wind turbines, and algae for biodiesel for implementation at CA. A number of quotes for PV systems were obtained and payback calculations were produced. A wind speed, power output profile, and payback period for wind turbines was done using wind data for Amberley Air base which is located within sight of CA. The current state of algae production for biodiesel was assessed to see if it has reached an economically viable stage for use at the abattoir however no payback period was calculated due to the underdevelopment of this industry. If a technology did not meet a reasonable payback period of less than or equal to 5 years (as stipulated by CA), then that technology was considered not viable for CA.

2.1.1 CA energy consumption

The energy consumption at CA needed to be determined before appropriate renewable energy technologies could be assessed. CA uses an 8 MW coal fired Thompson boiler that produces steam at 160°C that is fed into the cooker at around 135°C with a total plant steaming rate usage of 11-12 000 kg/hr. Figure 2 shows a schematic of the water circulation through the boiler. The boiler runs for approximately 16 hours from start up to shut down five days per week. The steam

from the boiler is fed into a jacketed cooker and return steam condensate is returned to the boiler. The gases extracted from inside the cooker pass through a heat exchanger then pass to the biofilter. The heat exchanger produces clean hot water to 70°C, which passes to two more tanks. One tank has cold water added to create the 42°C hot water, the other tank uses another heat exchanger to create the 84°C hot water needed by the abattoir. Steam from the boiler also passes to this heat exchanger and flows back to the boiler.

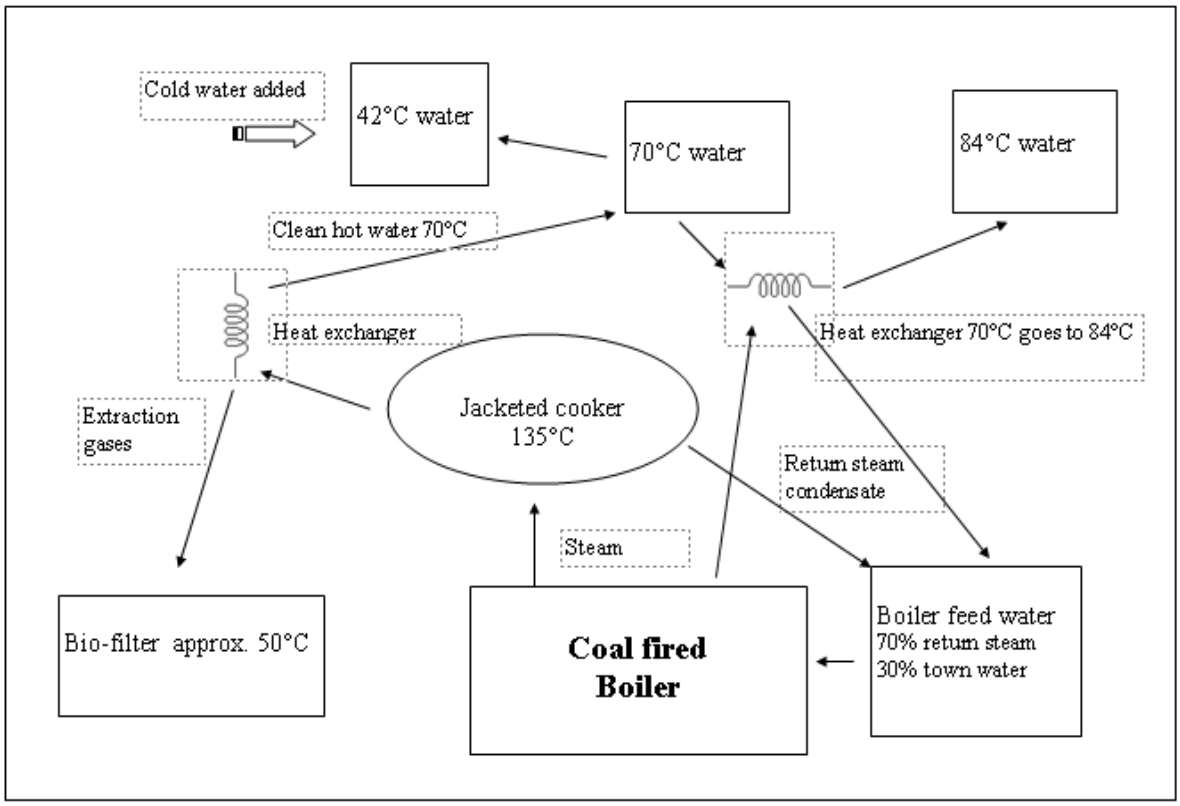

Figure 2 - Schematic of the water circulation from the boiler at CA to the cooker, heat exchangers, and bio-filter.

CA uses approximately 200 ML of water per year, max. 1.2 MWh of electricity per day (although this is seasonal due to the use of cold rooms), and 3000 tonne per year of coal, as well as ammonia to cool the refrigeration units. CA produces approximately 60 - 90 cubic metres of paunch per week with a moisture content of approximately 75%. Wastewater containing the remainder of the paunch, cattle yard waste (dirt, manure), fat, and blood is primary treated then sent to anaerobic/aerobic lagoons and then irrigated to crops/pasture.

National Greenhouse and Energy Reporting (NGER) was carried out for CA to help determine energy usage. NGER is a government initiative that requires companies to report their energy consumption, production, and emissions. The acquired NGER will also be useful as a baseline of energy use, will allow easy comparisons to be made after the (possible) implementation of renewables, and for use with further studies. Table 3 demonstrates the information gathered for NGER at CA: energy consumption, emission, and production. Values have been rounded to retain a level of commercial confidentiality for CA. However, precise values are available by request from the author.

Table 3- Energy consumption, emission, and production reportable under NGER. The amount values have been rounded to retain some confidentiality for CA.

Type	Period	Units	Amount	Criterion	Criterions
Electricity	July 2009-June 2010	kWh	5 900 000	A	A = data from invoices
Coal	July 2009-June 2010	Tonnes	3 000	A	AA = data from invoices and adjusted for changes in stockpile
Ammonia (refrigerant)	June 2009 - July 2010	kg	500	A	AAA = data measured at point of consumption via equipment calibrated to Aus standards
LPG	July 2009-June 2010	Tonnes	60	A	BBB = data derived from simplified consumption measurements
Paunch	July 2009-June 2010	Paunch is sent off site. According to page 55 worked example in NGER reporting guidelines for meat and livestock industry the paunch will be excluded from the NGER report.			
steam	July 2009-June 2011	GJ	700 000 000	BBB	
Diesel (off road)	July 2009-June 2012	L	20 000	A	
petrol (off road)	July 2009-June 2013	L	1 000	A	
Diesel (on road)	July 2009-June 2014	L	25 000	A	
petrol on road	July 2009-June 2015	L	3000	A	
Acetylene	July 2009-June 2016	GJ	not reportable		
Compressed air	July 2009-June 2017	GJ	not reportable		
Wastewater	July 2009-June 2018	CH4 in tonnes of CO2 equivalent	5 000	method 1	with actual plant water usage

The electricity, coal, and wastewater components are the most relevant information to this project. However, all the information contained in the NGER allows a complete picture of CA as a whole to be formed. CA energy use can be treated as a whole system or broken into component parts such as electrical energy consumption for the refrigeration system and coal consumption for the boiler.

2.1.2 Expected electricity increases 2011 to 2014

The cost of electricity is expected to rise and so it is important to try to predict future electricity prices for CA. EnergyAustralia's (2010) expected price trends till 2014, (Figure 3), show an annual increase of between 15% - 20% in the cost of electricity for each period until 2013/14. The price is then expected to only rise by less than 5%. CA has advised that it was paying between $0.05 - $0.11 per kWh for electricity in 2010 (Spence, M 2010, pers. comm., 19 April). This range would be expected due to the large variation between peak and off-peak electricity prices. The expected rise in electricity price for CA for each period starting in 2010 is then:

- 2010/11 is $0.06 - $0.13.
- 2011/12 is $0.07 - $0.15.
- 2012/13 is $0.08 - $0.18.
- 2013/14 is $0.08 - $0.19.

Figure 4 gives a graphical representation of these increases. This chart does not allow predictions to be made beyond 2014 as no further information was provided regarding predictions beyond this period. The information shows that by 2014 CA is expected to be paying between $0.08 - $0.19 per kWh. These predictions appear to be accurate as CA quoted paying between $0.07 - $0.12 per kWh for electricity pre 1st of July, 2012 and expect this to rise to a maximum of $0.14 per kWh from 1st July, 2012 (Spence, M 2012, pers. comm., 9 July). These increases since 2010 fall within the predicted range given by EnergyAustralia (2010).

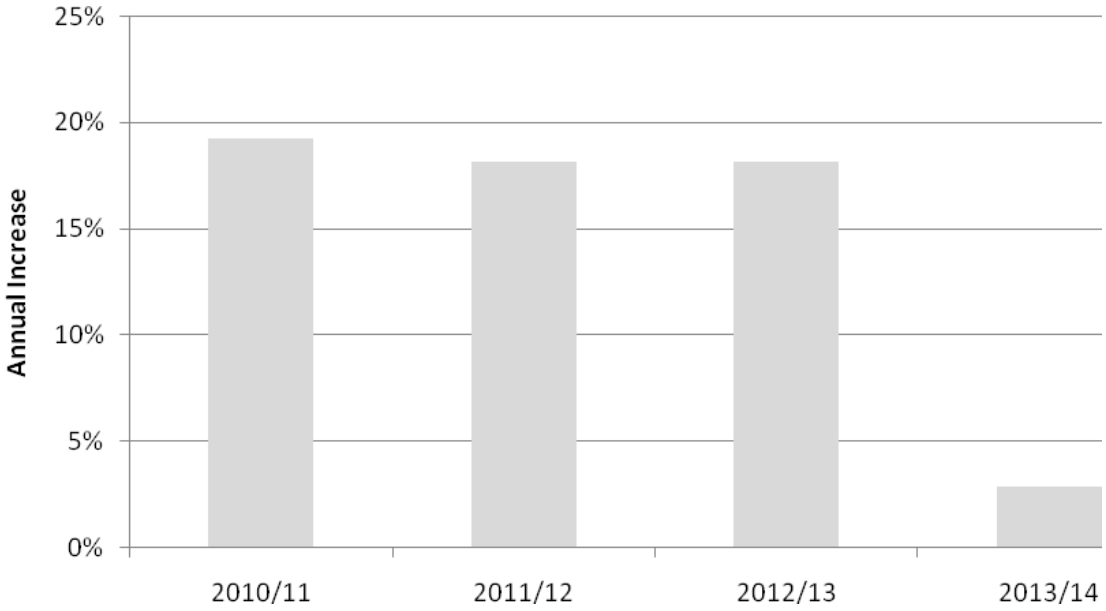

Figure 3 - EnergyAustralia's (2010) graph of expected yearly average electricity price increases for the period 2010 to 2014.

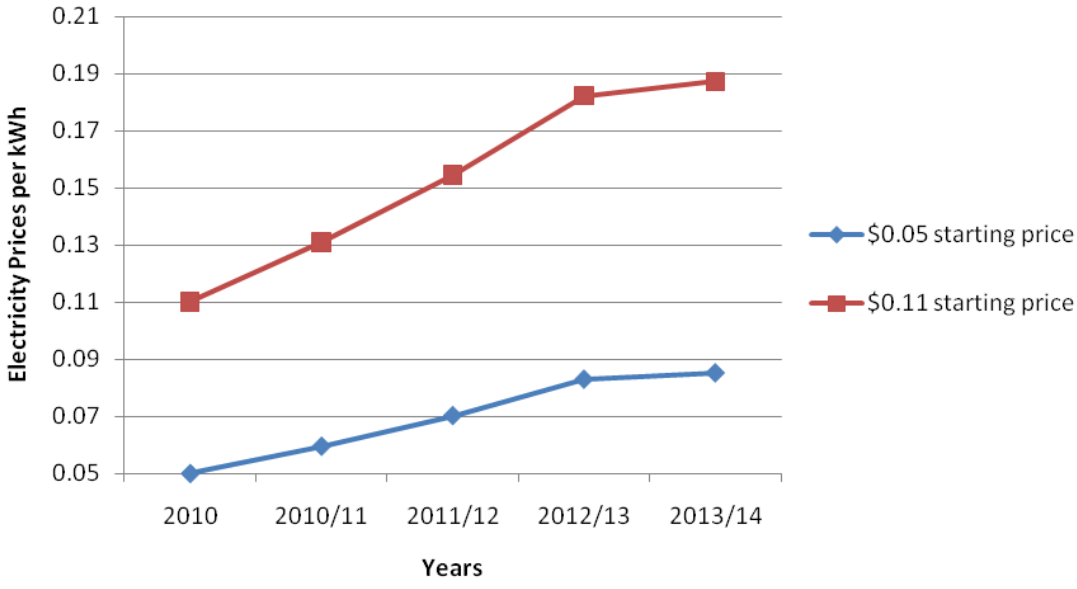

Figure 4 – The predicted electricity price increases from 2010 to 2014 (EnergyAustralia 2010). The non-linearity of the graph does not allow for price predictions beyond 2014. The starting point is CA's current (2010) electricity price of between $0.05 and $0.11 per kWh (Spence, M 2010, pers. Comm., 6 January).

2.1.3 Australian incentives for renewable energy use

Feed in tariffs, rebates, and funding opportunities can increase the viability of some renewable energy technologies by either increasing the value of electricity generation or reducing the capital cost. The Queensland feed in tariff for PV's is capped at 30 kW on a 3 phase system basically; three separate 10 kW systems, one on each phase. The return is $0.44 per kWh for excess power returned to the grid. However, this is only valid for residential and small businesses that consume less than 100 MWh per year of electricity (QLD Government 2011). For businesses such as CA, due to their large energy consumption, they are not eligible for this scheme.

The Renewable Remote Power Generation Program (RRPGP) was set up to increase renewable energy use in remote parts of Australia by providing financial support. A number of photovoltaic systems were installed under this scheme however, the RRPGP closed on 22 June 2009 (Queensland Government 2011). Other government funding opportunities for CA may include programs such as the Regional Food Producers Innovation and Productivity Program and can be found on the Queensland government business website. However, these programs are competitive, intermittent, and frequently aimed at innovative projects as opposed to installing existing technology. The benefits of these types of funding is that they can reduce the capital cost of installing a renewable technology that can, as in the case of PV, make a non-viable technology become economically viable. However, some of the emerging renewable technologies can have high operational costs that make them unfeasible, even with a reduction in capital cost.

The Renewable Energy Target (RET) was broken into two parts as of January 2011. These two sections are the Large-scale Renewable Energy target (LRET) and the Small-scale Renewable Energy Scheme (SRES) (Australian Government 2011). LRETs are aimed at, but not limited to, power stations to encourage additional electricity produced from renewable sources and is based on the amount of renewable energy produced above their baseline (Australian Government 2011). The baseline for CA would be zero due to the electricity being generated for the first time after January 1997 (as per regulations). However, although LRET's are aimed at power stations anything that generates more than the SRES unit capacity and annual electricity output limit is then classified as a power station.

The SRES is relevant to CA as it provides financial incentives to small-scale renewable energy producers (Australian government 2011) which is a more likely starting scenario for CA. Table 4 shows the requirements set by the Australian government for small generation units. The most relevant for CA being the unit capacity and annual electricity output for solar PV units installed after 14 November 2005. This limit is a unit capacity of not more than 100 kW with a total annual output of less than 250MWh (Australian government 2011).

Table 4 – Information provided by the Australian government (2011) on the requirements of small generation units. The relevant information for CA is the requirements for solar PV units installed after November 2005.

Unit type	Unit capacity and annual electricity output	Installation periods
Solar PV units	No more than 100 kW and a total annual electricity output less than 250 MWh	On or after 14 November 2005
Solar PV units	No more than 10 kW and a total annual electricity output less than 25 MWh	Between 1 April 2001 and 13 November 2005
Small wind turbines	No more than 10 kW and a total annual electricity output less than 25 MWh	On or after 1 April 2001
Hydroelectric units	No more than 6.4 kW and a total annual electricity output less than 25 MWh	On or after 1 April 2001

A small-scale technology certificate (STC) is created for 1MWh of renewable electricity created by the small generation unit. The online STC calculator shows that for the Ipswich postcode, a 100kW PV system, over 5 years would create 732 STC (inclusive of solar credits) or 691 STC (without solar credits). Assuming that these STC are sold through the clearing house at a set price of $40 then that would equate to $29 280 worth of STC (Australian government 2011). However, with all incentives it is important to check the current guidelines before making a decision to install a renewable technology as these incentives appear to change regularly.

To determine the applicability of a renewable technology for CA, incentives to increase economic viability are only one part of a feasibility study. Information regarding the different types available for each renewable technology is needed, including an understanding of manufacturers information to allow reasonable assessment of the renewable technology under consideration to be made.

2.1.4 PV user information

Before any renewable energy source can be tested for viability it is important to understand the manufacturers information available for that particular renewable technology. An important concept in understanding PV's is the I-V curve and given characteristics. Voltage (V, measured in Volts), current (I, measured in amps), and power (P, measured in Watts) can be graphically represented to show characteristics of a PV (Figure 6). Resistance, R, can be given by:

$$R = \frac{V}{I};$$

Power can be given by:

$$P = IV;$$

Current is also directly proportional to the amount of radiation falling on the PV, so the more radiation, the more current that can flow. Figure 5 demonstrates the different characteristics that can be gained by graphing an I-V and P-V plot for a PV.

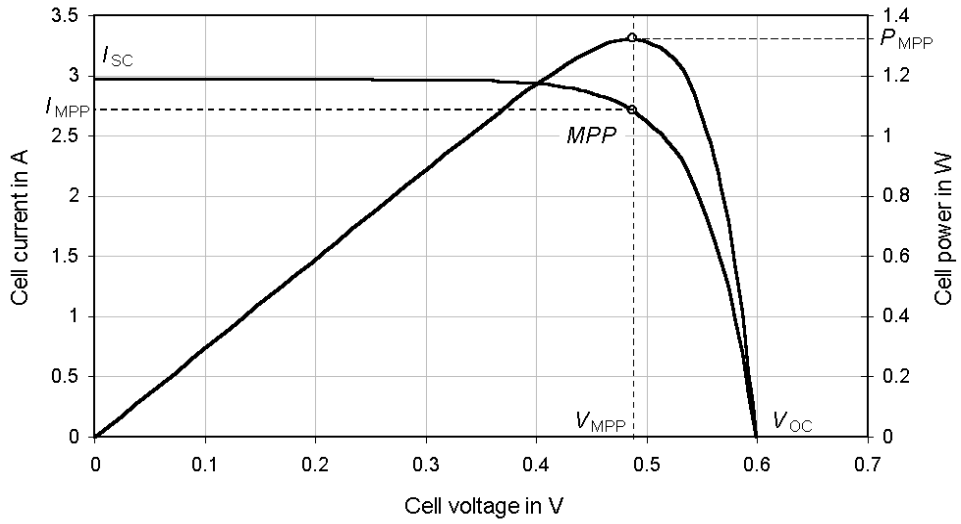

Figure 5 - I-V and P-V characteristic of a PV. The graph gives the maximum power point (MPP) which is the ideal operating point for maximum power delivery from the PV (Quaschning 2007).

The point I_{SC} is the short circuit current. This is the point where the graph cuts the y-axis, so there is no voltage at this point and therefore the cell can deliver no power. The point V_{OC} is the open-circuit voltage. This is the point where the graph cuts the x-axis, so there is no current and again the cell can deliver no power. I_{MPP} and V_{MPP} are the maximum power point (MPP) current and voltage respectively. The P-V graph is obtained for P by multiplying each point from the I-V graph. This also has an MPP point for power, (P_{MPP}). The MPP point is where PV's should aim to run at for maximum output. The fill factor (FF) is a quality rating for PVs which is the P_{MPP} divided by the product of the I_{SC} and the V_{OC}. The FF is a ratio of the maximum obtainable power to the theoretical power. Commercial-grade crystalline panels should have an FF >0.7 with grade B (inferior) crystalline panels having an FF of 0.4 to 0.65. Thin film panels have a FF of 0.4 to 0.7. Another characteristic generally given on information sheets for PVs is the temperature coefficient of P_{MPP}. This is a negative number (in % per ºC) which shows how much the power output will go down per degree that the cell temperature rises (usually starting from 25ºC) (Wright 2000).

PV efficiency is affected by natural and human factors which reduce the amount of radiation reaching the Earth's surface. It is then further influenced by the PV's ability to capture this radiation and to process it. Efficiency (η) is given by

$$\eta = \frac{output}{input} = \frac{\text{profitable energy}}{\text{expendable energy}};$$

The efficiency of a PV cell is related to the irradiance and is given by:

$$\eta = \frac{P_{MPP}}{IA};$$

Where P_{MPP} is the maximum power point, I is irradiance and A is area.

The efficiency of the PV to capture and process the incoming solar radiation is then reduced further by:

1. The tilt angle of the panel.
2. Heat and shading losses.
3. Conversion of energy.

Spreading light of the same intensity over a larger area (eg. Incident light radiation hitting the surface of a PV on an angle) reduces the energy per unit area (Parisi, Sabburg & Kimlin 2004). What this means is that light that hits a tilted PV that is positioned perpendicular to the incoming radiation will receive more irradiance than a horizontal PV. The irradiance that is spread over a greater angle is reduced to I_D *cos(θ)* where I_D is the direct irradiance, and θ is the incidence angle between the incoming radiation and the vertical to the surface (Parisi, Sabburg & Kimlin 2004). The ideal position for a fixed PV panel in the southern hemisphere is approximately 30º facing north. Panels can be set to a tilt equal to the latitude of where they are installed however, a better scenario would be using the solar zenith angle as this includes latitude and declination which depends on the time of year.

As previously shown current is directly proportional to the amount of radiation falling on the PV. Therefore, direct and diffuse shading of the panel will result in

less current being produced. Heat is also a problem for PVs as shown by the temperature coefficient. In Australia this is a problem as most panels are rated to perform at 25ºC however, during an Australian summer operating temperatures can be greater than 60 ºC (Turner 2007). This can result in quite significant losses of output.

Inherent efficiency losses in PVs are due to the amount of photon energy that can be converted into current. Photons with energy smaller than the band gap cannot jump an electron from the valence band to the conduction band (refer to appendix 3). For photons near the band gap not all the energy is converted to electricity due to the PV surface reflecting part of the incoming light and some being transmitted through the cell. For photon energies higher than the band gap only the band gap energy is used and the rest is passed on to the cell as heat (Quaschning 2007).

2.1.4.1 Types of PV

As well as understanding the manufacturers information it is also essential to have an understanding of the different types of PV available. There are three types of PVs: monocrystalline, polycrystalline, and amorphous (thin film). Silicon is one of the most common elements on Earth with the majority of panels being made of this and therefore, the focus here will be on silicon panels. Silicon is not found in a pure form and is mainly extracted from quartz sand. After the extraction process a high purity silicon rod is formed. Polycrystalline cells can be made from this material and monocrystalline material can be seeded from it to make a single crystal. Monocrystalline cells have less internal losses than polycrystalline due to their single crystalline structure. The crystalline rods are then cut into wafers (between 200 – 500 μm slices) which are then cleaned and doped. Metal contacts are then screen printed on with thin contacts on the front and, generally, the whole back section covered. The front section is only covered in thin strips to minimise the amount of reflection caused by the contacts and to allow maximum light to be available to the cell. The cell is then covered in an antireflective coating to help reduce reflection and then joined together into a module (Quaschning 2007).

Thin film panels are generally considered less efficient than poly and monocrystalline panels but have the benefit of being cheaper to produce, not requiring inter-cell connections, and maintain good efficiency when exposed to heat or shading (Turner 2007). Thin film panels are made, like their name suggests, by depositing a thin film of silicon straight onto a base substrate, usually glass, which has been coated in transparent tin oxide strips (connections). The glass substrate will then function as the front of the panel. After the p and n thin film layers have been

applied aluminium is used to create the back contacts and the whole panel is coated in some form of protection coating such as a polymer to allow the panel to be able to withstand climatic conditions (Quaschning 2007). When deciding on a PV it is important to weigh up the benefits of cost versus efficiency and the temperature co-efficient. For Australian climates it may be more beneficial to install thin film PV panels as they have a better efficiency when exposed to varying climatic conditions.

Another important consideration is the energy costs of producing the PV. It is now possible to acquire an embodied energy rating as part of the information provided by the PV manufacturer. This embodied energy rating tells how many years it will take to counteract the amount of energy used to produce the panel (Turner 2007). Most modern PV panels however have 25-year warranties so they will more than repay even a 4-year embodied energy debt. This means that they will produce far more clean energy than the energy used to produce them.

Steenblik (2005) states that the lifetime emissions from the entire life cycle of a PV system would create less than 100 grams per kilowatt-hour of emissions. This is far less than fossil fuels which produce 10 to 20 times that amount. Turner (1999) concluded that a 1kWh PV panel would save 1330 kg of CO_2 per year by replacing fossil fuels after it paid back its embodied energy debt. This reduction in GHG emissions will help to mitigate climate change and PV systems also have the benefit of being able to be standalone systems. This makes them ideal for use in remote areas which removes the high economic and energy cost of installing grid connection lines to remote areas (Steenblik 2005). However, PV systems are still not as cost

effective as, for example, renewable wind power generation or the traditional fossil fuel energy plants.

2.1.5 Wind turbines

The power output of a wind turbine is affected by wind speed and each turbine will have a characteristic wind speed-power curve. As the name suggests the wind speed-power curve is a graph of electrical power output versus wind speed. The equation governing these graphs is:

$$P = c_P \frac{\rho}{2} v^3 A;$$

Where P is the electrical power output, c_P is the power coefficient of the wind turbine, ρ is the density of air, v is the wind velocity, and A is the area swept by the rotor (Hau 2000). However, if there is not a known power coefficient available, then a theoretical graph or manufacturer's graph can be obtained or created.

Speed-power graphs are useful for determining what the actual output of the turbine will be for a specific site. A theoretical graph can be obtained using the rated power of the wind turbine with its rated speed. For example, the 5.5 m HUSH wind turbine has a rated power output of 20 kW at 15 m/s and a cut-in speed of 2 m/s (HUSH Wind Power n.d). The cut-in speed (or velocity) is the minimum wind speed that a turbine needs to start generating power. To create a wind speed-power graph for this turbine, we divide (varying) wind speed by the rated wind speed then multiply by the power output. We then set the cut-in speed to zero, and for all wind speeds greater than the rated output speed we set the power output to the rated value. The only information this graph lacks is the cut-out velocity which is the highest speed that

the turbine can operate while still delivering power. The benefit of these types of graphs is that they allow for site specific wind speeds to be used to generate the graph. Figures 6 and 7 demonstrate a theoretical graph for a 5.5m HUSH wind turbine and a 9m Proven wind turbine with a rated 15kW at 12m/s.

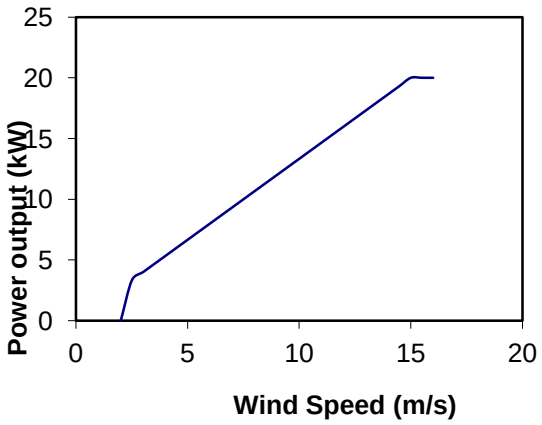

Figure 6- Electrical power output vs wind speed for a 5.5m HUSH wind turbine. A theoretical speed-power graph using the rated output and speed information available from the manufacturer for a HUSH wind turbine.

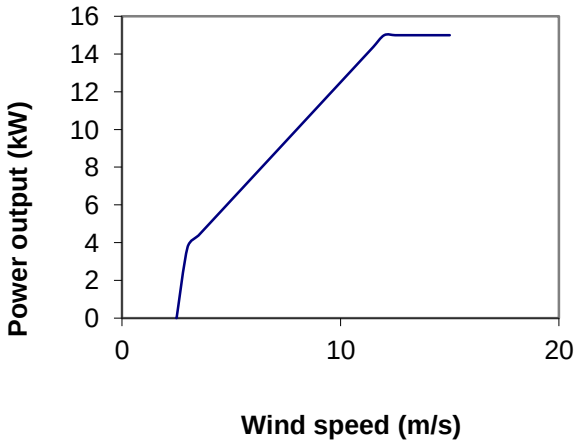

Figure 7 – Electrical power output vs wind speed for a Proven 9m wind turbine. A theoretical speed-power graph using the rated output and speed information available from the manufacturer for a Proven wind turbine.

The manufacturer's wind speed-power graph is part of the performance guarantee of the wind turbine. However, Gipe (2004) states that there are fewer rules governing small wind turbine testing and energy calculations compared to medium sized turbines that undergo independent testing. Therefore, the data provided by small wind turbine manufacturers should be viewed with care. The guidelines/ recommendations for a manufacturer to produce a power curve are based on three threshold points (Hau 2000). These are the cut-in speed, the rated wind velocity, and the cut-out velocity, and are used to determine the shape of the graph. The rated wind velocity is the wind speed where the maximum power output is reached. The power is also considered to be the net power, so it should include losses caused by the turbines' internal parts (Hau 2000).

2.1.5.1 Types of wind turbines

Wind turbines designs generally fall into two categories, horizontal or vertical axis (Figure 8). Horizontal axis turbines are the most common type used today. A common sight seen in the Australian outback is the horizontal axis "American multivane" windmill used for pumping water. Horizontal axis turbines range from these multivaned blade types to one, two, or three blade streamlined wind turbines (Hinrichs & Kleinbach 2006). Multivaned units are described as high-solidity devices while the types with fewer blades are conversely known as low-solidity devices. Modern horizontal axis turbines are low-solidity devices and owe their design to recent improvements in our understanding of aerodynamics (Boyle 2004).

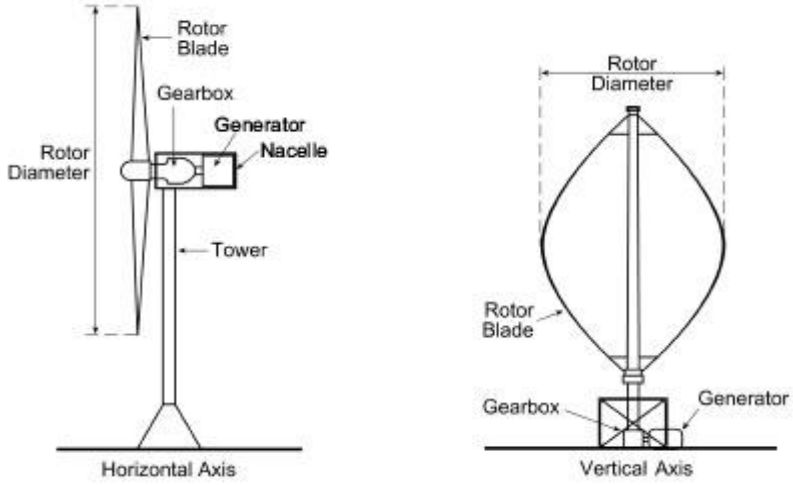

Figure 8 - The diagram shows horizontal and vertical axis wind turbine design (Scottish government 2010).

Vertical axis wind turbines are relatively modern designs and were invented in 1925 by Georges Darrieus. Thus, the Darrieus is one type of vertical axis turbine, and bears some resemblance to an eggbeater. These turbines can harness wind from any direction without needing to reposition the rotor. However, they are generally difficult to transport, install, and manufacture, which makes them less economically viable than horizontal axis turbines. Vertical axis turbines are believed to offer advantages over horizontal axis turbines when it comes to larger sizes and are thus the focus of current research that may eventually make them more economically viable than their horizontal counterparts (Boyle 2004).

No matter the type of turbine selected there is always the need for wind to make these turbines operate. Joselin Herbert et al. (2007) state that the wind availability (average wind speed and wind speed distribution at the site), the influence of height of installations above ground, and the total cost of the turbine system must be taken

into account to ensure the feasibility of wind turbine installation. These authors suggest that sites with average wind speeds of 20 km/h at a hub height of 30 m with a power density of 150 W/m^2 are economically viable. For Australian sites that do not have their own wind data it is possible to use data from the Bureau of Meteorology to create a wind profile for their site. However, on-site data is to be preferred when available as the most accurate information for a given time period.

2.1.6 Algae for biodiesel

The third most likely renewable technology reviewed was algae for use as biodiesel. A bioreactor is the most likely design to grow algae efficiently for biodiesel. Historically, the first bioreactors were not designed to grow algae for biofuel but instead used to study photosynthesis or as a feedstock for fisheries. One of the first photobioreactors was developed in the early 1940s by Myers and Clark (1944) to allow them access to a source of algae of high uniformity and to stabilize internal variables so that the relation of culture conditions to photosynthetic behaviour might be explored.

In 1979 the need for a large scale algal culture vessel to grow feedstock for seeding oysters led to the development of a 200 L bioreactor being constructed at the Fisheries Experiment Station at Conwy (Helm, Laing & Jones 1979). The Conwy reactor placed fluorescent lamps inside white tubes. The major drawbacks are the use of artificial lighting in conjunction with a non-continuous culture. Basically, this bioreactor is constructed from tubes made of white pigmented glass-fibre with a fluorescent lamp inserted into the middle of the tubes (Figure 9). The light from the lamp is reflected off the outer white surface increasing the exposure of the algae to

the light source. The temperatures were maintained at 18° C with the use of cooling water and CO_2 was added to aeration ports which also served to agitate the culture. The output showed that these vessels were capable of producing 52 litres per day of *Tetraselmis* at a density of 1000 cells μL^{-1}, and the average lifespan of cultures was 64 days (Helm, Laing & Jones 1979).

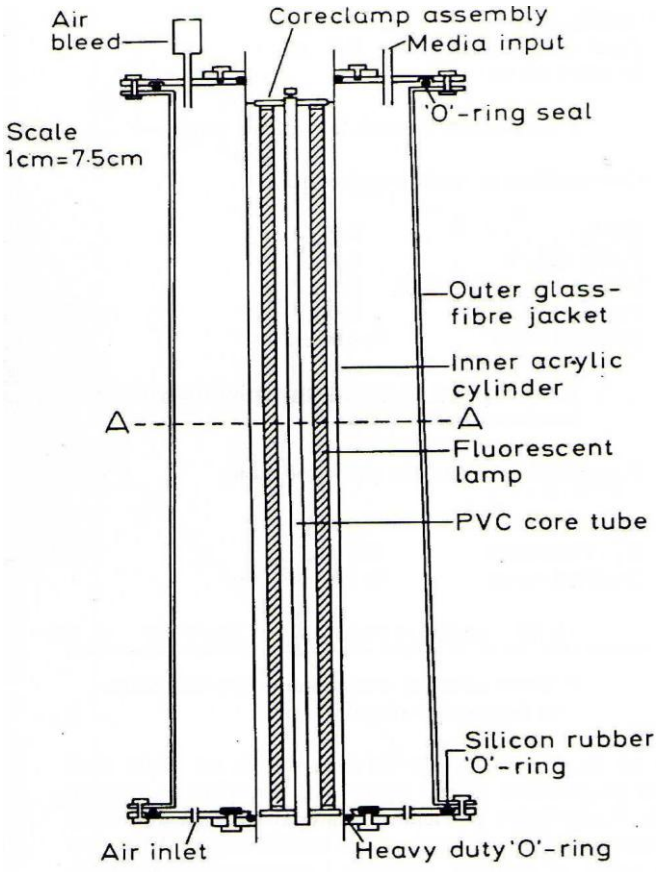

Figure 9- A longitudinal section through a Conwy vessel. Note the fluorescent lamp placed in the centre of the reactor. The outer walls are white to help reflect light back into the reactor (Helm, Laing & Jones 1979).

At the same time a very simple design was developed for the growth of algae as a feedstock for larval fish (Baynes, Emerson & Scott 1979). These 480 L vessels use polythene bags that are supported vertically by tubes of galvanised mesh (Figure 10).

The polythene bags are made of clear tubing that have been heat-sealed at the top and bottom and are relatively contaminant free and therefore require no pre-sterilization. Air-lines and outlet taps are inserted straight into the bags as the stretched polythene creates a firm seal around the inserted pipes. The system is able to be used inside or outside, with natural or artificial light and has a small ground area yet a large surface area which allows for light penetration. The most limiting factor with this design is light availability as the light is reduced within the bag due to self-shading by the algae. This can be reduced by removing part of the culture periodically to encourage cell division. Trials with 12 bags placed outside indicated that they maintained their yield even in dull weather by three bags at a time having ¼ of their volume removed every fourth day which allowed the culture time to replace that amount in the non-harvesting days. These cultures had a lifespan of 6-8 weeks before contaminants began to influence their growth after which new bags were set up (Baynes, Emerson & Scott 1979). These 'big bag' vessels have been the most commonly used large scale systems for the growth of algae in the aquaculture industry (Borowitzka 1999). This system appears to be a fairly cheap yet effective system to set up, with reliable yield and a simple, replaceable bag design. However, Borowitzka (1999) states that for temperature control this system needs to be indoors, resulting in the need for artificial lighting. In addition, this system inadequately mixes cultures, resulting in recurrent culture crashes, and thus creating a much higher production cost.

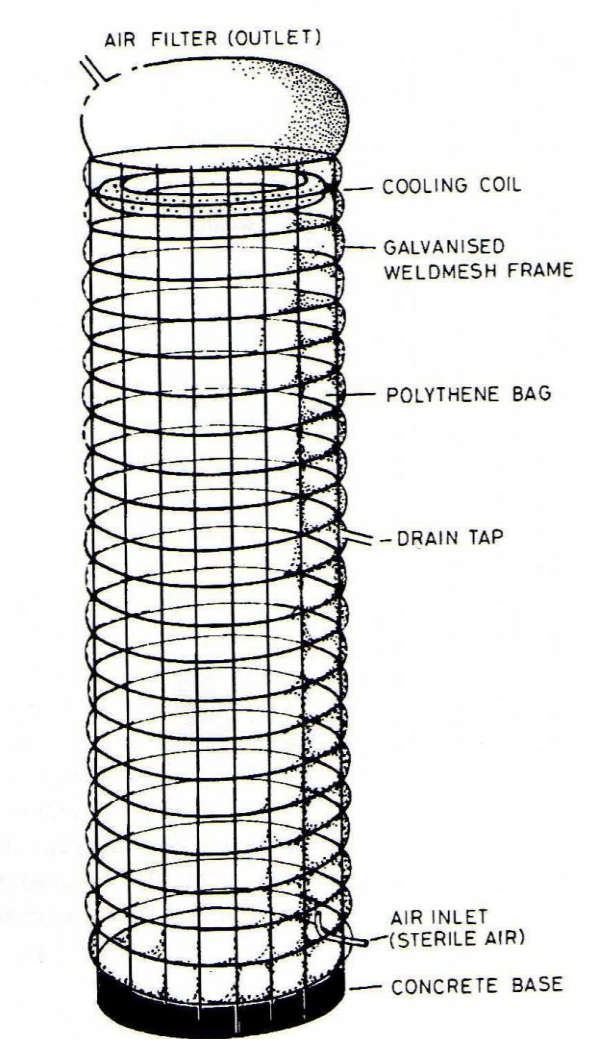

Figure 10 -"Big bag" vessel diagram. The outer frame supports polythene bags, which are replaceable in this type of reactor (Baynes, Emerson & Scott 1979).

2.1.6.1 Photobioreactor designs for the production of biofuel

Flat plate and tubular photobioreactors are currently the design of choice for the growing of algae for biodiesel production. Tubular and flat plate bioreactors enable a consistent composition and quality of alga by having high light efficiencies, controllable temperatures, sustainable cultures, and being contamination free. They are also able to be operated both in and outdoors and in differing climates and higher operating cell densities reduces harvesting costs and land use area (Borowitzka 1999).

Fine tuning designs on flat plate reactors and tubular photobioreactors now appear to be the direction that designs for efficiency are heading. Borowitzka (1999 p. 319) states that 'the fundamental principle in all of these designs is to reduce the light path and thus to increase the amount of light available to each cell'. There are a number of patents and designs around for flat plate and tubular bioreactors all with slight variations (e.g. Hu, Guterman and Richmond 1996). Nevertheless, they all follow the principle stated by Borowitzka. The various designs will be discussed in the pages below.

2.1.6.2 Flat plate photobioreactors

Hu, Guterman and Richmond (1996) developed a version of the flat plate photobioreactor called a Flat Inclined Modular Photobioreactor (FIMP) for use outdoors. The FIMP utilizes both direct and diffuse sunlight and incorporated variable tilt angles to maximise the amount of direct radiation throughout the year. Cascades of flat glass reactors were set up tilted, facing the sun and with a vigorous agitation system to enable mixing of the culture. The width between the glass plates (sitting on top of each other) is 2.6cm with the individual reactors being 90 by 70 cm and connected in series by PVC tubing (Figure 11). Maximum daylight temperature was maintained at 34 ºC, 35 ºC, and 40 ºC, depending on the type of algae used. The temperature was controlled by a temperature control sensor that was calibrated to 23 ºC and used a type of water sprinkler. A tube with sprinklers set 6 cm apart ran across the upper side of the front panel and used evaporative cooling by spraying water onto the top irradiated surfaces. This intermittent spray used an average rate of 50 litres per hour. CO_2 was added to the air mixer and hence to the air supply lines

which were perforated tubes running along the bottom and halfway through the reactor. The FIMP was able to be run continuously with high cell densities due to the short light-path and vigorous agitation system (Hu, Guterman & Richmond 1996). A possible drawback for using this type of system in Australia may be the amount of water required for cooling purposes. Also it is assumed that opaque waste water would be unable to be used as any darkening of the front glass panels would reduce the amount of radiation passing into the system though it may be possible for some types of grey water to be used. Hu, Guterman and Richmond (1996) however, do state that excess flow due to cooling can be collected into troughs placed alongside the reactors and fed back into the cooling water reservoir.

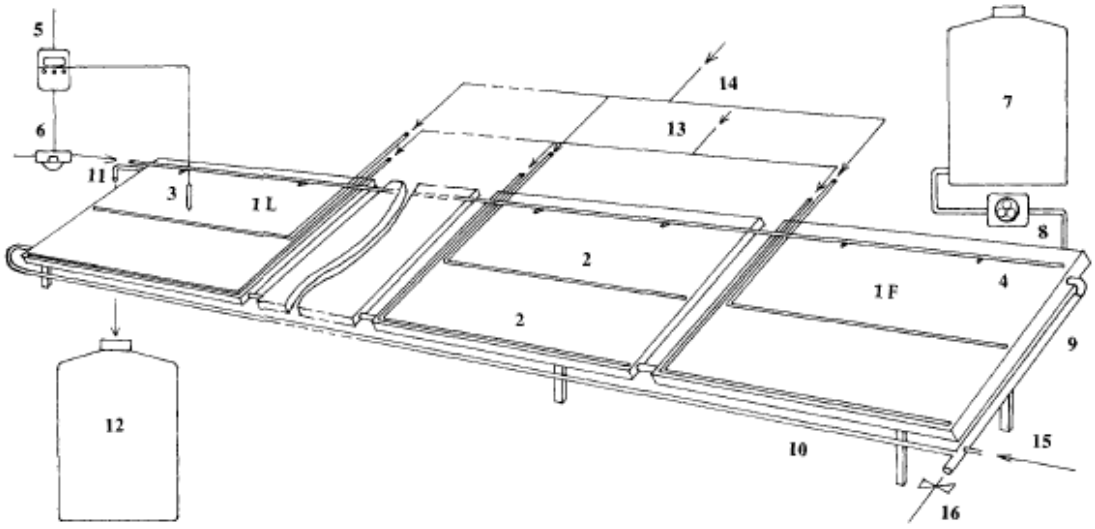

Figure 11 -'Schematic diagram of the flat inclined modular photobioreactor (FIMP) showing the first (1F) and last (1L) units in the cascade, (2) perforated tubes for bubbling compressed air, (3) thermosensor, (4) cooling water line and sprinklers, (5) thermostat, (6) solenoid valve, (7) culture medium reservoir, (8) pump, (9) airlift pipe, (10) recycling tubing, connecting the first with the end reactor in the row, (11) harvesting outlet, (12) harvesting reservoir, (13) compressed air supply, (14) line supply 2% CO_2 enriched air, (15) compressed air port for the airlift, and (16) sampling port.' (Hu, Guterman & Richmond 1996)

2.1.6.3 Tubular photobioreactors

Tubular bioreactors come in a variety of designs from horizontal tubes to tubes coiled vertically around a cylindrical frame (Lee 2001). The Centro di Studio dei Microrganismi Autotrofi of Florence started development of a horizontal tubular bioreactor in 1976 due to an increased interest in *Spirulina,* and the negative effect the climatic conditions in Italy had on its growth, as the ideal growth temperature is around 35 ºC (Tredici & Materassi 1992). The tubular photobioreactor is made of plexiglass tubes connected by PVC u-shape joins to create loops (Figure 12). The tube loops are laid on white polyethylene sheets and mixing is done by a diaphragm pump that lifts the culture up to a tank 3m above the ground and discharges back into the bioreactor every 4 minutes. The study found that this pulsing mixing worked better than continuous mixing. The 5 year tests on these systems showed an average productivity of 30-33 t $ha^{-1}y^{-1}$ (Tredici & Materassi 1992) which is equivalent to 8.219 g $m^{-2}d^{-1}$. It should be pointed out that at the time of Tredici and Materassi's report the cost of plexiglass was high and so it was not thought that this design would be suitable for translation into large scale industry (Tredici & Materassi 1992).

Figure 12 - The plexiglass tubular photobioreactor. The tube loops are placed on a white sheet to help reflect light back into the reactor (Tredici & Materassi 1992).

As an example of the wide range of bioreactor designs that have been developed for commercial use, in 1999 a tubular bioreactor was patented, based on the improved productivity of photosynthetic algae (Amnon Yogev & Dan Yakir 1999). This design is interesting to note as it has incorporated a Compound Parabolic solar Concentrator (CPC) into the design. The tube is placed in the centre of the CPC, which increases the light efficiency and distribution of radiation to the tubes (Figure 13) (Amnon Yogev & Dan Yakir 1999). This design approach thus bears similarity to the use of the polyethylene sheet in the horizontal tubular system and the white pigmented glass-fibre of the Conwy system, where the white surface reflects the radiation.

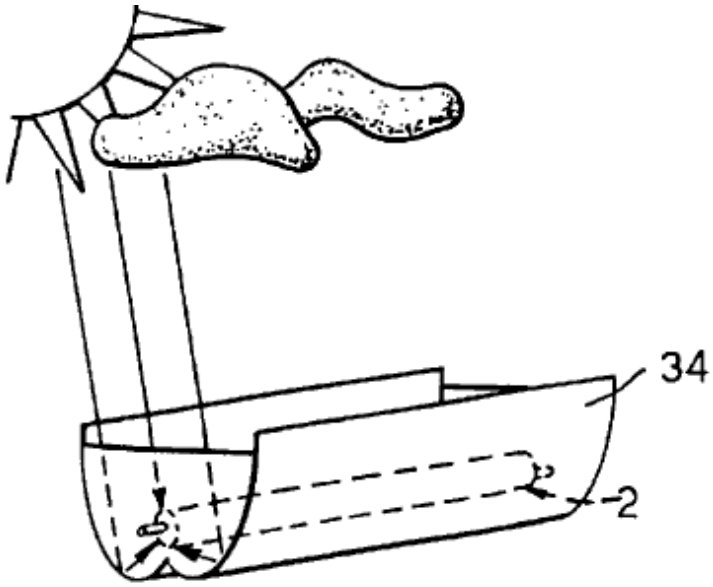

Figure 13 - Tubular photobioreactor with Compound Parabolic solar Concentrator (34) incorporated into the design. The parabolic reflector concentrates light back into the tube (2) of the reactor (Amnon Yogev & Dan Yakir 1999).

There are a number of draw backs and comparisons to be made with both tubular and flat plate reactors. Nerantzis et al. (n.d) state that 'reliability, scalability, control, low outputs, large energy and labour inputs are the main problems that in some cases override the benefits' for the mass production of algae. Accumulation of photosynthetically generated oxygen or dissolved oxygen (DO) is a problem, especially in tubular photobioreactors and many designs need some form of degassing vessel as high levels of DO reduce productivity (Nerantzis et al. n.d). Many algal species cannot survive exposure for 2-3 hours to oxygen levels above air saturation (Tredici & Materassi 1992). Tubular systems seem to have more problems with DO and a comparison can be seen in the amounts of DO in the FIMP compared to horizontal tubular reactors. The highest FIMP amount of DO concentration was 10.5 mg l^{-1} compared to 30-40 mg l^{-1} for the tubular reactors (Hu, Guterman & Richmond 1996). The lower rate in the FIMP had to do with a reduction of

photosynthesis at night, a short oxygen path, and the high rate of aeration (Hu, Guterman & Richmond 1996).

Thermal heating of outdoor bioreactors is also a problem as the solar energy not used in photosynthesis can heat the reactor 10-30 ºC above ambient temperature for several hours a day (Nerantzis et al. n.d). This could be a serious problem for Australian photobioreactors during the summer months if there is no cooling system in place. Otherwise, thermotolerant species of algae (Shen & Lee 1997) or chlorophyll reduction (Kizililsoley & Helvacioglu 2008) may be a solution for the Australian climate.

A study comparing the efficiencies of sunlight utilization between tubular and flat plate photobioreactors was carried out by Tredici and Zittelli (1997). They used for the outdoor study a coiled tubular, near horizontal straight tubular, and a near horizontal flat panel reactor. For the laboratory studies under artificial illumination they used a flat and tubular chamber reactor (Figure 14). Photosynthetic efficiency (PE) and dry biomass concentration was measured daily to estimate the productivity of the cultures in the different reactors. The near horizontal tubular reactor had the highest volumetric output and the second highest PE, with the coiled tubular design showing the highest PE. The Tredici and Zittelli (1997) study showed that the curved surface of the tubular reactors spread the incoming radiation over a greater surface area, thus reducing the light saturation effect and increasing PE. This study also showed the importance of the design of photobioreactors in regards to reducing the intensity of solar radiation to limit the light saturation effect. [The light saturation effect is where further increases in light will not increase the rate of photosynthesis.

Spreading light of the same intensity over a larger area (e.g. Incident light radiation hitting the surface on an angle) reduces the energy per unit area (Parisi, Sabburg & Kimlin 2004)]. The curved surface of the tubular reactors increases the PE, giving them a greater utilization of sunlight.

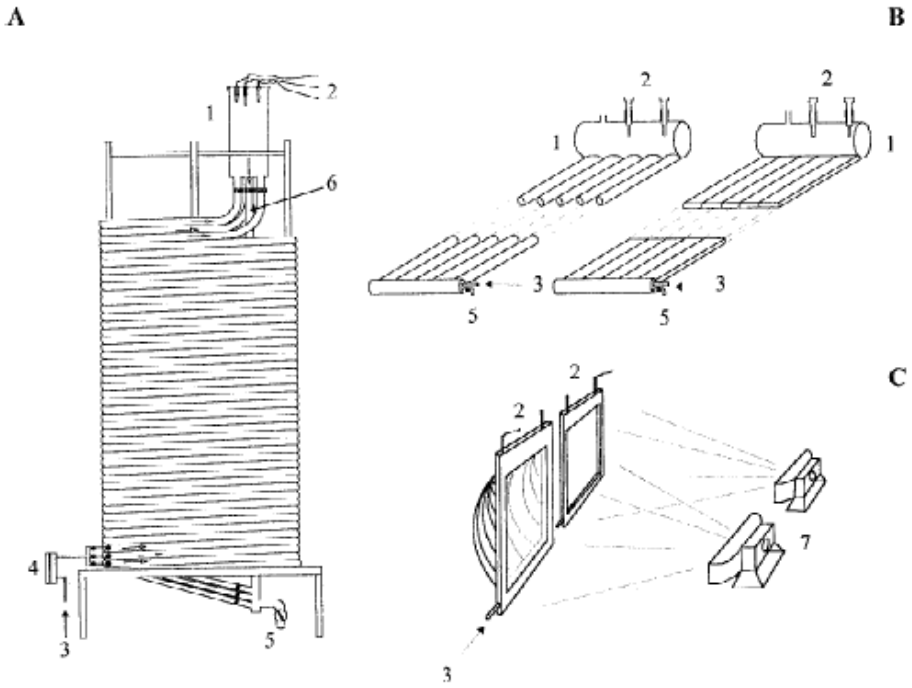

Figure 14 - Diagrams of the photobioreactors used in the comparison study. (A) is the coiled tubular reactor, (B) are the near horizontal flat and tubular reactors, and (C) are the flat and curved chamber reactors (Tredici & Zitelli 1997).

As the processing of algae into biodiesel is a set process the only factor for industries to decide before growing algae for biodiesel is based on: what is the best photobioreactor for their needs, and are they economically viable? Flat-plate and tubular technology appear to be appropriate for industries that aim to develop biodiesel as their primary product for the replacement of fossil fuel. These photobioreactors provide continuous culture and allow for optimum control of environmental factors (such as light availability) to provide ideal growing conditions

for the algae. The continuous culture output and the need for continuous production of their main product balances the higher structural costs for building these types of bioreactors.

Chapter 3: Part 1 Renewable Energy Results

3.1.0PV

Payback period calculation for PV was made using the method given by Boyle (2004, p.434). This method uses the capital cost, energy output, and the competing energy price to calculate the number of years needed to pay back the initial cost. The value of annual electricity generation is given by:

$$\text{Value of annual electricity generation (dollars)} = \frac{output \times price}{100};$$

Where the output is the annual energy output of the renewable in kWh per year and price is the cost of the competing energy price (such as coal or electricity) in cents per kWh.

The payback time is then calculated by:

$$\text{Payback time (years)} = \frac{capital}{generation};$$

Where capital is the initial capital cost in dollars, and generation is the value of annual electricity generation in dollars.

A number of quotes for PV systems were obtained. Information provided by Ekoenergy (2010, pers. comm., 25 October) stated that Ekoenergy could provide a 10 kW system that would produce 40 kWh per day for $38 800 or a 3 phase system

at 10 kW per phase, 162 panels, for $125 300 not including ancillary costs such as installation. Using the supplied data and a competing electricity price of $0.05 kWh the payback period is 53 years. Using the supplied data and a competing electricity price of $0.11 kWh the payback period is 24 years. Table 5 demonstrates the payback calculations for varying electricity prices based on the information received from Ekoenergy.

Table 5 - Demonstrates the payback calculations for Ekoenergy using a competing energy price of $0.05 and $0.11 per kWh, giving payback periods of 53 and 24 years respectively.

Ekoenergy			**Competing energy price**	
System	**Produces per day**	**kWh per year**	**$0.05 electricity**	**system cost**
10 kW	40 kWh	14600		$38,800
	value annual electricity generation	730		
	Payback	53.15 yrs		
System	**Produces per day**	**kWh per year**	**$0.11 electricity**	**system cost**
10 kW	40 kWh	14600		$38,800
	value annual electricity generation	1606		
	Payback	24.16 yrs		

Information provided by Solar Guys (2010, pers. comm., 22 October) gave the cost per Watt as $4.50 and a production of 4.4 kWh per kW. For CA this would mean $4.50 times 1.5 million (to cover peak load) giving a total cost of $6 750 000.

Table 6 demonstrates the payback calculations for varying electricity prices and for a $1 per Watt PV system. Using the supplied data from the Solar Guys and a competing electricity price of $0.05 kWh the payback period is 56.04 years. Using the supplied data and a competing electricity price of $0.11 kWh the payback period is 25.47 years. Using the supplied data and a competing electricity price of $0.50 kWh the payback period is 5.6 years.

Using the supplied data, a competing electricity price of $0.11 kWh, and the cost of $1.00 per Watt, the payback period is 5.66 years.

Using CA's electricity use reported in the NGER, 5 898 407 kWh per year, a basic capital cost calculation can be made based on the value of annual electricity generation (PV) and a 5 year payback period. The needed payback period is 5 years, using the current competing energy price of $0.11 kW/h, and value of annual electricity generation of $648 824 then;

Capital cost (dollars) = Payback x *value of annual electricity generation*,

gives a capital cost of $3 244 123. Thus, if a PV system cost $3 244 423.00 and produced 5898407 kWh annually then it would become viable with a payback period of 5 years.

Table 6 - Demonstrates the payback calculations for Solar Guys using differing competing energy prices and a calculation based on a $1 per Watt PV system. The viable payback periods belonging to the $0.50 competing electricity price and the $1.00 per Watt PV system.

Solar Guys			Competing energy price	
System	**total kWh per day**	**kWh per year**	**$0.05 electricity**	**system cost**
generic	6600	2409000		$6,750,000
	value annual electricity generation	120450		
	Payback (yrs)	56.04 yrs		
System	**total kWh per day**	**kWh per year**	**$0.11 electricity**	**system cost**
generic	6600	2409000		$6,750,000
	value annual electricity generation	264990		
	Payback (yrs)	25.47 yrs		
System	**total kWh per day**	**kWh per year**	**$0.50 electricity**	**system cost**
generic	6600	2409000		$6,750,000
	value annual electricity generation	1204500		
	Payback (yrs)	5.6 yrs		
System	**total kWh per day**	**kWh per year**	**$0.11 electricity**	**system cost**
generic	6600	2409000		$1, 500,000
	value annual electricity generation	264990		
	Payback (yrs)	5.66 yrs		

3.1.1 Wind Turbines

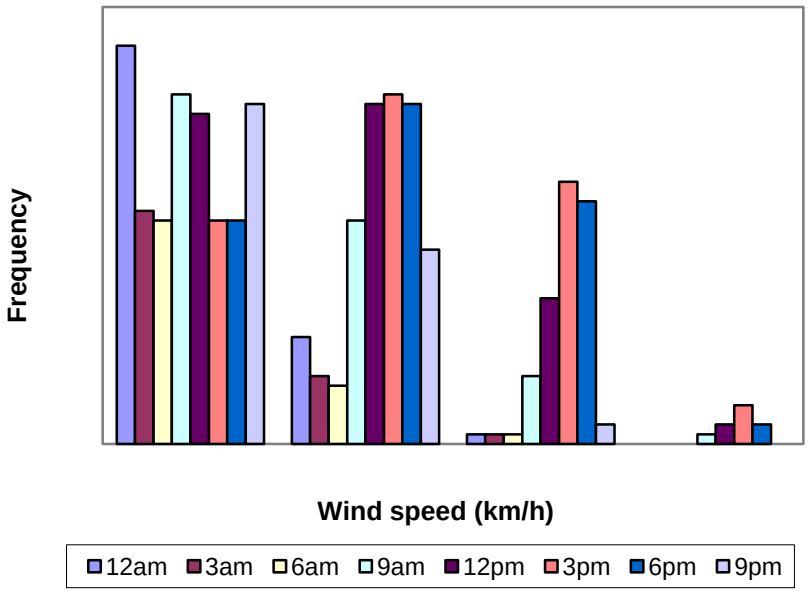

Figure 15 - A histogram demonstrating the frequency of wind speeds for Amberley air base using data obtained from the Bureau of Meteorology spanning from June 1952 to March 2010. The majority of wind speed falls within the 1 -10 km/h range.

A graph demonstrating the frequency of wind speeds at the Amberley air base is presented in Figure 15. Amberley Air Base is located within sight of CA and therefore, was considered an appropriate source for wind data. The data obtained was from the Bureau of Meteorology. This graph shows that the majority of the wind speed falls between 1 to 10 km/h. Hinrichs and Kleinbach's (2006) method was used to prepare a wind turbine power output profile for Amberley Air Base (and therefore, CA) using the rated wind speed output and rated wind speed for a HUSH wind turbine (rated output for HUSH wind power 5.5m turbine: 20 kW at 15 m/s with cut-in speed 2m/s). Where the power at each wind speed (calculated using the wind

speed-power profile method) is multiplied by the number of hours at that speed per month, and then summed to give the number of kWh produced per month.

To calculate the energy output it was assumed that the times 9am and 3pm represented average wind speed for the site. Therefore, for each 24hr period half the wind speed was calculated for 9am and the other half for 3pm wind speed. Wind speeds below the cut-in speed of 2 m/s were set to 0 as they would produce no output. Table 7 shows the monthly average wind speeds for the site for the years 1941- 2010 and 1981- 2010 (with zeroes added where the wind speed was less than the minimum cut in speed of the turbine). For the final calculation the years 1981-2010 were chosen to represent the data. The amount of kWh per month were then divided by the maximum power output per month of the wind turbine to give a percentage of the actual output to maximum rated output. The month of May shows the lowest output as 10% of the rated power. October shows the highest percentage as 26% of the rated output.

Table 7 - Demonstrates using Hinrichs and Kleinbach's (2006) method for calculating energy output for specific wind turbines. As shown by the figures below the wind turbine will be operating at far below the rated output capacity and thus will be ineffective.

Rated output for HUSH wind power 5.5m turbine: 20 kW at 15 m/s							
	Mean wind speed for Amberley (km/h)						
	Jan	**Feb**	**Mar**	**Apr**	**May**	**Jun**	**Years**
9am	8.8	8.4	7.9	6.1	5.2	5.5	1941-2010
3pm	16.5	15.1	14.3	12.3	11.1	12	1941-2010
9am	8.7	8.5	8.8	6.9	5.6	5.7	1981-2010
3pm	16.1	15	14.7	12.8	11.1	12.1	1981-2010
	No. kW per hour						
9am	3.26	3.11	2.93	2.26	1.93	2.04	1941-2010
3pm	6.11	5.59	5.30	4.56	4.11	4.44	1941-2010
9am	3.22	3.15	3.26	2.56	2.07	2.11	1981-2010
3pm	5.96	5.56	5.44	4.74	4.11	4.48	1981-2010
Assuming average wind speed is the average of the 9am and 3pm values.							
	Avg. per month using 1981-2010 data						
	38.67	37.78	39.11	30.67	24.89	25.33	
	71.56	66.67	65.33	56.89	49.33	53.78	
total kWh per day	110.22	104.44	104.44	87.56	74.22	79.11	
total kWh per month	3416.89	2924.44	3237.78	2626.67	2300.89	2373.33	
	max output						
20kW for 24hrs	480	480	480	480	480	480	
times days a month	14880	13440	14880	14400	14880	14400	
ratio of kWh per month	0.23	0.22	0.22	0.18	0.15	0.16	
%	22.96	21.76	21.76	18.24	15.46	16.48	

	Jul	Aug	Sep	Oct	Nov	Dec	Years
9am	5.3	5.8	7.4	8.5	9.2	8.6	1941-2010
3pm	12.6	13.8	15.8	17.9	17.9	17.6	1941-2010
9am	5.9	6.4	8.2	9.1	10	9.1	1981-2010
3pm	13.1	14.3	16.7	18.3	17.8	17.4	1981-2010
9am	1.96	2.15	2.74	3.15	3.41	3.19	1941-2010
3pm	4.67	5.11	5.85	6.63	6.63	6.52	1941-2010
9am	2.19	2.37	3.04	3.37	3.70	3.37	1981-2010
3pm	4.85	5.30	6.19	6.78	6.59	6.44	1981-2010
Assuming average wind speed is the average of the 9am and 3pm values.							
	26.22	28.44	36.44	40.44	44.44	40.44	
	58.22	63.56	74.22	81.33	79.11	77.33	
total kWh per day	84.44	92.00	110.67	121.78	123.56	117.78	
total kWh per month	2617.78	2852.00	3320.00	3775.11	3706.67	3651.11	
20kW for 24hrs	480	480	480	480	480	480	
times days a month	14880	14880	14400	14400	14400	14880	
ratio of kWh per month	0.18	0.19	0.23	0.26	0.26	0.25	
%	17.59	19.17	23.06	26.22	25.74	24.54	

Another method to visualise the expected output for a wind turbine is to prepare a speed-power graph and superimpose on it the sites' actual wind speed. Figure 16 demonstrates the Amberley air base wind speeds for 9am and 3pm included on the speed-power graph for a Proven 9m wind turbine. This shows that the site would receive a maximum of roughly 6 kW at their maximum wind speed. The maximum rated speed of 15 kW is not produced at all.

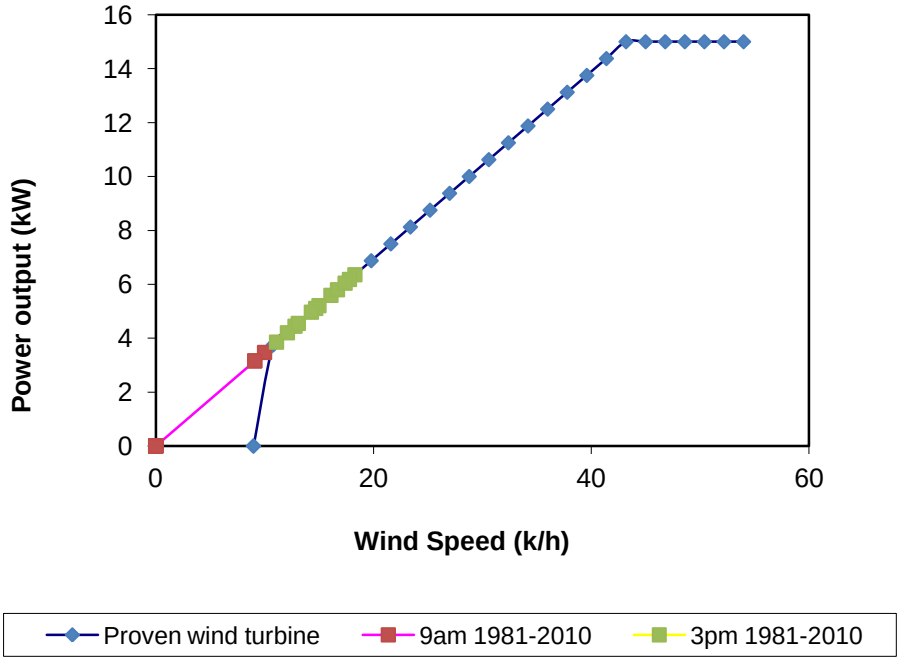

Figure 16- Speed-power graph for a Proven brand (9m) wind turbine with wind speeds and output for Amberley air base shown in pink and yellow. Note the 9am wind speed is below the cut-in speed and therefore is not producing power.

A payback calculation was made for CA using an example wind turbine as representative of the wind turbine industry. Using the power output figures (given by the company) for the annual output as 15000 – 30000 kWh for the Proven 15kW, 9m diameter, 15m high wind turbine and the capital cost of the system ($100 550) the payback period for wind turbines at a competing electricity cost of $0.05 is 67 years. This calculation does not take into account the low wind speed profile of the site which would increase the payback period.

3.1.2 Algae

A number of companies were contacted to attempt to get some quotes for photobioreactors. For example, Global NRG (n.d) advertised that they have produced a closed bioreactor 'design'. They state that "A Green NRG algae farm will consume approximately 500 metric tons of CO_2 per hectare per year" (Global NRG n.d). They claim an average growth rate of 80 grams of algae per metres squared per day, or roughly 25 kg/m^2y, that the algae contains 25% of their weight as oil, and will consume 1.9 times the amount of biomass produced in CO_2 (Global NRG n.d). However, when Global NRG were approached for a quote for one of these bioreactors it was found that these types of bioreactors are not yet available due to suffering from culture crashes and were therefore still in the testing stage (Bartlett, M 2010, pers. Comm., 1 September). Most bioreactors appear to be in pilot stages, large dedicated algal farms exist but there doesn't appear to be smaller scale designs suitable for industry that have moved beyond these pilot studies. Designs are available but their viability needs to be demonstrated through further research and development. Therefore, it was not possible to calculate a payback period for photobioreactors.

Algae grown in abattoir wastewater do seem to offer some promise to the industry. A study done on the use of high rate algal ponds for the treatment of abattoir waste was successful and appears promising (Fallowfield, Cromar & Evans 2001). The study found that abattoir wastewater that had been pre-treated in anaerobic digesters was suitable for the high rate algal ponds. The ponds in conjunction with the anaerobic digester removed 95 – 99% of the BOD, 73 – 80% of the COD, 50 – 60% of the nitrogen, and 14 – 28% of the phosphorous. These removal rates in the wastewater

could help abattoirs in their wastewater treatment while also producing a resalable item in the algae. Unfortunately the Fallowfield, Cromar and Evans (2001) study did not progress to a full scale treatment plant but was successful in showing that abattoir wastewater is suitable to grow algae. So the problem with deciding if algae is a viable renewable energy source lies in the lack of full scale/available/trialled systems.

Chapter 4: Part 1 Renewable Energy Discussion

4.1.0 PV

The payback periods for PV show that they are not currently economically viable for implementation at CA. The payback periods ranged from 24 to 56 years for CA using current PV capital costs and CA's current electricity prices. CA had stipulated that they desired a renewable energy source to have a 5 year payback period to make it economically viable. Therefore, PV is not currently economically viable. However, an economically viable payback period of 5.6 years was calculated using either the capital cost of $1 per watt for a PV system or a competing energy price of $0.50 per kWh. In either of these cases then PV would become economically viable for CA.

A report by IT Power (Franklin et al. 2010) performed case studies at a number of Australian meat processing plants to assess options for renewable energy and energy efficiency. In these case studies plant B most closely resembles CA. Plant B is a beef processing plant with similar kill rates and facilities eg, kill floor, refrigeration, and rendering and with similar energy consumption and electricity costs of less than

$0.10 per kWh. IT Power's study determined that for plant B the payback period for PV would range between 20 – 25 years making PV not viable. Their payback is however consistent with the results of the present study, and their results also support the findings of the current study that rising electricity costs and falling PV capital cost will make PV viable for industry in the near future.

4.1.1 Wind

The wind speed and power output profile for CA demonstrates that wind turbines are not an appropriate technology for CA. The month of May showed the lowest output as 10% of the rated power while October showed the highest percentage as 26% of the rated output. These very low percentages due to low site wind speeds demonstrate that CA would not get even 50% of the rated energy output of a wind turbine, making wind unsuitable for CA as a renewable energy technology. Thus no attempt has been made to include building height and obstacles into the wind speed profile, and the calculations limited to the average wind speed of the site at 9am and 3pm each month. The calculated payback period of 67 years also did not take into account the low wind speed profile of the site, which would further increase the payback period. Wind turbines are clearly not economically viable for CA.

The low output percentages obtained from the calculations demonstrate the hazards of purchasing a wind turbine without preparing a wind speed profile, and assuming that a wind turbine will produce output similar to its rated output for its expected life span. The reality is that in low wind areas wind turbine output performance can drop dramatically and seriously reduce economic viability.

The report by IT Power (Franklin et al. 2010) did a payback calculation for plant B based on a theoretical output for a wind turbine based on a percentage of its rated output. The IT Power calculations showed that wind turbines were not economically viable for plant B due to a payback period of 14 – 95 years. It is noted that such a calculation was not based on the sites' actual wind speed, and so it would not be possible to know whether the site could attain the predicted percentage output.

The basic payback calculations for solar PV and wind demonstrate that these two renewable energy technologies are not currently economically viable for CA, CA is however an appropriate site for PV technology and should become viable in the future. On the other hand, unless there is significant meteorological change at the site or better developed low wind speed wind turbines, wind is not likely to ever become viable for CA.

4.1.2 Algae

Photobioreactors using algae to produce biodiesel do offer great promise as a renewable energy source. Algae produced for the use as biodiesel have many factors that clearly demonstrate the viability of this technology over foodcrop systems for biodiesel production, and help mitigate climate change, especially through carbon capture. While photobioreactors have varying outputs of algae and reactor-specific drawbacks they are at a stage that industries can take advantage of their multi-purpose function, that of producing algae for biodiesel and their added environmental benefits such as CO_2 capture. The cost of algae production for biodiesel is still comparatively high to fossil fuel. However, improvements in photobioreactor design, in combination with molecular engineering, (rising fossil

fuel costs, and rising environmental awareness) will reduce the cost of algal biodiesel, helping to make it become more economical and environmentally benign (Christi 2007).

Biodiesel from algae is a far more practical solution for the replacement of petroleum derived transport fuels than using food crops. It is able to capture carbon, treat wastewater, and uses less area than foodcrops (Patil, Tran & Giselrod 2008). As noted by Sheehan et al. (1998):

> Algal biodiesel is one of the only avenues available for high-volume re-use of CO_2 generated in power plants. It is a technology that marries the potential need for carbon disposal in the electric utility industry with the need for clean-burning alternatives to petroleum in the transportation sector (Sheehan et al. 1998).

Christi (2008) compared the land area required for oil palm and algae to produce the required annual amount of biodiesel to replace the petroleum derived transport fuel for the United States. Based on the rate needed of 0.53 billion m^3 per year of biodiesel the oil palm would need to be grown over an area of 111 million hectares or over 61% of all agricultural cropping land in the United States. Assuming 30% oil content, algae would require 5.4 million hectares or 3% of the agricultural cropping land. This comparison of land use required for oilcrops such as oil palm (one of the most productive oil crops) compared to algae show the unrealistic choice of land crops for biodiesel production. Algae are also not in competition with food stocks. Reijnders (2009) states that the shortfall in food and fodder production that takes place when European wheat is diverted to the production of ethanol can lead to

expanding crop production elsewhere, which can result in land clearing, and which adds to environmental damage and climate change and to rising food prices.

Through the process of photosynthesis, algae are able to capture carbon from the atmosphere. In a study done by Miron et al. (2003) it was found that the elemental composition of an algal biomass was 49.2 % and was contained mostly in carbohydrates and lipids. The carbon was from photosynthesis fixation of CO_2 and the rate of carbon fixation was 2.5 mg C per litre per hour. Christi (2008) therefore states that algal biomass fixes 183 tons of CO_2 when 100 tons of biomass are produced. Tests done by CK Environmental showed that over seven days the photobioreactors reduced nitrogen oxide emissions by 85% and CO_2 emissions by 82% on sunny days and about 50% each on very cloudy days (Davidson 2006). Thus photobioreactors can be used to remove CO_2 from flue gases and reduce green house gas emissions (Patil, Tran & Giselrod 2008).

Waste water treatment can be economically and technically demanding. Therefore using wastewater as the nutrient source for the bioreactors increases the environmental and economical benefits. Algae can effectively remove heavy metals, nitrogen, and phosphorus from aqueous solutions (Patil, Tran & Giselrod 2008).

A benefit of biodiesel is that it can be stored and transported using existing diesel tanks and equipment. As it is oxygenated biodiesel is also more of a lubricant than diesel and is combusted more completely, thus increasing the life of engines. Biodiesel also has a higher flash point than diesel, making it safer to use, handle and store, and it has a low emission profile (Vasudevan & Briggs 2008).

Dedicated algal farms for biodiesel do look likely to be a viable market option. However, for CA, algae for biodiesel production is not viable. Three litres of algae are needed to produce 1 litre of biodiesel (assuming algal oil content of 30%). This would equate to 135 000L of algae needing to be produced at CA each year to cover their current diesel usage. Assuming that a photobioreactor will produce 25 kg/m^2/year as given by Global energy (n.d) then CA would need an area of 5400 m^2 to produce enough algae to cover their diesel usage. Thus a large scale plant is required for the production of algae for the purpose of creating biodiesel and therefore, algae for the production of biodiesel does not appear currently feasible for CA. However, algae to treat wastewater and produce methane may be a viable solution for CA.

Part 1 of the feasibility study of renewable energy for CA shows that of the top three renewables studied there are none that are currently viable for immediate implementation. With changing electricity prices and dropping PV capital cost PV should be viable in the (near) future. Wind turbine energy shows little hope of ever becoming viable due to the lack of high wind speed at the site. Algae for use other than biodiesel shows some promise, but further feasibility studies need to be done.

Chapter 5: Part 2 – The viability of paunch for use as a Biofuel

5.1.0 Paunch literature review

During the 1970s and early 80s a number of studies were published regarding the benefits of drying paunch, although research on this topic has decreased until now. One of the first people to suggest that paunch be dried for beneficial uses (as a feed additive) was Baumann (1971), due to his research into reducing water pollution caused by blood and paunch. Baumann (1971) made recommendations to the beef processing industry that all abattoirs should install dehydrators for both blood and paunch. The abattoir where the study was conducted slaughtered 1,368 head of cattle per day, and a gas-fired dehydrator was run for 6 months to produce 588 tons of dried paunch in 1,260 hrs (Baumann 1971). Converting these numbers to their metric equivalent gives:

$$\frac{533.42\ tonne\ dry\ paunch}{52.5\ days\ (\text{assuming 24hr per day dehydration})} = 10.2\frac{tonne\ dry\ paunch}{day}$$

The costs calculated in 1971 were $38.46 USD dehydration cost/ton (Baumann 1971). Using an inflation calculator this would equate to $204.70 USD in 2010 (Friedman n.d). While the output rate of 10.2 tonne of dry paunch produced per day is an excellent rate for drying paunch the cost is more than double the cost of 1 tonne of coal ($100) which would be the competing fossil fuel. Solar drying of the paunch could reduce the dehydration costs per tonne making it a more cost competitive product. If an economically viable method exists for drying paunch today, then Baumann's recommendation of 1971 should still stand.

In an attempt to reduce environmental damage and financial burdens at abattoirs eds Witherow and Scaief (1976) identified numerous methods for handling paunch. The methods with the most potential and interest for this report are:

1. *Lagooning or stockpiling*

   Stockpiling relies on evaporation and moisture transference to soil or land. This method showed that it is possible to lower the moisture content by 2 to 5 % in a few hours and by 65% over a few weeks. Paunch has a high BOD which prevents it from being allowed to enter surface or ground water thus, presenting drainage issues (eds Witherow & Scaief 1976). However, there is also a large odour problem associated with this method as well as flies, rain, and drainage problems.

2. *Rotary dryers* (Baumann as cited in eds Witherow & Scaief 1976)

   See the previous discussion (Baumann 1971) regarding gas fired dehydrators.

3. *Solar & air drying*

   Yin and Farmer (as cited in eds Witherow & Scaief 1976) successfully used air drying to dry paunch to 16 to 20 % moisture content in a week. They turned a 10 cm layer of paunch daily to stop a crust forming along the top. Paunch forms an outer crust that acts to seal the paunch and significantly reduce the migration of moisture from the interior (De Baerdemaeker & Horsfield 1976, cited by Farmer, Farouk, Brusewitz 1980). This can be seen at CA as the paunch left in the sun develops a dry crust that insulates the

interior and prevents further drying. Therefore, paunch agitation is an important factor in drying. Also of note is that paunch starts to compost after 24 hrs (Spence, M 2010, pers. Comm., 19 April). Other problems encountered with Yin and Farmers' study were rain rewetting the paunch through the open sides of the drying shed, fly and odour problems. They dealt with these problems through the building of a solar still with mechanical agitation as opposed to hand stirring of the paunch (eds Witherow & Scaief 1976).

4. *Presses*

Presses are any mechanical means used to dewater paunch. Paunch has a tendency to clog a wide range of presses but in eds Witherow and Scaief (1976) report it was determined that screw presses were the most suitable for dewatering paunch. This has remained true as many abattoirs currently use screw presses to dewater the paunch and separate the liquid from the solid paunch waste stream.

5. *Incineration*

A number of incineration designs were suggested but only one appears to have been completed. Of note from these reports is that paunch incineration is self-sustaining when the solids content is over 30 % (eds Witherow & Scaief 1976).

6. *Pyrolysis*

   A pyrolysis study was done using steer manure and the outcome of the report suggests that paunch would be a suitable candidate for pyrolysis if there was a suitable market for the by-products (eds Witherow & Scaief 1976).

Editors Witherow and Scaief (1976) demonstrated that there are a number of paunch handling techniques that could be incorporated into an abattoir and that, if dried, paunch could be used as a beneficial biofuel.

Ricci (1977) set about to design and demonstrate a fluidized bed incineration system to handle the paunch waste stream produced by (beef) abattoirs. The design had two separate dewatering systems in place to handle the coarse and fine particles contained in the paunch. These streams then passed into a settler and/or filter before entering the incinerator. The two stage dewatering system was developed due to the poor filtration rates and dewatering characteristics of the paunch in filtration and compressibility testing. Simple and pressure dewatering was then investigated with the solids concentration increasing to a maximum of 27% by being fed between rollers. From these studies it was suggested that a modified screw press be used as the primary dewaterer to separate the streams before passing into a second dewaterer and filter or settler and filter combination. This design was produced for an Illinois company and was prompted due to the cost of using Chicago's sewerage system. At the time of printing (Ricci 1977) it was implied that this design would proceed and results in the implementation be presented in a subsequent report. Data are not

readily available to indicate whether this study was successful or would be economically viable in today's market.

A study by Farmer, Brusewitz and Moustafa (1979) identified that solar dried paunch has the potential to become a fuel source for abattoirs. They modified a simple solar still design to test their hypotheses on drying paunch with a solar still type design. Their results suggest that;

- 'An open mesh tray bottom significantly increases the drying rate.
- Breaking of the crust on the second or third day increases the condensate production rate. Continued stirring on subsequent days is not necessary.
- Covering the dryer at night extends drying later into the evening.
- Forced air circulation had negligible effect for dryers of this size
- Output from the double length dryer was twice that of the standard length dryer. Although the average moisture content was similar, the variability was greater in the double – length dryer (Farmer, Brusewitz & Moustafa 1979, p 224)'.

Additional information contained in the above study includes:

- The removal of surface moisture by pressing was easiest for high forage rationed (grass fed) cattle as this moisture was of low viscosity. Whereas high concentrate ration (grain fed) cattle moisture was more viscous and therefore harder to remove.
- Pre-frozen paunch delays the drying rate by a minimum of 2 days.

- The paunch temperature lagged the internal temperature of the dryer by about 1 to 2 hrs during the afternoon.
- Condensate was still produced 3 to 4 hrs after dusk.
- A relationship between ambient temperature and humidity and the internal temperature of the dryer needs to be determined.
- The drying time was increased by 10 to 12 days if the crust was not agitated during drying (Farmer, Brusewitz & Moustafa 1979).

These results from the Farmer, Brusewitz and Moustafa (1979) study can benefit future efforts into paunch drying, as their conclusions should be applicable to all types of solar dryers, and not just modified solar still designs.

Griffith and Brusewitz (1980) performed a study using a tunnel dryer to determine a drying constant as a function of air relative humidity, material depth, and time after slaughter in order to optimise paunch moisture reduction. This drying constant characterises the rate of drying by combining all the transport properties of drying (i.e. thermal conductivity, moisture diffusivity, interface heat, and mass transfer coefficient) into a simple exponential function (Mujumdar 2007). Drying constants are applicable to constant air conditions and are themselves a function of moisture content, material temperature and thickness, air humidity, temperature, and velocity (Mujumdar 2007). To obtain a drying constant Griffith and Brusewitz (1980) used a set temperature of 35°C with varying relative humidity at 20%, 50%, and 80%. Their study found that paunch composition (i.e. grass or grain fed) had the greatest effect on drying rates compared to humidity, age, or depth. These authors found that the drying time for a high concentrate ration feed was five times higher than that for a

high forage diet. There was also an age - humidity relationship for medium to high humidity and fastest drying occurred at low humidity and shallow depth. Griffith and Brusewitz's (1980) data suggests that there is no effect on the drying rate for depths of 2cm to 10cm. However, they only used solid wall drying pans which therefore restricted the flow of moisture transfer to the upward direction. Older paunch can also reduce the drying constant along with high humidity. It was found that all drying constants were high for humidities up to 20%.

The drying constant, k, determined in this study was determined using the drying equation for an unsaturated surface:

$$MR = M_i e^{-kt};$$

Where *MR* is the moisture ratio, M_i is the initial moisture ratio, k is the drying constant, and t is time (Henderson & Perry, cited in Griffith & Brusewitz 1980, p. 1016). The moisture ratio was used to compare samples with different initial moisture content and was calculated by:

$$MR = \frac{(M - M_e)}{(M_i - M_e)};$$

Where *MR* is the moisture ratio, *M* is the moisture content, M_e is the equilibrium moisture content, M_i is the initial moisture content (Griffith & Brusewitz 1980).

Griffith and Brusewitz's (1980) preliminary drying constant for paunch ranged from 0.005 – 0.108 per hour and was most affected by paunch content as opposed to the drying conditions. There then appears to be a number of typographical errors in their paper regarding the main experiments' drying constants. In the main body of the text they state that the average drying constant is 1.17 (per hour) with a standard deviation of 0.41. However, this average is from the average of the data contained in table 2 of their results, which instead gives an average of 1.17×10^2 per hour with a

range between 0.47 - 2.21× 10^{2} per hour. In addition, Griffith and Brusewitz's (1980) figure 3 is an example of run# 2 in their table. When the data contained in this figure are analysed it shows a slope of -0.0114 per hour. Further examination of the drying constants in their figures 4, 5, and 6 shows the drying constant ranges from approximately 0.005 to 0.022 per hour. Therefore, it appears that their drying average is 1.17× 10^{-2} per hour for the main experiment. It is also unclear as to whether their figure of 0.108 per hour is correct for the preliminary experiment. This rate is much higher than would be expected for the drying conditions and when compared to the rates found in their main experiment.

It is interesting to note the range of more than an order of magnitude in the drying constant values provided by Griffith and Brusewitz (1980). This indicates that paunch is highly susceptible to internal and external conditions that either help or hinder the drying process. As expected the drying constant is thus only applicable to certain conditions.

Farmer, Farouk, and Brusewitz (1980) using direct solar energy and solar-regenerated desiccant for low-insolation days found that they could reduce paunch moisture from 80% to 30% in 5 days. The dryer was designed to operate independently as a modified solar still on high insolation days or in conjunction with the desiccant during low insolation days. This study was noteworthy due to the size of the dryer (pilot-plant size as opposed to laboratory studies) and an innovative concentrating solar air collector. The concentrating solar air collector (Figure 17) was 1.10 m × 1.75 m, adjusted to remain perpendicular to incoming solar radiation, and Farmer, Farouk, and Brusewitz (1980) claim that it produced equivalent energy

compared to a 1.5 times larger flat plate collector. Also of note from this study are the following results:

- Internal dryer temperature reached its maximum between 2 – 3pm,
- Drying without using the desiccant was slow with an average daily moisture removal rate of 30%,
- More uniform moisture distributions were achieved by using desiccant and forced convective air,
- Drying averaged out over 24 hr period showed a constant rate drying period with the falling rate period of little importance as it could be averaged into the constant period,
- Although the drying to 30% in 5 days occurred using the combined direct solar radiation and desiccant night drying it would be possible to obtain the same result in regions of higher insolation.

This dryer design was again a modified solar still design. It would be interesting to determine if a faster drying rate could be obtained using a different type of solar dryer. However, Farmer, Farouk, and Brusewitz's (1980) results shows that it is possible using a pilot-plant sized dryer to dry paunch in 5 days.

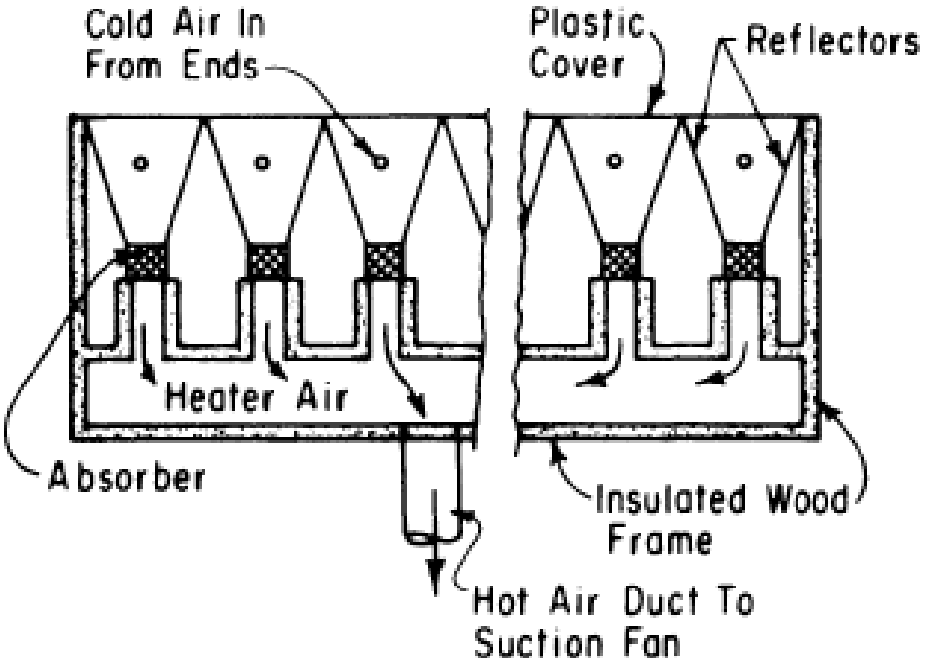

Figure 17 -The concentrating solar air collector was 1.10 m × 1.75 m, adjusted to remain perpendicular to incoming solar radiation and produced energy equivalent to a 1.5 times larger flat plate collector (Farmer, Farouk, and Brusewitz 1980)

Brusewitz, Moustafa and Farmer (1981) claim that pneumatic dewatering of paunch to remove loosely held moisture could be done with less energy and in a fraction of the time compared to evaporation techniques. Their study showed that dewatering soon after slaughter removed the most amount of liquid and that storage at low temperatures (10°C) resulted in 10 to 50% less water being removed. They also found that larger mesh sizes did not increase the amount of solids in the expressed liquid and that small mesh sizes still allowed the liquid to be expressed for up to an hour and did not need mesh cleaning between trials. Farmer, Farouk, and Brusewitz (1980) showed that the fastest expressed liquid removal rate was for 40 mesh (0.400mm wide openings), 20 mesh (0.841mm wide openings), and 16 round-hole screens and that they could dewater paunch to 10% moisture content in maximum time of 16.5 min with 20 kPa and 40 mesh size. They also suggested that a possible

way of dewatering paunch would be by using the positive pressure created by using a column of paunch as the creator of its own positive pressure. The weight of the paunch would press down, enabling it to dewater itself of some of its surface moisture.

Bridle (2010) undertook a desktop study to review waste pyrolysis using paunch and DAF sludge (DAF sludge is fat and protein, meat slivers and fat, that gets into the wash water). The study identified that there are potential economic and environmental benefits using abattoir waste for pyrolysis or gasification. However, the report showed that the paunch and DAF sludge would need to be dried to 20% moisture content (80% total solids) or below prior to being used as moisture contents higher than this would require a much higher energy from the pyrolyser and produce poor quality syngas, thus rendering it uneconomical.

After the previous desktop study Bridle (2011) undertook to design a programme to dry, characterise, and use paunch and DAF sludge in two systems; Pacific Pyrolysis, and BiGchar gasification. He also undertook a desktop review on the use of paunch and DAF sludge in abattoir boilers. The study predicts that pyrolysis and gasification are the most attractive for the meat industry with possible gains of GHG credits up to 1 tonne CO_{2e} and net energy credits up to 3.2 GJ per tonne of feedstock. However, he claims that thermally dried paunch and DAF sludge is not economically viable for co-combustion in boilers, whereas dewatered paunch is viable for co-combustion due to some environmental benefits and as a disposal method.

The process to dry the paunch for the two system tests and for use in the desktop study was done by spreading 2 to 3 m^2 (estimated 1350 kg wet weight) of paunch was over an area of 25 m^2 at a depth of 10 to 15 cm and sun dried over a period of two weeks. The area was increased to 50 m^2 after the first week and the paunch was hand stirred twice a day. The evaporation rate was determined to be 2.1 kg water per day which Bridle (2011) claims is half the typical drying rate of a solar dryer. The calculated final weight of the dried paunch was 270 kg. Analysis of data taken from these samples showed that paunch has a reasonable (dry) gross calorific value of 18.74 MJ/kg.

The desktop study for co-combustion examined current boiler practices, possible problems, and economics associated with using abattoir waste mixed with coal in the boilers. It was noted that solid waste material is only suitable for solid-fuel fired boilers and not liquid or gas fired boilers. It was shown that abattoir waste could create about a quarter of the energy needed for boiler operations. Problems that were identified in the Bridle study were;

- Potential clogging and feed problems due to waste particle size and bulk density,
- Ash fusion/ melting,
- High particulate carry-over,
- Increased corrosion.

The economic factor that made co-combustion unattractive was the high cost associated with drying the paunch. However, this was based on the cost and maintenance of a fossil-fuel run dryer. The dewatered paunch approach as a waste disposal system was economically attractive due to paunch only needing a total solid of 30% to burn self-sustainingly. This is around the total solid count from

dewatering systems such as a screw press. However, this method was only suggested for use as a waste disposal method with little or no energy recovered.

Bridle (2011) then undertook an assessment of dewatered paunch for use in a co-combustion boiler. The results of this study show great promise for paunch waste to be used in co-combustion with a net economic benefit of $1.58 million over 20 years for use in existing boilers and a net economic benefit of $2.85 million over 20 years for a new boiler able to co-fire biomass. Paunch could provide 30% of boiler fuel requirements with potential for GHG credits. There were minor environmental impacts and no impact on boiler combustion performance (at 5% paunch rate with total solids of 30%). The environmental impact of increased stack emissions remained within regulatory guidelines.

Paunch needs to be dried cost effectively to be used as a biofuel. Horsfield (1973) did a calculation on the cost to use fossil fuel to dry pig manure based on the amount of manure produced per pig and the latent heat of vaporization for water. This calculation can easily be modified for paunch. One cow produces approximately 25 kg of paunch at 85% moisture content, Therefore, 21.2 kg of water needs to be removed to produce 3.8 kg dry weight. If the latent heat of water is 2260 kJ/kg then 47912 kJ is needed to remove the water. If diesel costs $1.50 per litre (BP Australia 2010) and has an energy content of 38 MJ/L (BP Australia 2010) then it would cost $1.95 per head of cattle to dry its paunch using a fossil fuel. This is unfeasible as it would cost on a daily basis $195 if only 100 head of cattle were processed each day. On a yearly basis this cost would equate to more than is currently spent on coal

(which paunch would possibly be replacing). Therefore, to enable paunch to be used as a biofuel, a cheaper method of drying is needed.

5.1.1 Concluding remarks regarding this review of literature

The studies discussed here have helped our understanding of the factors involved in drying paunch. They also demonstrate a common theme that paunch needs to be dried before it can become a useful biofuel. Thus a method needs to be developed to dry paunch quickly and easily as well as cheaply as possible (for example a 5-day drying time would create a backlog of wet paunch due to the large amount of paunch produced weekly at CA). In the present study the properties of drying paunch are investigated through laboratory tests to determine optimum factors for fastest drying times and test the idea that solar drying of paunch is likely to lead to a viable source of biofuels for abattoirs such as CA.

5.2.0 Paunch Methods

In the second part of the present study organic waste streams, meat and bone meal, tallow, and paunch have all been investigated in search for a viable renewable energy source. Of these, dried paunch was identified as a potential renewable energy fuel for boilers, or for pyrolysis. The focus of the study then turned to the drying properties of paunch, to determine if paunch could be dried quickly to create an economically viable fuel source.

5.2.1 The Meteorological conditions at CA

For paunch (for use as a biofuel) to become an economically viable choice for abattoirs it needs to be dried cheaply and quickly. The simplest method for reducing the drying costs is to use a "free" energy source such as the sun. The Sun is our own nuclear fusion reactor. Under immense temperature and pressure the Sun fuses hydrogen into helium mostly using the proton-proton chain whereby four hydrogen nuclei are used in a series of reactions to produce one helium nucleus. During this process a small proportion of the mass is converted into energy. Solar electromagnetic radiation is emitted from the sun as radiant energy. Electromagnetic radiation ranges from gamma rays (10^{-12}m) to radio waves (10^{4}m) and includes visible light (10^{-7}m). The Sun emits substantial amounts of infrared, ultraviolet, and visible light (Giancoli 1998). In one year the sun produces around ten thousand times more energy than the annual total global energy demand (Quaschning 2007).

The power of electromagnetic radiation incident on a surface, per unit area (Wm^{-2}), is given the term irradiance, I. Irradiance is the total amount of radiation present at all frequencies, and global irradiance is made up of direct, diffuse and reflected radiation. Measurements have shown that the amount of power which falls on each square metre of the Earth's surface is about 1400 watts. That is, each square metre could light 14 standard 100W light bulbs (Jefferys & Robbins 1981).

Terrestrial solar radiation reaching the earth's surface is influenced by a number of factors. These include:

1. The solar zenith angle or height of the sun above the horizon.
2. The changes annually of the earth-sun distance.
3. The chemistry of the atmosphere.
4. Cloud cover.
5. The albedo of the ground and surroundings.
6. Altitude above sea level.

The solar zenith angle (SZA) affects how much of the atmosphere the solar radiation is passing through. The higher the sun is in the sky the smaller the SZA, meaning that the radiation has less atmosphere to travel through before reaching the Earth's surface and therefore undergoes less atmospheric scattering and absorption. As the SZA increases (the sun is lower in the sky) therefore, the radiation is spread over a larger surface area which thus reduces the direct irradiance.

The SZA is calculated by:

$$SZA = 90^{o} - \text{solar altitude}$$

The solar altitude can be found at: http://aa.usno.navy.mil/data/docs/AltAz.php by entering the appropriate longitude and latitude details (NASA 2008).

The distance between the Earth and sun varies between 1.47×10^{8} km and 1.52×10^{8} km throughout the year, which causes variation in the irradiance between 1325 W/m^2 and 1420 W/m^2. The average value of irradiance is the solar constant I_o = 1,367 ± 2 W/m^2 (Quaschning 2007). Seasonal changes in sunlight are due to the tilt of the

Earth as it spins on its axis as it orbits the sun. The Earth is tilted at an angle of 23.5^{o} to its plane of motion about the sun. This means is that during summer the South Pole is tilted towards the sun and during winter is tilted away from the sun. Conversely the North Pole, during their summer, is tilted towards the sun during the southern hemisphere's winter. Winter months receive less radiation due to the same principle as the solar zenith angle. Due to the tilt the radiation is spread over a larger area and passes through greater depth of atmosphere and thus faces more absorption and scattering (Hinrichs & Kleinbach 2006).

The chemistry of the atmosphere influences the amount of radiation present due to the natural chemistry of the atmosphere and to pollution caused by humans. Mie and Rayleigh scattering are the two forms of scattering due to particles. Mie scattering is due to dust and pollution where the particles are larger than the radiation wavelengths. Rayleigh is due to molecular scattering where the particles are smaller than the radiation wavelengths. The effect of clouds on the radiation is due to Mie scattering and also the reflecting of radiation back into space. Therefore, clouds can reduce (and sometimes increase) the amount of radiation reaching the surface of the earth (Quaschning 2007).

Albedo is the fraction of light hitting a surface that gets reflected away and can be expressed as a ratio of the upwelling irradiance to the downwelling irradiance (Parisi & Kimlin 1997). As shown in:

$$A = \frac{I_r}{I_i};$$

Where A is the albedo, I_r is reflected irradiance and I_i is incoming irradiance (Lenoble 1993).

The Earth has an albedo of 0.39 and therefore reflects 39% of incoming solar radiation back into space and is mostly caused by clouds. To put albedo into perspective; a surface with an albedo of 1 would be perfectly white, it would reflect all incoming radiation, and a surface with an albedo of 0 would be perfectly black, it would absorb all incoming radiation (Seeds 2008). Solar radiation is also affected by altitude above sea level. This again is due to how much of the atmosphere through which the radiation must pass.

Meteorological conditions at CA were investigated to determine its suitability for solar technologies. Solar radiation (insolation) reaching the Earths' surface on average per day ranges between 6.8 MJ/ m^2/d to 23 MJ/m^2/d (Hinrichs & Kleinbach 2006). Ipswich, Australia has on average 18 – 21 MJ/m^2/d (Figure 18) (BOM 2011). The average annual daily sunshine hours for Ipswich are approximately 7 – 8 hours with the monthly averages ranging from 6 – 9 hours, the highest averages being in the periods August through to December (Figure 19) (BOM 2011). This high insolation in conjunction with good average annual daily sunshine hours shows promise for solar technologies.

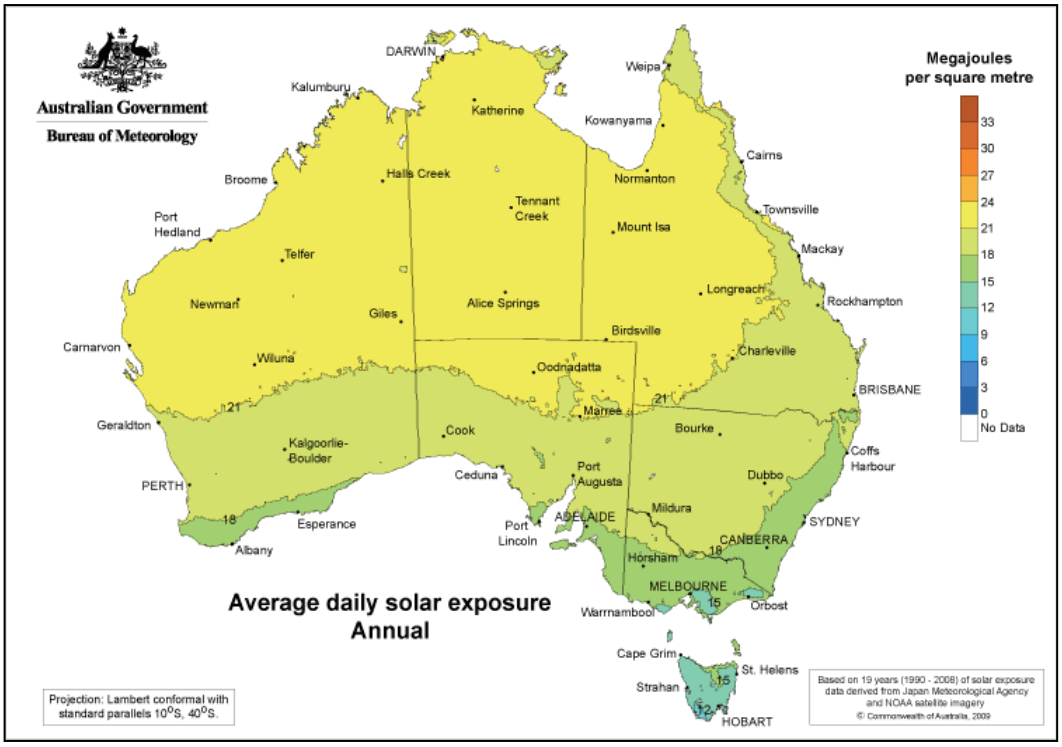

Figure 18 – Shows the annual average daily solar exposure for Australia in MJ/m^2. Ipswich, Australia has on average 18 – 21 MJ/ m^2/d (BOM 2011).

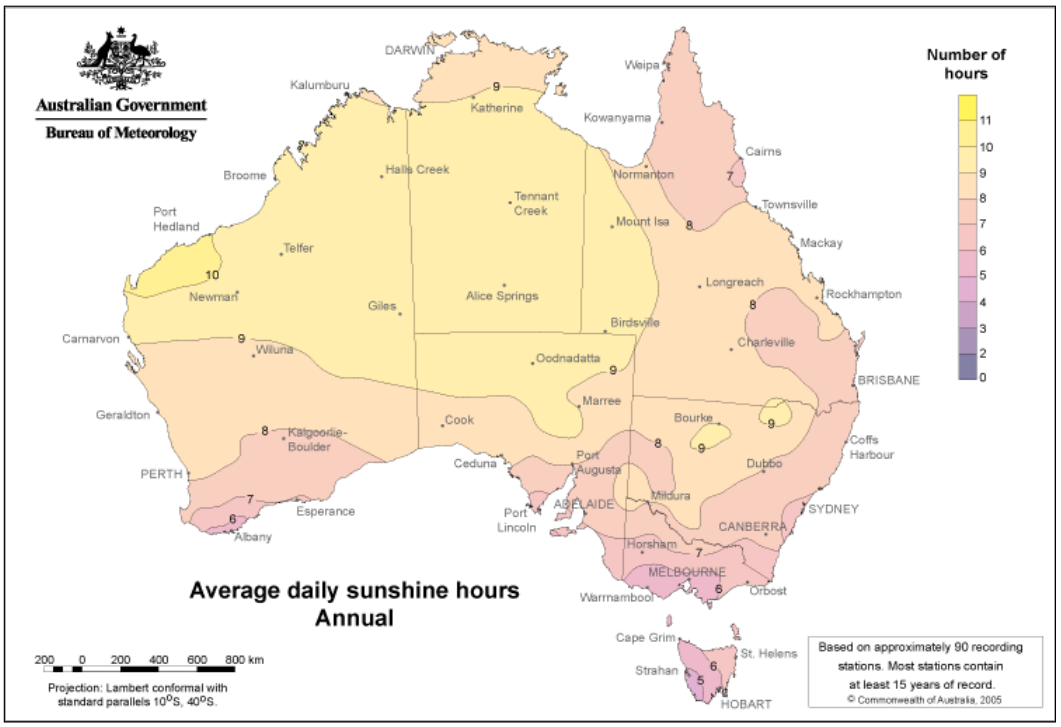

Figure 19 - Shows the Australian annual daily sunshine hours average. Ipswich annually has between 7 to 8 hours of sunshine daily (BOM 2011).

Cloud cover data also suggests that Ipswich is a suitable site for solar technology. Clear, cloudy, and cloud cover data was obtained from the Bureau of Meteorology (2011) for Amberley air base, which is situated within sight of CA. Figure 20 gives a graphical representation of this data. It demonstrates that there are on average more clear days than cloudy from May to October and that there is a large portion of clear days (> 10 days) per month from June to October each year. The mean 3pm cloud cover for those months is less than 4 octas, where 1 octa is equal to 1/8th of the sky being obscured by clouds. Therefore, less than half the sky is obscured by cloud. This means that during periods of lower insolation, such as winter months, there are still a large amount of clear skies. The months with the clearest days that correspond to the longest sunshine hours are August to October.

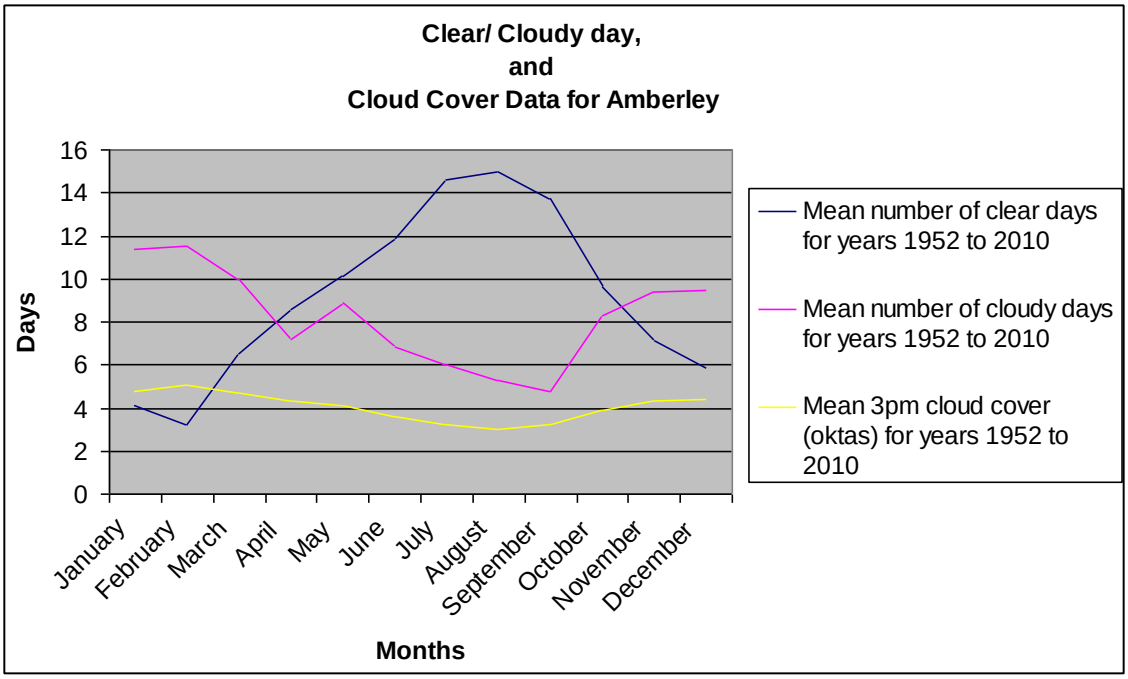

Figure 20- Clear/ cloudy day, and cloud cover data for Amberley. The months of June to October each year show greater than 10 clear days per month (BOM 2011).

Relative humidity (RH) also has an effect on solar drying technologies. Relative humidity is a percentage of how much water is in the air compared to how much water the air can hold. Warmer air can hold more water and therefore, has a lower RH than cooler air (BOM 2011). RH is important when it comes to drying as this ability of air to contain water can limit how fast things can dry as the water acts as a medium to remove moisture. The Ipswich area has a range of RH between 40 – 80 %. As expected the 3pm RH is less than the 9am RH with August and September showing the lowest average RH (Figure 21). The RH can be lessened by an absorber on a solar dryer (due to heating the air), and hence the ambient RH is not as great a meteorological concern as insolation, sunshine hours, and clear days. Therefore, solar technologies would be suitable for use at CA as far as meteorological conditions are concerned due to the large number of clear days combined with the high solar insolation.

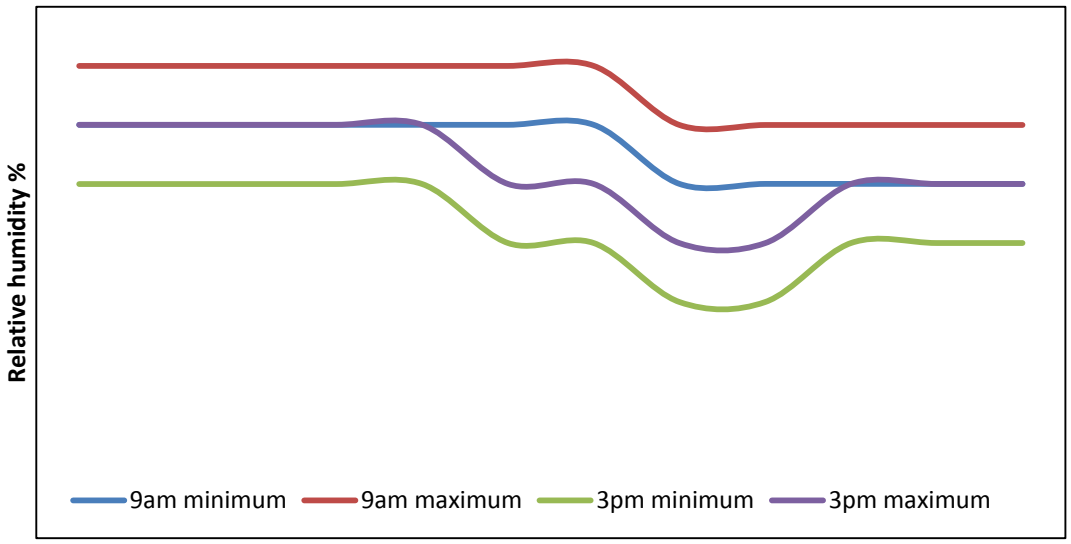

Figure 21– Average maximum and minimum monthly relative humidities, 9am & 3pm, for the greater Brisbane area, Australia (BOM 2011).

5.2.2 Solar drying

The global situation regarding solar drying has been reviewed by Brenndorfer et al. (1985):

> …solar drying is still far from being a widely used technology. Apart, perhaps, from the incorporation of solar collectors into grain drying and storage silos in North America, there is not one instance of widespread and widely acceptable use of solar dryers for the drying of crops and foodstuffs. Although solar drying has received appreciable research interest worldwide in universities and technical institutes this has been mainly in the form of thermodynamic studies, a comparison of sun and solar drying rates, or in very recent years, computer modelling techniques, all performed in an academic environment….Perhaps the principal and most important failing of many projects is a lack of appreciation of the environment for which the dryer is intended. The final design is frequently inappropriate and the subsequent transfer of technology from researcher to end-user is anything but effective….and to some extent, the tendency has been that a dryer is designed and then an application sought (Brenndorfer et al. 1985).

A solar dryer is an enclosed unit that uses solar thermal energy to dry substances as opposed to open air sun drying which as the name suggests is just spreading the substance to be dried out in the sun. There are a number of drawbacks to open air drying such as, the large surface area required to spread the product, possible infestation from insects, the product is exposed to the elements such as rain, possible odour problems, etc. Solar dryers do not face these problems and are also capable of increasing temperature and air movement, and decreasing the RH which not only increases the drying rate but also increases the throughput of the product (e.g. Belessiotis & Delyannis 2010).

Solar dryers can be broadly classified into two groups: passive and active dryers which can be further broken down into three sub-categories (e.g. Weiss & Buchinger n.d, Brenndorfer et al. 1985). In essence, an active solar dryer incorporates a

mechanism such as a fan that requires a source of power (which can be supplied by a PV). In contrast, a passive dryer relies on natural convection to move the air passing over the product, and can run independently of a power supply. The sub-categories for solar dryers are; direct, indirect, and mixed mode type dryers (Weiss & Buchinger n.d). Direct dryers expose the product to be dried directly to the solar radiation, whereas indirect dryers dry the product in the shade. Mixed-mode dryers use both direct and indirect drying modes. Active dryers can improve drying time by up to three times and decrease the size of the solar absorber by 50%, through forced convection. Therefore, active drying shows promise when considering the design of future paunch solar dryers.

Solar drying, e.g. solar tunnel dryers, have been used with success for many years. Solar dryers are typically made up of an absorber, a drying chamber, and an exhaust or ventilation holes. Depending on the design these components may be separate or all part of the one unit. There are numerous solar dryer designs available from simple solar stills (a hole in the ground covered by a weighted clear plastic sheet) to solar tunnel dryers which use a transparent plastic covered flat plate collector and a drying tunnel (with fans) to blow hot air over the item needing drying (Bala & Mondol 2001). The fans in the tunnel dryer can be run by PV panels which have the added benefit of self-regulating the dryer as on high insolation days the fans run faster than on low insolation days (Bala & Mondol 2001). This use of fans and variations on this technique have proved successful for drying fish, fruit, and vegetables.

The absorber component of a solar dryer can elevate ambient air by greater than 40°C. Absorbers also come in a variety of designs with greater or less capacity to

raise the ambient air for example, a double pass flat plate collector passes the incoming air both under then over the absorber, which increases the path length travelled by the air, and thus increasing the absorbers' capacity to increase the air temperature (Brenndorfer et al. 1985). Therefore, solar drying using an active dryer with a suitable absorber appears to be a possible solution to cheaply drying paunch. However, in order to design the optimum solar dryer, the drying properties of paunch need to be understood.

5.2.3 Churchill Abattoir

Cattle paunch was obtained from CA which is an energy intensive medium sized facility and is representative of the Australian meat industry. CA paunch is first dry dumped where the contents are dumped out without the addition of water and then the emptied paunch is umbrella washed. The paunch then passes through a Bauer screw press separator which is situated above a cemented holding area (Figure 22). The screw press dewaters the paunch of most of its surface water, thus separating the liquid from the solid. The resulting liquid waste stream, once separated from the solids, passes to holding ponds. The solids pile is cleared two to three times per week and sent off site to a composting facility. CA make no money from this practice but benefit from the reduction in their National Greenhouse and Energy Reporting (NGER) as paunch is not reportable under NGER if sent off-site Nevertheless, the assumption of non-reportability doesn't take into account CA's net carbon footprint. CA's treatment of paunch is a generally accepted treatment method in Australia.

Figure 22 - Paunch on site at CA passes from the screw press to fall into a pile in the cement holding area.

The use of solar dried paunch nevertheless has the potential to significantly offset CA's energy costs. Approximately 23 – 25 kg of paunch is produced per head of cattle (wet weight) or roughly 3.8 kg dry weight (Ricci 1977, eds Witherow & Scaief 1976, Doyle & Lant 2001). CA produce between 60 – 90 m^3 of paunch per week, which equates to 60 – 90 tonnes per week when wet, or about 15 tonnes dry weight per week. Assuming a 51 week operating year would mean there is potentially 765 tonnes of paunch (dry weight) available to use as a coal substitute. Therefore, it may be possible to reduce CA's coal consumption and gain GHG and energy credits.

5.2.4 Factors that affect drying

Theory predicts how paunch will dry. There are a number of external, general factors that affect paunch drying. These factors can be placed into two groups depending on the different stages of drying. The first stage is evaporation which has a constant drying period and the second is the internal migration of water from the interior which has a falling rate drying period (Brenndorfer et al. 1985). Evaporation from a wet surface (as long as the surface remains wet) can be considered the same as for evaporation from a free water surface and is mostly affected by temperature and humidity (Brenndorfer et al. 1985). This behaviour can be seen in the rate of evaporation, which is proportional to the difference between the saturated vapour pressure of water at the surface and the partial vapour pressure of water in the adjacent air (Brenndorfer et al. 1985). Using Daltons development of evaporation theory we set:

$$E = f(\bar{u})\ (p_s - p_a);$$

Where E is the rate of evaporation, f is a function of the mean wind speed, $\bar{u}$ is mean wind speed, p_s is the saturated vapour pressure at the temperature of the water surface, and p_a is the partial vapour pressure of water in adjacent air.

Daltons' law of partial pressure says that the partial pressure is the sum of the pressures of the individual gases present in the air. The equation for the rate of evaporation shows that temperature and humidity are the largest contributors to the rate. This behaviour rises as the saturated vapour pressure, p_s, increases as temperature increases at constant humidity while the partial vapour pressure, p_a,

increases with humidity at a fixed temperature. Therefore, as the rate is dependent on the difference, $p_s - p_a$, it follows that the evaporation rate will increase with temperature and decrease with increased humidity (Brenndorfer et al. 1985).

Penman also developed an equation for evaporation from an open water source which gives the kilograms of water evaporated every second for each square metre of area:

$$E = \frac{mR_n + \rho_a c_a Dg}{L(m + K_s)};$$

Where m = psychrometric slope, Rn = net irradiance, ρ_a = density of air, c_p = heat capacity of air, g = surface aerodynamic conductance (represents the intensity of the near-surface vertical turbulence that transports heat and moisture), D = saturation deficit, L = latent heat of vaporization, K_s = psychrometric constant. Temperature, relative humidity, and wind speed impact the values of m, g, c_a, ρ_a, and D.

The Penman equation can be reduced to:

$$E = AR_n + B(a+bW)D;$$

Where E is the evaporation rate, R_n, is the net radiation, W is the wind speed, A and B are coefficients that contain physical properties of air and water vapour, and D is the saturation deficit of the air (Mason & Hughes 2001).

The saturation deficit, D, gives the evaporation capability of air and is the difference between the saturation vapour pressure and the vapour pressure of a volume air:

$$D = e_w - e;$$

Where e is the actual vapour pressure for a given volume of air and e_w is the saturation vapour pressure of the volume at a given temperature.

The saturation deficit can also be expressed in terms of the relative humidity (RH):

$$D = e_w(1-\frac{RH}{100});$$

This equation shows that the saturation vapour pressure will thus rise with rising temperature. So the same *RH* will correspond to a greater saturation deficit creating greater evaporation at warmer temperatures.

The reduced Penman equation shown above also demonstrates the factors that influence drying rates. The evaporative rate can be broken into two terms. The radiation term, AR_n, is dependent on the amount of radiation energy available for evaporation. The aerodynamic term, B(a+bW)D, depends on temperature and relative humidity as related to, D, the saturation deficit and wind speed, W. The aerodynamic term contains the factors that control the movement of water vapour and sensible heat away from the evaporative surface. A large D term is generated by hot, dry air and produces greater evaporative rates. The saturation deficit is then related to the wind speed whose effect is also greatest for hot, dry air and therefore a larger contributor to the potential evaporative rate (Mason & Hughes 2001).

The second stage of drying is the internal migration of water from the interior. In this stage temperature and particle size are of most importance. Table 8 shows the two different drying stages and the factors that affect them. For moisture to migrate from the interior there are two underlying principals, diffusion and capillary flow (Brenndorfer et al. 1985). The equation for diffusion of a liquid through a solid tells us that moisture content in time is proportional to a change in moisture gradient and the moisture rate decreases with bigger particle size (Brenndorfer et al. 1985). Therefore, this second drying stage is the limiting factor in drying times, as when there is sufficient moisture (moisture gradient) in the material there is a constant flow of moisture to the surface which is then evaporated. However, once the material starts to dry this rate drops and then tends to zero once equilibrium moisture content has been reached (Brenndorfer et al. 1985).

Table 8 - Factors that affect the two stages of drying

Surface evaporation	**Internal migration**
Temperature; Warmer air > evaporation rate	Temperature is important
More humid < evaporation rate	Humidity not important (apart from where it affects the evaporation from the surface).
Velocity (movement of air) > evaporation rate but the gain is limited above certain velocities	Air velocity is no longer important
Unaffected by particle size of the sample to be dried	Size of particle is important
Heat conduction and radiation of drying chamber can also add to rate	Physical structure of the solid, solid porosity. Moisture content.

Equilibrium is met when the rate of evaporation equals the rate of condensing of a substance. What this means is that due to kinetic energy molecules will leave a substance, and then due to an attracting force, will return. When the amount of molecules leaving the water equal the amount of molecules condensing (or returning) then equilibrium has been reached (Giancoli 1980). Equilibrium moisture content is important in terms of drying in that once it has been reached, no further drying is possible.

Ficks' laws of diffusion tells us that a substance will flow from an area of high concentration to an area of low concentration. His second law tells us how diffusion causes the concentration to change with time:

$$\frac{\partial \emptyset}{\partial t} = D \frac{\partial^2 \emptyset}{\partial x^2};$$

Where $\emptyset$ is the substance concentration, t is time, D is the diffusion coefficient, x is the position or length.

From Ficks' law a general equation for the diffusion of liquid through a porous solid can be generated:

$$\frac{\partial MC}{\partial t} = D \frac{\partial^2 MC}{\partial x^2};$$

In this equation MC is the moisture content, t is time, D is the diffusion coefficient, and x is the distance through the solid (distance from the surface of the particle/solid) (Brenndorfer et al. 1985).

The above equation tells us that if x is big then the rate of change of moisture content over time is small. Therefore, particle size is important, and increasing surface area increases both the evaporative stage and internal migration. The diffusion

coefficient, *D*, increases with increased temperature, thus increasing the rate of change (Brenndorfer et al. 1985).

In some cases where the second stage is predominant, a hard impermeable skin is formed on top of the product. The material is then called casehardened and such behaviour is characteristic of paunch. A possible method for dealing with casehardening is to retard evaporation and keep it in time with the internal migration of moisture from the interior, thus not allowing a crust to form. This improvement could be achieved by increasing the relative
humidity and therefore lowering the evaporative rate, while not affecting the second stage of drying (Mujumdar 2007).

5.2.5 Moisture content

Moisture content is the amount of water contained in the material and is given as a ratio or percentage, where 0 is completely dry, and 1 (or 100%) is completely saturated. The moisture content can be given as a wet or dry moisture basis.

Wet basis is a ratio of the weight of water to the wet weight of the product (Teter 1987) given by:

$$Mw = 100\ \frac{W-D}{W};$$

where *Mw* is the wet basis moisture content percentage, *W* is the wet weight, and *D* is the dry weight.

Dry basis is the ratio of the weight of water to the dry weight of the product (Teter 1987) given by:

$$Md = 100\frac{W-D}{D};$$

where *Md* is the dry basis moisture content percentage, *W* is the wet weight, and *D* is the dry weight.

A useful way to understand and gain insightful knowledge into paunch drying is Farmer, Farouk and Brusewitz's (1980) equation for an average daily drying rate, given by:

$$MC = MC_i - ADR \times T;$$

Where *MC* is the final moisture content, MC_i is the initial moisture content, *ADR* is the average daily drying rate, *T* is time.

This equation was used to graph the change in moisture content versus time in hours to give the average daily drying rate for varying temperatures. This allows calculations to be made regarding the times to dry to certain moisture contents.

Blending wet product with dry product is also a valid way to aid in moisture reduction. The equation for the quantity required for blending is given by (NDSU 2011):

$$Quantity\ required\ for\ blending = \frac{dMC-kMC}{dMC-rMC} \times kQ;$$

Where *dMC* is the desired *MC*, *kMC* is known *MC*, *rMC* is required *MC*, and *kQ* is known quantity. The total product produced at the desired moisture content is the total of the quantity required for blending plus the known quantity.

The equation for the quantity required for blending allows for calculation of blending with another product as well as blending with the same product where one has been dried more than the other. Thorough mixing is required using this method to avoid creating wet spots and warmer temperatures, and aeration will aid in equalizing the moisture content (NDSU 2011).

5.2.6 Experimental equipment

A study was undertaken with the main objective to measure the effect of varying temperature on the drying time of paunch. The experimental equipment for paunch drying comprised of several components:

- Tunnel dryer,
- Ohaus MB45 Moisture Analyser,
- Psychrometer,
- Remmington hot air blower,
- Davis instruments Turbo Meter (wind speed indicator),
- Digital thermometer.

The design of the tunnel dryer was similar to Griffith and Brusewitz's (1980) design and can be seen in figures 23 and 24. In their design they passed heated air over their

samples which were contained in solid wall drying pans. They measured air temperature, humidity and dew point before and after the samples. In the current study the tunnel dryer had a heat source at the entry which blew hot air over the samples. The sample was situated in the centre of the box at a depth of 2.5cm, Figure 24. The paunch was enclosed on all sides except the top which allowed the air to pass over the sample. Therefore, drying was restricted to the upward direction. The psychrometer was placed into a resealable hole in the box lid to enable entry air temperature and relative humidity measurements to be taken. Another reading was done on the outside of the exit air vent to determine the temperature and relative humidity leaving the box. Thermocouples and alcohol thermometers were also placed at these locations as a backup means of measuring the temperature (refer to appendix 2).

The dimensions of the tunnel dryer were 1.055m x 0.2m x 0.21m. As air can be considered a fluid it is possible to calculate the volumetric flow rate (volume of fluid passing a point in the system per unit time) of the air passing over the paunch. The volumetric flow rate (airflow rate) for inside the box is calculated by:

$$Volumetric\ flow\ rate = airflow\ \frac{m}{s} \times cross\ sectional\ area\ m^2;$$

The cross sectional area is the area perpendicular to the flow rate. Therefore, the cross sectional area is the width times the depth of the box, 0.042m^2.

The volumetric flow rate for each temperature is:

- 41°C volumetric flow rate = 0.45m^3s^{-1}
- 55°C volumetric flow rate = 0.38m^3s^{-1}
- 72°C volumetric flow rate = 0.39m^3s^{-1}

This volumetric flow rate will allow fan power calculations to be made for future dryer designs if the new design is to match the experimental conditions achieved in the lab scale tunnel dryer.

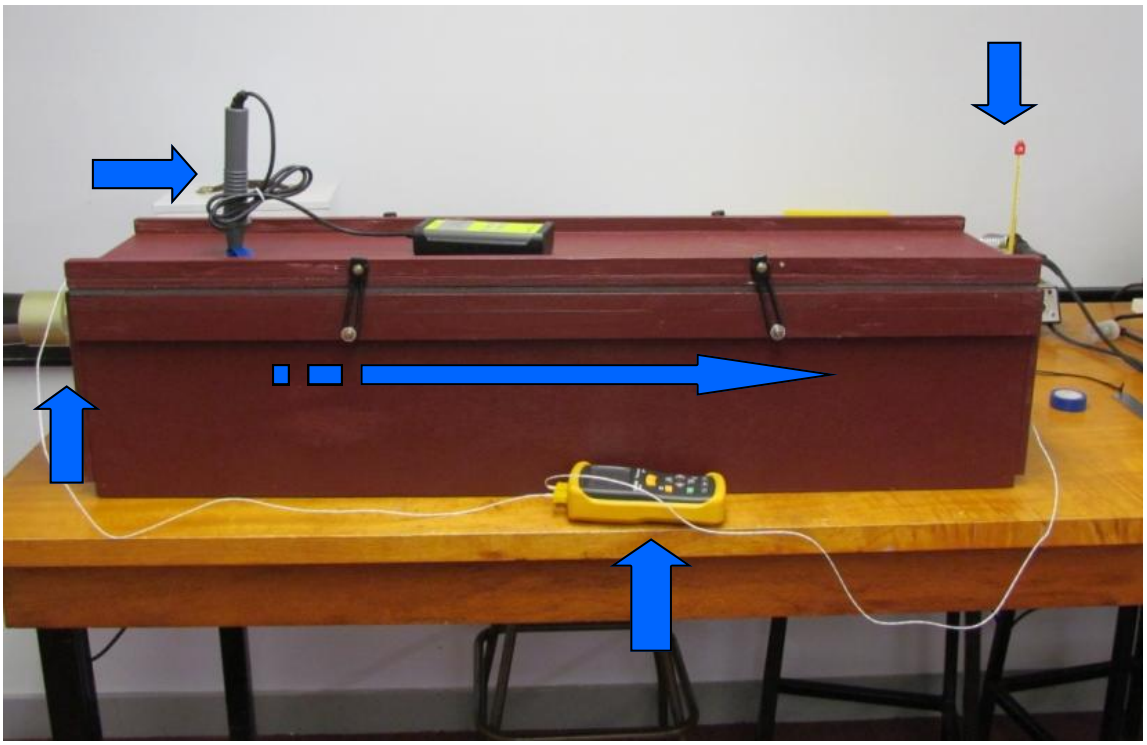

Figure 23 - Tunnel dryer; hot air passes from the entry at left, over the paunch and out the air vent at the end on the right.

Figure 24- Paunch inside the tunnel dryer.

The moisture contents were measured using an OHAUS MB45 moisture analyser (Figure 25). The moisture analyser was used to measure initial and final moisture contents for each experimental run. The drying profile for the analyser was a step profile, with step 1 set at 200°C for 7 min, step 2 set at 150°C for 1 min, and step 3 set at 105°C for 37 min, for a total run time of 45 min. This profile was based on the operation manuals' suggested setting for wet vegetables and tested for repeatability for paunch. This operating profile produced dry weight without burning (or overly browning) the paunch.

Figure 25 –The Ohaus MB45 moisture balance.

5.2.7 Experimental procedure

The collection of data on paunch drying was done on-site at CA. Paunch samples were collected as the paunch passed out of the screw press and therefore, all samples were less than a day old. The maximum age of paunch on-site at CA is 2 – 3 days before removal off-site. The three temperature settings were chosen to represent possible solar dryer operating temperatures. 41°C was picked as the lowest setting as CA has fairly high daily insolation and 40°C would be fairly easy to achieve with a solar dryer. The maximum temperature was picked as a good solar absorber can raise ambient temperature by 30°C quite easily. The initial moisture content of the paunch was measured in the moisture balance before being placed inside the tunnel dryer. The temperature and humidity inside the entry and outside the exit were taken at

half-hour intervals for each sample run. The initial runs at each temperature setting were done for 1, 2, 3, 4, and 5 hours. At the end of each run the final moisture content was measured by the moisture balance. All relative humidities were below 10% based on Griffith and Brusewitz (1980) results that suggest that fastest drying times for paunch occur at relative humidities below 20%. This was a reasonable factor as the temperature of the heated air naturally produced relative humidities below 20%, except for the lowest temperature setting of 41°C entry air, which had humidities above 20% (but below 40%). Multiple initial and final moisture contents were taken and the average values graphed. After the data were analysed it was decided to run another set of tests for periods of time greater than 5 hours to test the experimental average drying rates (ADRs). The second set of tests were run up to 12 hrs for 72°C entry air, up to 14 hrs for 55°C entry air, and up to 16 hrs for 41°C entry air.

Chapter 6: Part 2 – Paunch Results

6.1.0 Operating temperature inside tunnel dryer

The operating temperature and relative humidity of the tunnel dryer were measured at half-hour intervals inside the box at the entry and at the exit via the exhaust hole. Figures 26 and 27 are examples and demonstrate the variation between entry and exit and start up time. As expected, the temperature dropped at the exit due to heat loss/ transfer inside the box, and humidity increased at the exit due to air picking up moisture (evaporation) from passing over the paunch. Temperature and RH generally reached a steady operating range within an hour of start-up. Measurements were carried out on hot, cold, and rainy days. However, the operating temperature and humidity remained largely consistent for and between each run. Most variation was seen on days with high humidity (rainy days), and this can be seen in figure 27 at approximately two and a half hours, where there is a slight rise in RH due to an onset of rain which increased the ambient RH. Variations in operating conditions for the experiment between runs remained small in all cases.

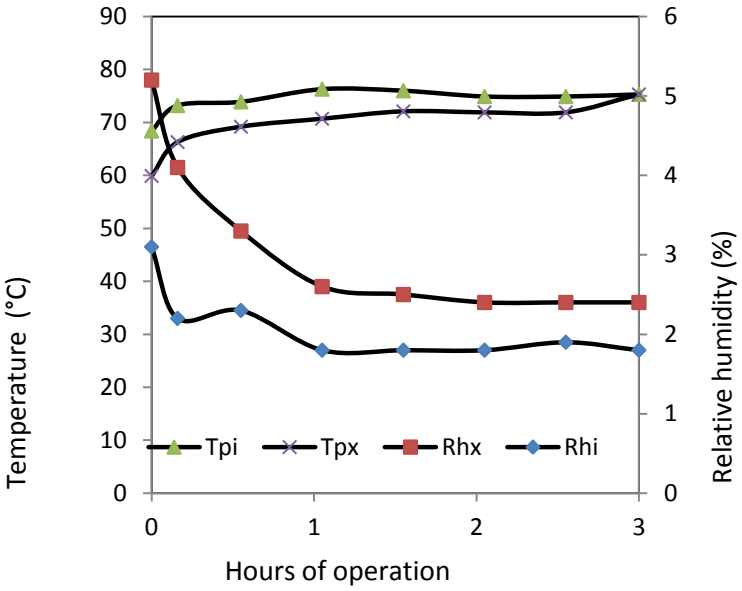

Figure 26 - The variation of entry (i) and exit (x) temperature (Tp) and relative humidity (RH) in the tunnel dryer averaged for all 3 hr runs at 72°C entry air.

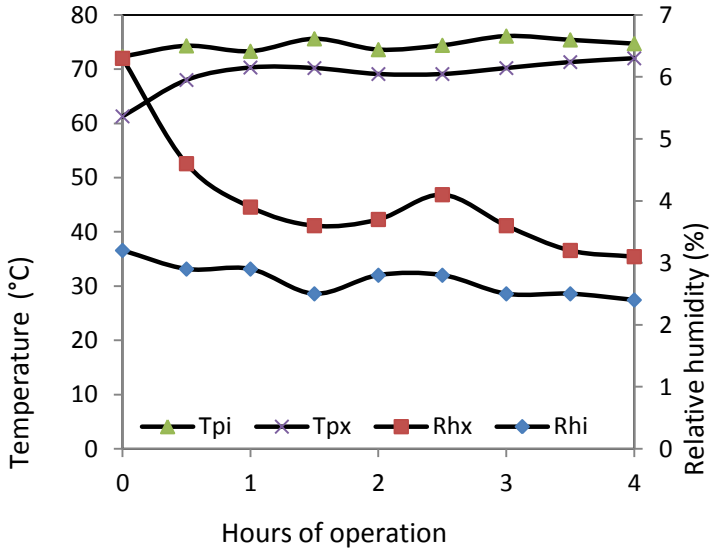

Figure 27 - The variation of entry (i) and exit (x) temperature (Tp) and relative humidity (RH) in the tunnel dryer for one run at 72°C entry air for 4 hr. The run on this particular day had a period of rain which increased the RH inside the box at two and a half hours into the measurement sequence.

6.1.1 Average drying rates

Paunch drying times varied according to temperature. The average drying rates (%ΔMC/ hr)

for varying temperature (wet and dry basis) for up to 5hrs are shown in table 9. These are based on Farmer, Farouk and Brusewitz's (1980) equation for an average daily drying rate which is given by:

$$MC = MC_i - ADR \times T;$$

Where *MC* is the final moisture content, MC_i is the initial moisture content, *ADR* is the average daily drying rate, *T* is time.

Table 9- Paunch average drying rates (ADR) for wet and dry basis up to 5 hrs.

Temperature	ADR wet basis (up to 5hrs)	ADR dry basis (up to 5hrs)
72 °C	6.1	36.4
55°C	2.8	29.7
41 °C	2.6	20.7

The 72 °C entry air showed a significant increase in the ADR when compared to the 55°C and 41°C entry air. This variation and increased drying rate for higher temperatures was expected due to the theory that increased temperature increases the rate of drying. The ADR for 72°C entry air suggests that if paunch continued to dry at this rate it would be possible to dry paunch to 20% moisture content in 8 hours. However, further experimentation indicated that the ADR changed after 5 hrs(refer to appendix 1 for ADR graphs up to 5hrs for 41 and 55°C entry air).

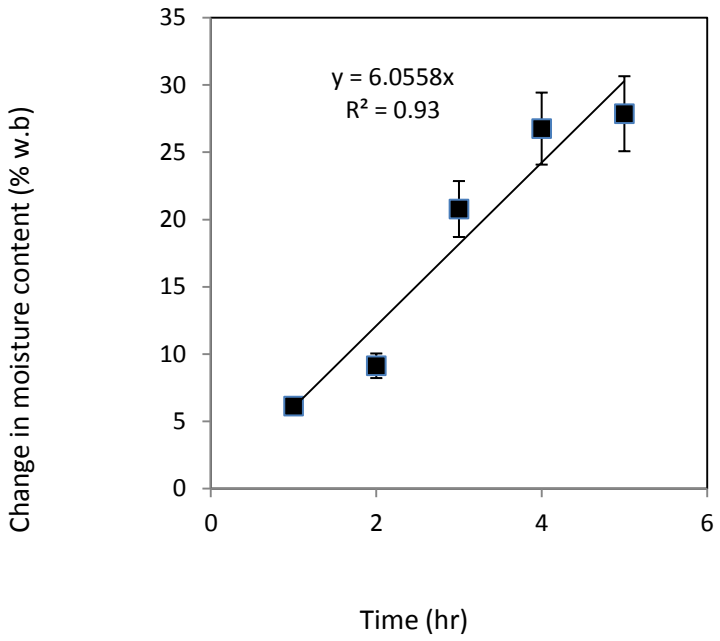

Figure 28- Change in moisture content (wet basis) versus time for 72 °C entry air temperature, paunch depth 2.5cm, time up to 5hrs. The data points have been fitted with a linear trend line.

Further experimental work was done for times greater than 5 hours. The ADR for the varying temperatures greater than 5hrs is shown in table 10. A single satisfactory ADR was difficult to find for 72°C entry air. There were two distinct rates of change between 0-5hrs and >5hrs. The ADR in wet basis shows this most clearly with a reduction in ADR of almost half at over 5 hrs of drying time. This is interpreted as the second phase of drying, where the ADR drops as it is restricted by internal moisture migration. There was a clearly observable drying zone in the paunch at the end of each run. There was a clear dry zone on top with a drying zone that extended from about halfway through the paunch to closer to the bottom of the container, depending on the number of hours the test had run. When the drying zone through the paunch was situated about halfway, there was a clear undried zone at the bottom

layer of the paunch. Figures 29 – 31 show the change in moisture content versus time for varying temperature for wet basis. The slope of the line gives the ADR.

Table 10 - Paunch average drying rates (ADR) for wet and dry basis for over 5 hrs.

Temperature	ADR wet basis	ADR dry basis
72°C	3.46 (up to 12hrs)	30.1
72 °C	6.1 (up to 5 hrs)	36.4
72 °C	3.03 (over 5hrs)	28.98
55°C	2.6	17.5
41 °C	1.3	11.2

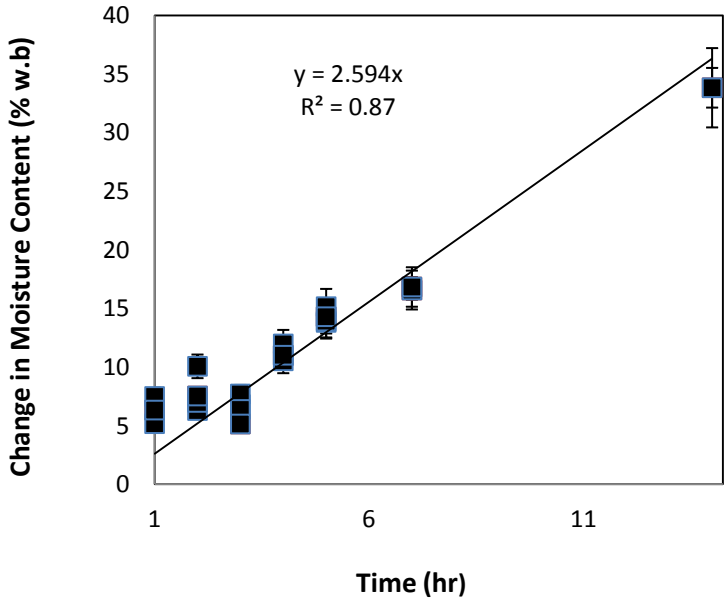

Figure 29 - Change in moisture content (wet basis) versus time for 55 °C entry air temperature, paunch depth 2.5cm, time over 5hrs. The data points have been fitted with a linear trend line.

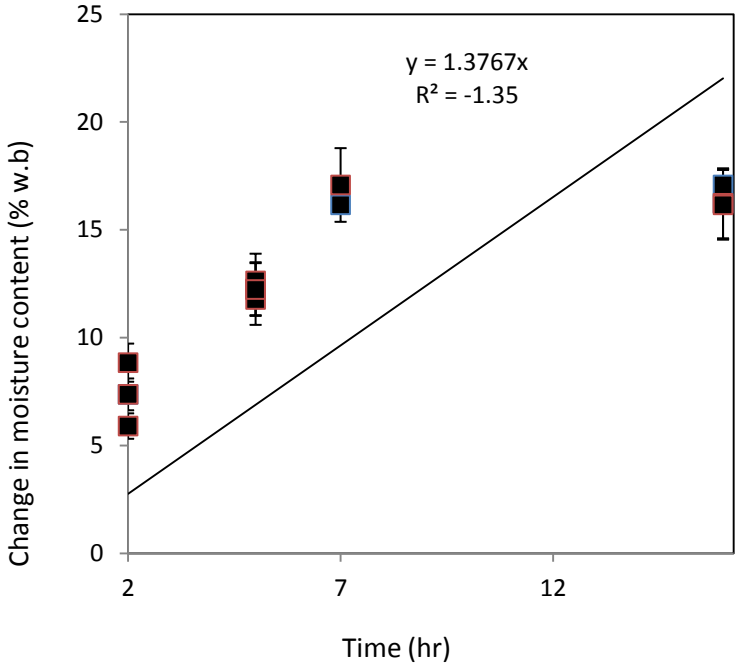

Figure 30 - Change in moisture content (wet basis) versus time for 41 °C entry air temperature, paunch depth 2.5cm, time over 5hrs. The data points have been fitted with a linear trend line.

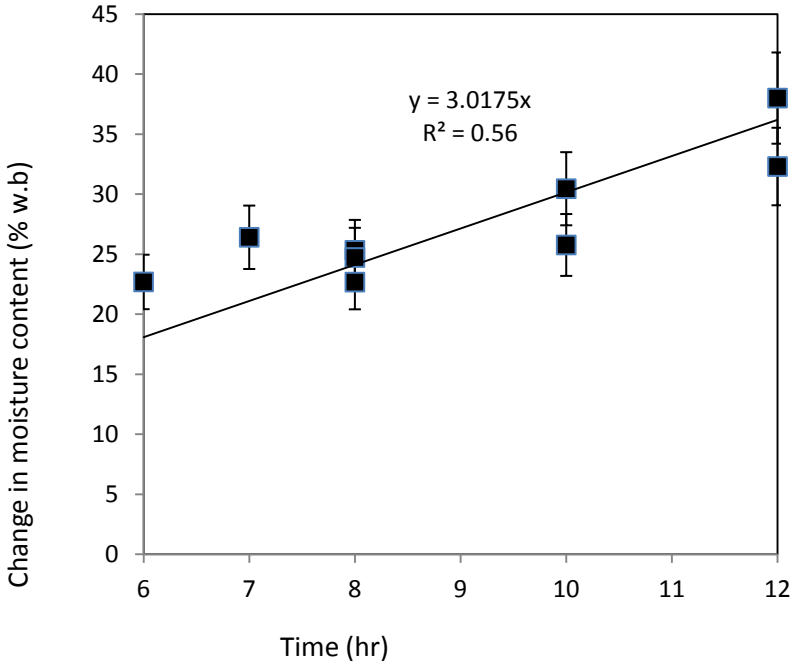

Figure 31 - Change in moisture content (wet basis) versus time for 72 °C entry air temperature, paunch depth 2.5cm, time over 5hrs. The data points have been fitted with a linear trend line.

The graphs were fitted with a linear trend line and error bars were based on a comparison between the values found for the 2 hour runs at 71 °C air temperature. Using percentage error calculations:

$$\frac{(experimental\ value - accepted\ value)}{accepted\ value} \times 100 = \%;$$

Of the two hour values at 71 °C air temperature the two values that were used were chosen as their initial moisture content varied by only 0.88% and were run under similar conditions (as were all tests). The resulting variations have been used to represent the percentage errors for individual measurements obtained in the experiment. The change in final moisture contents for the two values differed by 1.04% and gave a percentage error of ± 11.21%.

6.1.2 Equilibrium moisture content

Equilibrium moisture contents were based on yellow dent corn which was similar to soft and hard wheat moisture content (Grainnet n.d). This decision was made due to a lack of access to drying ovens to allow paunch equilibrium moisture contents to be determined, and instead use an existing published equilibrium moisture content similar to the feed given to feedlot cattle. Table 11 show the wet and dry basis equilibrium moisture contents for yellow dent corn.

Table 11 - Equilibrium moisture contents for yellow dent corn (wet and dry basis).

	Yellow dent corn equilibrium moisture content (grainnet n.d).	
Temperature	**RH 30%**	
40°	12% d.b	10.6% w.b
55°	11% d.b	9.6% w.b
70°	10% d.b	8.7% w.b

6.1.3 Drying constant

Drying constants, k, for dry basis were determined based on the drying equation for an unsaturated surface:

$$MR = M_i e^{-kt};$$

Here *MR* is the moisture ratio, M_i is the initial moisture ratio, *k* is the drying constant, and *t* is time (Henderson & Perry, cited in Griffith & Brusewitz 1980, p. 1016). Where the moisture ratio is given by:

$$MR = \frac{(M-M_e)}{(M_i-M_e)};$$

Here *MR* is the moisture ratio, *M* is the moisture content, M_e is the equilibrium moisture content, M_i is the initial moisture content (Griffith & Brusewitz 1980). This equation can be rearranged as:

$$\frac{LnMi-LnMR}{t} = k;$$

Thus, setting the initial moisture ratio to zero (as performed by Griffith & Brusewitz 1980) gives a plot of $\frac{-LnMR}{t}$ where the slope of the line is the drying constant k. Equilibrium values for yellow dent corn were used for equilibrium moisture content, and the linear regression was forced through zero. Figures 32 to 34 show the graphed

data fitted with a linear trend line. Table 12 summarizes these results and corresponding R^2 value.

Table 12 – Summary of drying constants, K, (dry basis) for present experiment.

Temperature °C	K value	R^2	Time
72	-0.173	0.195	1 - 12
55	-0.1187	0.923	1 - 14
41	-0.0643	-1.237	1 - 16

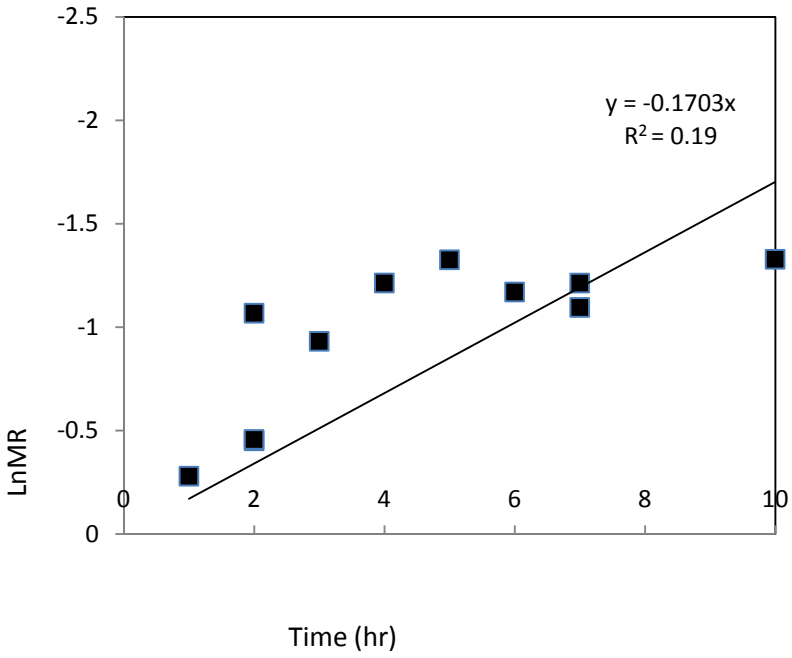

Figure 32 - Drying constant ,k, for 71°C entry air for up to 12 hours. Data have been fitted with a linear trend line.

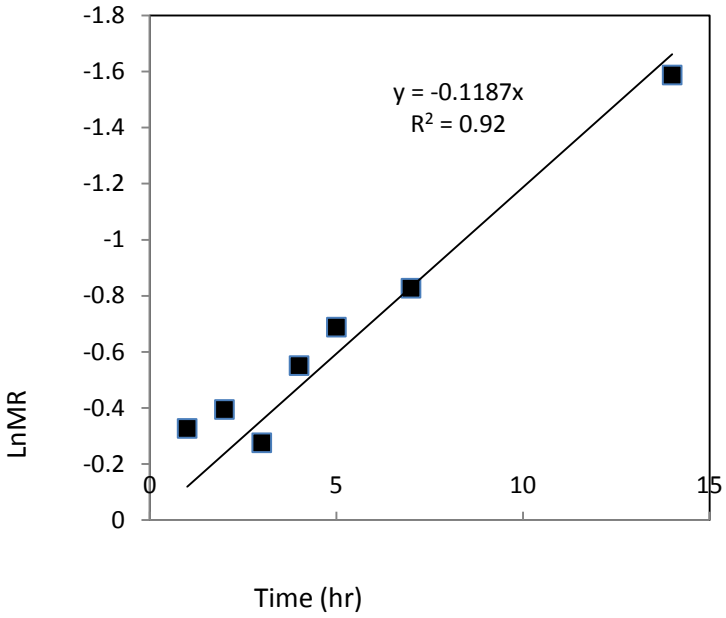

Figure 33 - Drying constant, k, for 55°C entry air for up to 14 hours. Data have been fitted with a linear trend line.

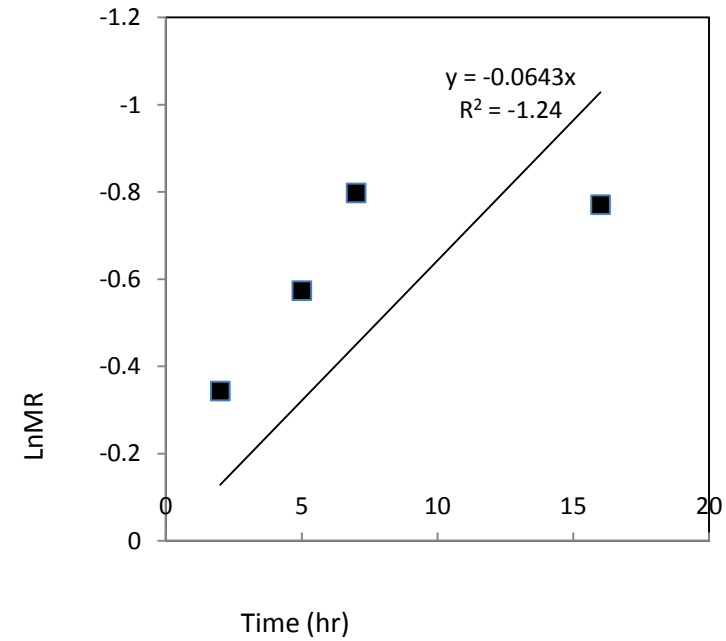

Figure 34 - Drying constant, k, for 41°C entry air for up to 16 hours. Data have been fitted with a linear trend line.

6.1.4 Optimal drying temperature and RH

The results of the measurements performed for this study show that optimal drying will require temperatures over 55°C and with relative humidity under 20% if drying is to be optimised. Due to the amount of paunch produced each week drying over more than a few days (without a very large capacity dryer) would produce an unacceptable backlog of paunch to be dried. Simple sun drying is thus not feasible as it requires a large spreading area, and up to two weeks drying time. An ageing paunch would further slow the drying process as Griffith and Brusewitz (1980) and Brusewitz, Moustafa and Farmer (1981) showed that increased paunch age reduces drying rates and dewatering, and would also create a need for an extra holding area, increased smell, and fly problems. So the need for a dedicated solar dryer is clear, and its required operating conditions can be established.

Chapter 7: Part 2 – Paunch Discussion

7.1.0 Effect of temperature

The results indicate the importance of temperature on paunch drying. It is clear from the variation of ADRs (1.2 for 41°C, up to 6.1 for 72°C) that higher temperatures will result in faster drying times. Theory tells us that there are two stages in drying; the evaporative period and the migration of moisture from the interior. Although these two stages are intimately linked it is the second phase, where moisture needs to be transferred to the surface via diffusion or capillary action to be evaporated, which is the limiting factor in drying. By knowing how much drying can be hastened an effective solar dryer can be designed. There were two distinct rates of change in the drying of paunch between 0-5hrs and >5hrs for 72°C entry air, with the second phase of drying apparently occurring after 5 hrs, where the ADR drops by being restricted by internal moisture migration. Nevertheless, a second factor that may also be at work for longer drying times is that the paunch may be insulating itself through the development of an outer crust.

The drying times are limited due to internal migration of moisture and experimentation is needed to find how limiting it will be. If the ADR of 72°C air was not limited by this then it would be possible to dry paunch in 8 hrs. Experimentation is needed to confirm whether it is possible to increase the ADR using methods suggested by Farmer, Brusewitz and Moustafa (1979), such as an open mesh tray, or agitation of the crust, and by manipulating the operating conditions that affect the second phase of drying. If these strategies could be used to increase the ADR it may be possible to reduce the moisture content to 20% in as short as 8 hrs (based on the

ADR of 6.1 for 72°C air). The existence of a drying zone that was observable for each run leads to a reasonable assumption that paunch can be dried at a faster rate than the discovered ADRs. This assumption is based on the fact that drying in the experiment was limited to the upward direction. By stirring the paunch or placing it in mesh holders will increase the surface area of the paunch, thus reducing the distance/path length needed to be travelled by the moisture. Clearly the ADRs would be much higher had the undried and drying zones also been exposed to the surface air conditions.

7.1.1 Viability of paunch for use in boilers

The experimental ADRs suggest that the time required to dry paunch may make it a viable option as a renewable energy source. Yin and Farmer (as cited in eds Witherow & Scaief 1976) sun dried (air dried) paunch in week, Bridle (2011) sun dried paunch in two weeks, Farmer, Farouk, and Brusewitz (1980) used a modified solar still to dry paunch to 30% in 5 days. This makes it feasible to expect that a well designed solar dryer at CA can achieve an ADR approaching the experimental results in this study and should be able to dry paunch in a few days, thus making paunch a viable energy source.

It is also interesting to note that Nippon meat packers conducted studies on burning 70% paunch mixed with 30% sawdust in their boiler. They bought a new $77 000 screw press to dewater their paunch to a moisture content of 47 – 49%. This firm had success with the boiler performance but were experiencing inconsistencies with the paunch from the screw press and were therefore unable to fully integrate paunch as a fuel source. This firm also stated that sun drying of paunch was not a viable option

for them due to the large area that would be required for spreading the paunch (Triance, A 2012, pers. comm., 16 May). In this case a solar dryer may thus allow a more consistent fuel source to be created. The screw press would create lower paunch initial moisture content for the dryer and increase drying times.

A possible solution for the problem of waste particle size and bulk density when burning paunch in a boiler (Bridle 2011) is to use a cheap pelletizer after paunch drying to allow easier feeding into boilers and storage. Global Energy produce a portable pellet mill that costs $6 400 and can pelletize 650 – 750 kg per hour (Bartlett n.d). This machine should be capable of handling the amount of paunch produced by CA with quite a low capital cost. However, no study has yet been done on pelletizing dried paunch and it would be interesting to determine if this was a suitable method for handling and storing dried paunch.

Paunch has a self-sustaining flame when the total solids are ≥ 30% (eds Witherow & Scaief 1976, Bridle 2011). Figure 35 graphically demonstrates that for inconsistent initial moisture content all final moisture contents are >30% for 72°C entry air, and are achievable in less than 15 hrs.

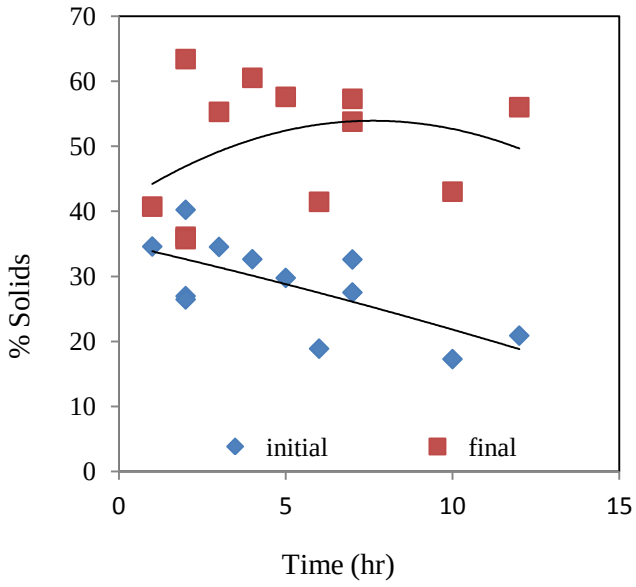

Figure 35 – Initial and final total % total solids versus time for 72°C entry air. All final total solids are >30% and were achievable in under 24hr.

Water content impacts boiler output, is boiler specific and can be found in boiler specification sheets. Hatt (1997) states that boiler efficiency loss is approximately 0.1% for each 1% increase in MC. Coal ranges in MC depending on the type:

- 2.8 – 16.3% for anthracite,
- 2.2 – 15.9% for bituminous,
- 39% for lignite (Engineering toolbox n.d).

CA currently uses coal with an inherent MC of 4.2% and a total MC of 6.5%. They then spray the coal with a mist to stick the finer coal (dust) particles to the larger coal stones (1 inch). This produces a total MC of 9 – 10% entering the boiler. If boiler output drops due to MC it is possible to increase the feed rate of the boiler to increase the output. However, this would significantly decrease the financial viability with the increased coal usage. In contrast, a more efficient way is to decrease the initial moisture content of the feedstock, in this case paunch. Therefore, for efficient

boiler output paunch should have a substantially lower MC than 70% (w.b). Also, as stated by Bridle (2011) burning paunch with 70% moisture content would only be suitable as a waste disposal method with the paunch itself providing little or no energy. Therefore, there are two ways to lower the moisture content. The first is using a solar dryer to lower the moisture content and the second is to mix the paunch with a dryer substance. It may be possible to mix the paunch with the coal prior to entering the boiler. This could act as a substitute for spraying the coal and capturing the finer dust particles. However, due to the need for thorough mixing to achieve a consistent MC it may not prove economically viable to pre-mix the paunch with coal.

7.1.2 Comparison of results with previous research

Farmer, Farouk, and Brusewitz (1980) found an ADR of 30.5 % ΔMC d.b per day for their solar dryer (a modified solar still) using direct insolation. The authors' ADRs ranged from 1.27 to 2.73 % ΔMC d.b per hour for direct insolation and desiccant drying. The present experimental ADRs ranged between 11 to 36 % ΔMC d.b per hour. This is a rate up to 24 times greater than Farmer, Farouk, and Brusewitz's (1980) value.

Comparison between Farmer, Farouk, and Brusewitz (1980) and the results of the present study is difficult as Farmer, Farouk, and Brusewitz (1980) had ambient temperatures between 10 - 25°C, with operating temperatures of 15 - 50°C at the high end of their dryer and 15-35° at the low end. It took Farmer, Farouk, and Brusewitz (1980) 5 days (compared to the present experiments 12 hrs) to reach

similar final moisture content from comparable initial moisture contents. It took these authors 6 hrs to reach just below 50°C at the high end where it then started to drop over the next 4hrs to below 40°C. Therefore, Farmer, Farouk, and Brusewitz's (1980) stated ADR is only useful for their dryer design, and not a true value for average drying rates of paunch as it includes large variations in temperature such as those experienced between day and night the dryer would have been inactive. The work of Farmer, Farouk, and Brusewitz (1980) suggests that during each night the paunch would have been undergoing much slower drying rates as it tried to reach equilibrium with the conditions inside the box. Therefore, as it is expected that Farmer, Farouk, and Brusewitz's (1980) drying mostly took place in the peak temperature range (not in the whole 24hr period), their true drying rate could be orders of magnitudes greater than that published. The experimental ADR from the present study were measured with consistent temperature and RH and give a more precise in time indication of the hourly changes of moisture content for paunch at those conditions.

It is interesting to note that Farmer, Farouk, and Brusewitz (1980) stated that their dryer would be suitable for use as a straight direct insolation dryer in areas with higher insolation. Their insolation for the testing of the dryer ranged from 4.45 – 14.27 MJ/m^2 per day. Ipswich has on average per day an insolation of between 18 – 21 MJ/m^2 which is significantly higher. This suggests that Farmer, Farouk, and Brusewitz's (1980) dryer would perform better in Ipswich, with higher internal temperatures, and faster dryer rates.

Griffith and Brusewitz (1980) measured a drying rate constant, k, of 0.005 to 0.108 /hr for their preliminary results and an average rate of 0.0117 /hr for their main experiment. In comparison, the new experimental k values obtained varied from 0.0643 to 0.1703 /hr. While these fall within the range given by Griffith and Brusewitz (1980) caution should be exercised in making direct comparisons with the results from the present study. This is because while both experiments have similar designs, Griffith and Brusewitz's (1980) experiment used a lower temperature of 35°C, and used RH that ranged higher, up to 80%. Griffith and Brusewitz's (1980) results also used paunch from just three different cows whereas the present experimental results used paunch obtained from the screw press at CA, for each separate run, with the paunch being either grass or grain fed in origin, or a mixture of both, from many cows.

Another point of difference between the present study and Griffith and Brusewitz's (1980) study is that equilibrium moisture content has been derieved differently. Griffith and Brusewitz's (1980) results used an experimentally acquired equilibrium moisture content for paunch that was not published in the paper, so the present experiment has used a published estimate from the literature based on yellow dent corn which should be similar to paunch. In addition, Griffith and Brusewitz's (1980) experiments were run from 1 to 88hrs (3.6 days) whereas the present experiment was operated for less than 1 day for each set of temperatures, which ranged up to 71°C compared to Griffith and Brusewitz's (1980) 35°C.

Temperature plays an important part in both the evaporative and internal moisture migration stages whereas humidity is only of importance during the evaporative

stage. As a result, a comparison of drying rates between Griffith and Brusewitz's (1980) and the present experiment is difficult, as the present experiment used varying temperatures which affected both stages of drying, whereas Griffith and Brusewitz's (1980) related only to the evaporative stage. Given that the present experiment operated at a higher temperature, lower humidity than Griffith and Brusewitz's (1980), the similarity of the resulting drying constants (0.0643 to 0.1703 /hr, 0.005 to 0.108 /hr, 1.17 /hr) remains surprising. Theory (refer section 2.2.4) suggests that higher temperature and lower humidity will have an increased effect on drying times. It appears more likely that Griffith and Brusewitz's (1980) drying constant has a typographical error and if out by a factor of 10^{-2} we get a more reasonable comparison. Figure 36 demonstrates the final moisture ratio obtained using the drying constant, k, in the exponential equation e^{-kt}. Series A represents the believed error in Griffith and Brusewitz's (1980) paper with series B being the corrected value. Series C, D, and E represent the k value found in the present experiment for 41, 72, and 55°C entry air respectively. Series A shows that if this constant was correct then it would reach a zero moisture content in approximately 5 hrs. From the present experiment it is clear that 35°C air with changing RH will not dry paunch in this time. Series B with the corrected drying constant for Griffith and Brusewitz's (1980) leads to a more reasonable outcome.

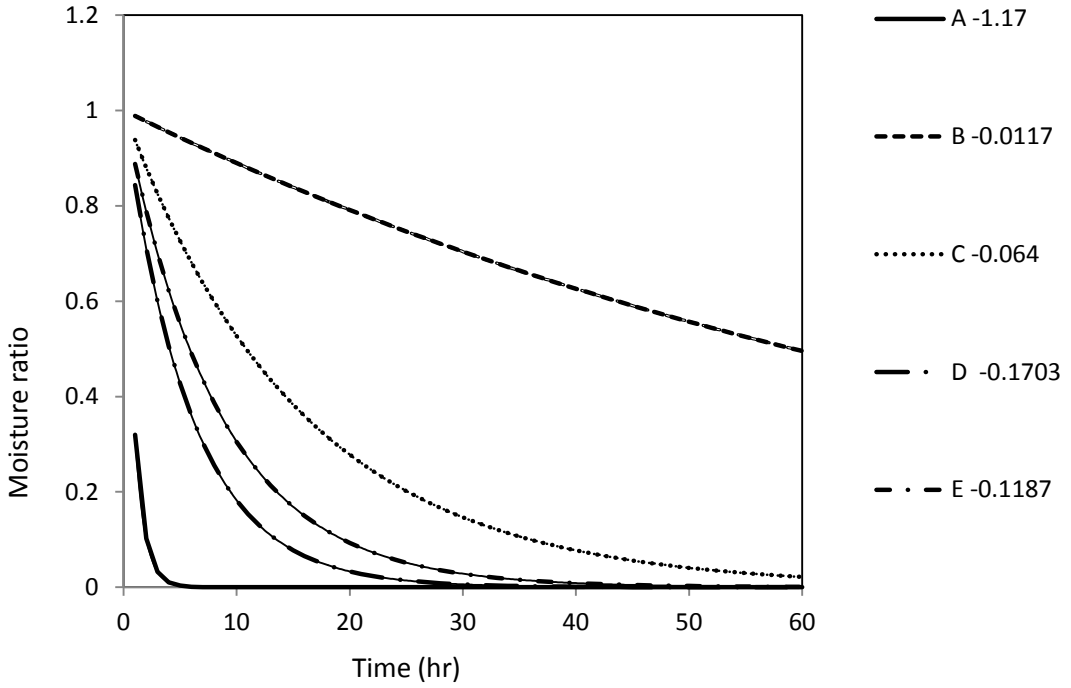

Figure 36 - Griffith and Brusewitz's (1980) and present experiment k values. The A series (-1.17) is the believed typographical error in Griffith and Brusewitz's (1980) paper and series B (-0.0117) is the corrected value. Series C, D, and E are the present experiment values for 41, 72, and 55°C respectively.

From Farmer, Farouk, and Brusewitz's (1980) solar dryer design it is known that it is possible to dry paunch in 5 days. Yin and Farmer (as cited in eds Witherow & Scaief 1976) used air drying to reach a final moisture content of 16 – 20% in one week. Griffith and Brusewitz (1980) demonstrated the relationship between RH, age, and depth of paunch. The experimental ADRs and k values show that it may be possible using higher temperatures to significantly increase the drying rate. Therefore, it should be possible to dry paunch within a maximum of 5 days, using Farmer, Farouk, and Brusewitz's (1980) solar dryer design as a baseline.

One way to create a more consistent dryer would be to change the dryer design and to use some of the abattoir excess heat as an initial air source for the solar absorber.

CA has a pipe that feeds the biofilter that contains air with a temperature of 34.3°C and a RH of 30.5% it could be possible to feed this air through an absorber and hence a solar dryer and then feed it back to the biofilter (to contain the smell). This would mean that on low insolation days with low ambient temperatures the air inside the dryer would still remain above 30°C which is higher than the maximum ambient conditions used in Farmer, Farouk, and Brusewitz's (1980) solar dryer. In contrast, the heated air produced using a biofilter pipe should lead to similar temperatures to Griffith and Brusewitz's (1980) study and so produce a similar drying constant.

7.1.3 Limitations of the present research

The experimental results are limited due to a number of factors:

- Direction of drying (moisture transfer in upward direction),
- Uncontrolled ambient temperature and humidity,
- No separation of grass from grain fed cattle paunch.

As the paunch was placed in an enclosed holder (pan) the direction of moisture transfer to the surface was limited to the upward direction. This is similar to Griffith and Brusewitz (1980) study and allowed favourable comparison with their work. Other factors that may have affected the results were uncontrolled ambient air temperature and humidity outside the box. This contributed to slight variations of temperature and humidity inside the box due to ambient air passing into the box after being heated by the Remington hot air blower and by changing the temperature of the air surrounding the box which may have increased or decreased the operating temperature due to heat transference between the box and ambient air. However, the box was constructed out of wood and lined with thick plastic sheeting which made the box fairly insulated and therefore, transfer of heat was kept to a minimum. Only

at the highest temperature setting did the plastic lining showed some signs of deformation.

It is noted that there was no separation of grass or grain fed paunch in the present study. Previous literature suggests that there can be an increase in drying times up to five times greater for grain fed cattle as opposed to grass fed (Farmer, Brusewitz & Moustafa 1979).

The limitations in comparing the present results with similar research do not impede the validity of the present results. In real-world situations any solar dryer will be exposed to uncontrolled ambient air conditions. In addition, it is not reasonable to expect paunch types to be separated before drying. Therefore, drying rates should be able to encompass mixed feed ration types of paunch.

7.1.4 Active dryers as an effective design

Tunnel dryers appear to be the most effective design for paunch drying. The drying times for paunch vary from one to two weeks for sun drying, to possibly 8 hours as found by the present study (Yin & Farmer as cited in eds Witherow & Scaief 1976, Bridle 2011). A modified solar still dried paunch to 30% in 5 days which is only slightly better than the air drying rate (Farmer, Farouk & Brusewitz 1980). The most promising rates appear to be for the tunnel dryer type design with drying constants that imply a maximum of a couple of days (Griffith & Brusewitz 1980). The experimental design forms the basis of a modified tunnel dryer design with the expectation that it will be the most likely candidate for scaling up into an industrial-sized paunch dryer.

Chapter 8: Conclusions and future work

8.1 Conclusions

Of the renewable energy sources assessed in part 1, none were found to be cost-effective at current electricity prices. Photovoltaics may soon however become viable if the cost of electricity rises and capital costs drop. Wind turbine energy shows little hope of ever becoming viable for implementation at CA due to the lack of high wind speed at the site, and algae for uses other than biodiesel shows promise, but further study needs to be done.

Photovoltaics offer a promising solution to reducing GHG emissions by replacing fossil fuels. The embodied energy shows that they will repay their environmental debt and continue to produce emissions free energy (Steenblik 2005). Research and development will help to improve cell efficiencies and production which will help to reduce the cost of PV systems. These costs could be further reduced by governmental policy which encourages the use of renewable energy over fossil fuels. The current rate at which photovoltaic technology is being implemented shows that there is an increasing global move towards renewable energy technology. This move towards renewables if coupled with further development and policy could well see photovoltaics playing a much larger part in world energy production. With changing electricity prices and dropping PV capital cost PV will likely be viable for implementation at CA in the near future.

Paunch is the most likely organic waste candidate for CA to implement to produce energy. The preliminary results provided in this thesis support the hypothesis that solar dried paunch is a viable Biofuel for CA. The preliminary average drying rates

(1.2 up to 6.1 w.b) and drying constants (0.0643 to 0.1703 d.b) show that increased temperature increases the drying rates previously shown in the literature. The average dying rates will allow drying times to be determined depending on the specific parameters inside a solar dryer. The apparatus used for the experiments in this study appears to form the basis for an industrial dryer, as opposed to previously tested modified solar still designs.

The results provided in this study indicate that solar drying of paunch holds promise as a cost-effective source of biofuel for abattoirs This will not only benefit CA but will then be easily implemented into the wider abattoir community and help them to reduce their environmental foot print and lower their energy costs, and help create a sustainable future.

8.2 Future work

Algae for the production of biodiesel does not appear feasible for CA. However, algae for cleaning up wastewater or for methane production may have benefit to the meat industry. The study done by Fallowfield, Cromar, and Evans (2001) confirms that abattoir wastewater is suitable for growing algae and shows that it can have a beneficial effect on removing 95 – 99% of the BOD, 73 – 80% of the COD, 50 – 60% of the nitrogen, and 14 – 28% of the phosphorous from the wastewater. David Batten and a team from CSIRO have developed a comprehensive pre-feasibility model for growing algae in wastewater (Batten, D 2011, pers. Comm., 15 February). Originally developed for a Melbourne sewerage treatment plant the model can be adapted for other sites. The model can produce different feasibility scenarios such as algae for use in a gasifier or anaerobic digester. Therefore, use of CSIRO's pre-

feasibility model could produce relevant data for CA and may be feasible grounds for a pilot study on integrating algae into abattoirs.

Photobioreactors in conjunction with open ponds may be a solution for abattoirs to allow them to grow algae. Huntley and Redalje (2007) developed the coupled photobioreactor-open pond cultivation system to solve the problem of open pond technology being affordable but unable to provide continuous cultures, while photobioreactors are able to provide continuous cultures but were not aimed at smaller industrial application. Their solution was to incorporate both systems into their designs. Closed photobioreactors are used for the first stage to produce a continuous supply of uncontaminated inoculum in large volume. Open ponds are used in the second stage where the most rapid growth rates occur. This system is continuous due to the bioreactors ability to supply new inoculum and the short algae retention time in the ponds. The algae only remained in the ponds for 1 day which removed the risk of contamination that ponds are normally susceptible to (unless the algae grown is of a type that has a high tolerance to extreme environmental factors). The batch cultures in the open ponds also quickly exhaust the nutrient supply also helping to avoid contamination by other species and also to increase the rates of oil productivity (Huntley & Redalje 2007), so the photobioreactors supply the initial culture and the open ponds grow the culture and also allow for greater oil content by the rapid removal of nutrients in the ponds. The removal of nutrients from the ponds is important as generally high oil strains of algae grow slower than lower oil strains (Vasudevan & Briggs 2008). This is how ponds quickly get contaminated by the unwanted lower oil species. The commercial scale demonstration facility for biodiesel production was run using this two stage approach for over a year and had

an average biomass energy production of 763GJ $ha^{-1}y^{-1}$(Huntley & Redalje 2007). Wang et al. (2008) state that this system is feasible, if fast growing algal species are used.

However, big bag photobioreactors appear to be an appropriate technology for industries that are not producing biodiesel as their main output. Smaller industries and industries, such as abattoirs, using photobioreactors to clean up waste water, capture CO_2 emissions and to produce biodiesel for private use would make more economic sense to use the big bag system. These systems are not continuous but have cheap structural costs and over 30 years of proven algal output. The culture crashes are easily remedied by bag replacement and research could be done into the possible effectiveness of bag rinsing or turning the bags inside out to limit the amount of bags used. They could also be used alone or in conjunction with open air ponds.

Further study could be done into the feasibility of a central processing plant where small industry could send the biomass for processing into biodiesel or other resalable uses such as feedstock. Sun drying of the algal biomass would make storage and transportation easy. A central processing plant could allow small industry the benefits of algal production without the cost of transesterification (turning the algae into biodiesel) for possible "small" amounts of biodiesel. A buy back scheme could also be implemented for the industries involved to be able to gain access to the biodiesel. Algae left over from the transesterification process could then be a cheap high protein stock feed for the wider meat industry such as livestock producers.

These strategies could then make photobioreactors viable for smaller industries or industries not wishing to produce biodiesel as their main product.

5.3 Paunch

The ADRs obtained are precursors to paunch becoming a viable biofuel. Future work will involve testing the ADRs to increase the drying rates. Farmer, Brusewitz and Moustafa (1979) suggest that drying times can be almost halved by using mesh holders or agitating the crust. Instead of finding more ADRs for enclosed bottom pans a better use of the time would be acquiring ADRs for mesh holders, breaking the crust, and continuous stirring to determine which of these will produce the fastest rate. This will then lead to the design of the drying chamber component of the solar dryer. During these tests it will be possible to concurrently acquire the "best" drying parameters. Longer drying times also need to be determined to see if it is possible to reach 20% final MC in a timely fashion. This would then allow a conclusion to be drawn as to whether solar drying paunch would be suitable for use in pyrolysis.

Another interesting study would be creating a drying chamber based on the results of the ADRs for different holders. This could be attached to the pipe at CA that feeds into the biofilter. This pipe looks to be an effective air source for a solar dryer as it has a temperature of 34.3°C and an RH of 30.5%. The drying chamber could be built without (yet) the need for an absorber and used to test minimum drying times that could be achieved without a solar absorber included. This would help determine the most effective drying chamber design in conjunction with the ADRs as well as provide the baseline drying times for cloudy days when there is low solar insolation.

Solar dryer types need to be evaluated to determine the most effective design. A definite focus should be on active dryers as opposed to passive dryers and tunnel type dryers over solar still designs. Absorbers should be investigated and a pilot size absorber should be built to allow air temperature and RH measurements to be determined. Fan power and air flow rates will need to be determined. Once these factors are known then it would be possible to make predictions for drying times in the solar dryer.

Stockpiling would also be interesting to test to see if there are any advantages to using this method before drying the paunch (eds Witherow & Scaif 1976).

References

ABC 2006, *Green group backs $270m wind farm*, ABC News, viewed 3 February 2012, <www.abc.net.au>.

Amnon Yogev, R & Dan Yakir, KE 1999, 'Bioreactor and system for improved productivity of photosynthetic algae', United States Patent, USA.

Arrow, K 2007, 'Global climate change: A challenge to policy', *Economists'View*, viewed 20 January 2010, http://www.bepress.com/cgi/viewcontent.cgi?article=1270&context=ev

Australian Government 2011, LRET/SRES – the basics, Office of the Renewable Energy Regulator, Australia.

Australian Government 2011, Small generation units; owners guide, Office of the Renewable Energy Regulator, Australia.

Bala, BK & Mondol, MRA 2001, 'Experimental investigation on solar drying of fish using solar tunnel dryer', *Drying Technology*, vol. 19, pp. 427-36.

Bartlett, M n.d, Major renewable energy project for WA, *Weekly Machinery*, article received from Global NRG.

Baumann, DJ 1971, 'Elimination of water pollution by packinghouse animal paunch and blood', *Office of Research and Monitoring, Environmental Protection Agency,* USA.

Baynes, S, Emerson, L & Scott, A 1979, 'Production of algae for use in the rearing of larval fish', *Fisheries Research Technical Report*, vol. 53, pp.13-18.

Belessiotis, V & Delyannis, E 2010, 'Solar drying', *Solar Energy*, viewed 1 June 2011, <www.sciencedirect>.

Bell, A 1980, 'Burning waste as it floats on air', ECOS Magazine, no. 26, pp. 10 – 12.

Bold, HC & Wynne, MJ 1985, Introduction to the algae, 2nd edn, Prentice-Hall Inc, New Jersey.

Borowitzka, MA 1999, 'Commercial production of microalgae: ponds, tanks, tubes and fermenters', *Journal of Biotechnology,* vol. 70, pp. 313-21.

Boyle, G 2004, *Renewable energy: Power for a sustainable future*, 2nd edn, Oxford University Press, United Kingdom.

Boyle, G, Everett, B & Ramage, J 2003, *Energy systems and sustainability*, Oxford University Press, United Kingdom.

BP Australia 2010, *Product specification – BP ultimate diesel*, BP Australia PTY Ltd, issued 1 May 2010, Master copy held by Marketing Technical Services, Australia.

Bradshaw, CJA, Giam, X, Sodhi, NS, 2010, 'Evaluating the relative environmental impact of countries', *PLoS ONE*, viewed 1 June 2010, http://www.plosone.org

Braun, M, Stetz, T, Brundlinger, R, Mayr, C, Ogimoto, K, Hatta, H, Kobayashi, H, Kropski, B, Mather, B, Coddington, M, Lynn, K, Graditi, G, Woyte, A & MacGill, I 2011, 'Is the distribution grid ready to accept large-scale photovoltaic deployment? State of the art, progress, and future prospects', *26th EU PVSEC*, Hamburg, Germany.

Brenndorfer, B, Kennedy, L, Trim, DS, Mrema, GC & Wereko-Brobby, C 1985, *Solar dryers – their role in post-harvest processing*, Commonwealth Secretariat, London.

Bridle, T 2010, 'Waste to energy: Alternative uses for paunch waste and DAF sludge, Waste pyrolysis review', *Meat and Livestock Australia*, Australia.

Bridle, T 2011, 'Pilot testing pyrolysis systems and reviews of solid waste use on boilers', *Meat and Livestock Australia*, Australia.

Bridle, T 2011, 'Use of paunch waste as a boiler fuel', *Meat and Livestock Australia*, Australia.

Brusewitz, GH, Moustafa, SMA, & Farmer, DM 1981, 'Pneumatic dewatering of paunch contents', *Transactions of the American Society of Agricultural Engineers*, article no.3709, pp.488 - 91.

Bureau of Meteorology 2011, Water and the land> Sunshine: average daily sunshine hours, viewed January 2011, <http://reg.bom.gov.au/watl/sunshine/>

Bureau of Meteorology 2011, Humidity, viewed January 2011, <http://www.bom.gov.au/jsp/ncc/climate_averages/relative-humidity/index.jsp>

Campbell, NA & Reece, JB 2002, *Biology, 6th edn*, Pearson Education Inc, San Francisco.

Christi, Y 2007, 'Biodiesel from microalgae', *Biotechnology Advances*, vol. 25, pp. 294-306.

Christi, Y 2008, 'Biodiesel from microalgae beats bioethanol', *Trends in Biotechnology*, vol. 26, pp. 126-31.

CSIRO 2011, *Coal gasification: from fundamentals to application*, CSIRO, Autralia, viewed 3 February 2012, <http://www.csiro.au/Outcomes/Energy/Energy-from-coal/coal-gasification.aspx>.

Cucchiella, F & D'Adamo, I 2012, 'Feasibility study of developing photovoltaic power projects in Italy: An integrated approach', *Renewable and Sustainable Energy Reviews,* vol. 16, pp. 1562 – 76.

Davidson, S 2006, 'Algae bioreactors that tackle CO_2 emissions', *ECOS,* vol. 133, pp. 34-5.

Diesendorf, M 2003, 'Why Australia needs wind power', *Dissent,* no. 13, pp. 43-8.

Dincer, F 2011, 'The analysis on photovoltaic electricity generation status, potential and policies of the leading countries in solar energy', *Renewable and Sustainable Energy Reviews,* vol.15, pp. 713 – 20.

Dismukes, JP, Miller, LK & Bers, JA 2009, The industrial life cycle of wind energy electrical power generation ARI methodology modelling of life cycle dynamics', *Technological Forecasting & Social Change,* vol.76, pp. 178-91.

Doyle, J & Lant, P 2001, 'An assessment of dry paunch dumping in red meat processing plants PRENV.008', *Meat and Livestock Australia,* Australia.

EnergyAustralia 2010, Statement of expected network price trends 2010/11 to 2013/14, viewed 12 December 2010, <http://www.energyaustralia.com.au/Common/Network-Supply-and-Services/Electricity-supply/Network-prices.aspx>.

Engineering toolbox n.d., Coal classification, viewed 2 February 2012, <www.engineeringtoolbox.com>.

Fallowfield, H, Cromar, N, & Evans, R 2001, The use of high rate algal ponds in the treatment of abattoir wastes project number RPDA 501 (previously 313), Meat and livestock Australia final report.

Farmer, DM, Brusewitz, GH & Moustafa, SMA 1979, 'Techniques for drying paunch contents with solar energy', *Transactions of the American Society of Agricultural Engineers*, article no.3438, pp.219 - 24.

Farmer, DM, Farouk, SM & Brusewitz, GH 1980, 'Paunch drying with direct solar energy supplemented by solar-regenerated desiccant', *Transactions of the American Society of Agricultural Engineers*, article no.3642, pp.1057 - 64.

Farrugia, RN 2003, 'The wind shear exponent in a Mediterranean island climate', *Renewable Energy*, vol. 28, pp. 647-53.

First flight, n.d. viewed 22 Febuary 2010 <http://weblab.open.ac.uk/firstflight/forces/#>.

Franklin, S, Jordan, J, McCracken, P, McDonald, J & Gordon, J 2010, 'Renewable energy and energy efficiency options for the Australian meat processing industry', *Meat and Livestock Australia,* Australia.

Friedmann, SM n.d, *Inflation calculator,* viewed 16 May 2010, <www.westegg.com/inflation/infl.cgi>.

Giancoli, DC 1998, *Physics*, 5th edn, Prentice – Hall of Australia, Sydney.

Gipe, P 2004, *Wind power*, James & James, London.

Global NRG n.d, Summary of Global NRG Report, Algae bioreactors another way to fuel cars, Global NRG.

Grainnet n.d., Equillibrium moisture content, Grainnet, viewed 3 February 2012, <www.grainnet.com>.

Griffith, CL & Brusewitz, GH 1980, 'The drying rate of cow paunch contents', *Transactions of the American Society of Agricultural Engineers*, article no.3586, pp.1016 – 23.

Grobbelaar, J 2000, 'Physiological and technological considerations for optimising mass algal cultures', *Journal of Applied Phycology*, vol.12, pp.201-6.

Gulyurtlu, I, Boavida, D, Ferrao, T & Abelha, P n.d, Combustion of MBM in fluidized bed, *48th IEA-FBC workshop: Future challenges for waste combustion and co-combustion in FBC*, Europe.

Halliday, D, Resnick, R & Walker, J 1997, *Fundamentals of physics, extended*, John Wiley & Sons, USA.

Hatt, R 1997, *Moisture impacts on coal handling and heat rate – or as published by World Coal "Sticky when wet",* Coal Combustion Inc, Versailles, KY, viewed 13 February 2012, <http://www.coalcombustion.com/PDF%20Files/MOISTURE%2003.pdf>.

Hau, E 2000, *Wind-turbines: fundamentals, technologies, application, economics*, Springer, Germany.

Helm, M, Laing, I & Jones, E 1979, 'The development of a 200 l algal culture vessel at Conwy', *Fisheries Research Technical Report*, vol. 53, pp. 1-7.

Hinrichs, RA & Kleinbach, M 2006, *Energy. Its use and the environment*, 4th edn, Thompson Brooks/Cole, Belmont, USA.

Horsfield, B 1973, 'Drying animal wastes with solar energy and exhaust ventilation air', *Annual meeting*, American Society of Agricultural Engineers, Lexington, Kentucky.

Hu, Q, Guterman, H & Richmond, A 1996, 'A flat inclined modular photobioreactor for outdoor mass cultivation of photoautotrophs', *Biotechnology Bioengineering*, vol. 51, pp. 51-60.

Huntley, ME & Redalje, DG 2007, 'CO_2 mitigation and renewable oil from photosynthetic microbes: A new appraisal', *Mitigation and Adaptation Strategies for Global Change*, vol. 12, pp. 573-608.

HUSH Wind Power n.d, Information sheet.

Jefferys, WH& Robbins, RR 1981, Discovering astronomy, John Wiley & Sons, New York.

Johns, MR 1995, 'Developments in wastewater treatment in the meat processing industry- a review'. *Bioresource Technology*, vol. 54, pp. 203-16.

Joselin Herbert, GM, Iniyan, S, Sreevalsan, E & Rajapandian, S 2007, 'A review of wind energy technologies', *Renewable and Sustainable Energy Reviews*, vol. 11, pp. 1117-45.

Kizililsoley, M & Helvacioglu, S 2008, 'Maximising areal productivity, light penetration capacity, photosynthetic efficiency while preventing overheating of dense micro algae cultures by chlorophyll reduction method', *Scientific pre-publication by Soley Institute*, Soley Institute, Turkey.

Kropp, R 2009, *Solar expected to maintain its status as the world's fastest-growing energy technology*, SRI World Group, viewed 14th January 2010, < http://www.socialfunds.com/index.cgi>.

Kubiszewski, I, Cleveland, CJ & Endres, PK 2010, 'Meta-analysis of net return for wind power systems', *Renewable Energy*, vol. 35, pp. 218-25.

Laing, I 1979, 'Recommended procedures for the culture of *Chaetoceros calcitrans*', *Fisheries Research Technical Report*, vol. 53, pp. 8-10.

Lee, YK 2001, 'Microalgal mass culture systems and methods: Their limitation and potential', Journal of Applied Phycology, vol. 13, pp. 307-15.

Lenoble, J 1993, *Atmospheric radiative transfer*, A. DEEPAK Publishing, Virginia, USA.

Li, Y, Horsman, M, Wu, N, Lan, Q & Dubois-Calero, N 2008, 'Biofuels from microalgae', *Biotechnology Program*, vol. 24, pp. 815-20.

Madigan, M, Martinko, J, Dunlap, P & Clark, D 2009, *Biology of microorganisms , 12th edn*, Pearson Education, USA.

Mason, N & Hughes, P 2001, *Introduction to environmental physics – planet Earth, life and climate*, Taylor and Francis, New York.

McLaughlin, S, Bouton, J, Bransby, B, Conger, B, Ocumpaugh, W, Parrish, D, Taliaferro, C, Vogel, K, & Wullschleger, S 1999, 'Developing switchgrass as a bioenergy crop', *Perspectives on New Crops and New Uses*, ASHS Press, Alexandria, VA, pp. 282 – 99.

MLA 2010, *Meat technology update – Covered anaerobic ponds* 2010, Meat and Livestock Australia, Australia, viewed 1 June 2012, <www.meatupdate.csiro.au>.

MIRINZ 1996, *Beef paunch processing*, MIRINZ Meat Research, New Zealand, no. 33.

Miron, AS, Garcia, MCC, Gomez, AC, Camacho, FG, Grima, EM & Christi, Y 2003, 'Shear stress tolerance and biochemical characterization of *Phaeodactylum tricornutum* in quasi steady-state continuous culture in outdoor photobioreactors', *Biochemical Engineering*, vol. 16, pp. 287-97.

Mujumdar, AS 2007, *Handbook of industrial drying*, Taylor and Francis, Florida.

Myers, J & Clark, LB 1944, 'Culture conditions and the development of the photosynthetic mechanism-II. An apparutus for the continuous culture of *Chlorella',* The Journal of General Physiology, vol. 28, pp. 103-12.

NASA 2008, *Sun or moon altitude/ azimuth tables*, U.S Naval Observatory, viewed 5 January 2010, <http://aa.usno.navy.mil/data/docs/AltAz.php>

NASA 2009, U.S centennial of flight commission, viewed 22 Febuary 2010, <www.centennialofflight.gov/.../DI5.htm>.

NDSU 2011, *Grain moisture content effects and management*, North Dakota State University, North Dakota, viewed 7 May 2011, <www.ag.ndsu.edu>.

Nelson, RG, & Schrock, MD 2006, 'Energetic and economic feasibility associated with the production, processing, and conversion of beef tallow to a substitute diesel fuel', *Biomass and Bioenergy*, vol. 30, pp. 584-91.

Nerantzis, E, Tzovenis, I, Stamatiadis, S, Giannakopoulou, E & Maniatis, L (n.d), '*Continuous production of Arthrospira (=Spirulina) plantensis in a helical photobioreactor'*, Greece.

NIWA 2010, Bio-crude oil from wastewater algae, viewed 18 August 2010, <www.niwa.co.nz>.

Oliver, M & Jackson T 2000, 'The evolution of economic and environmental cost for crystalline silicon photovoltaics', *Energy Policy*, vol. 28, pp. 1011-21.

Parisi, A & Kimlin, M 1997, 'Why do UV levels vary?', *Australasian Science*, Vol. 18, pp. 39-41.

Parisi, A, Sabburg, J & Kimlin, M 2004, *Scattered and filtered solar UV measurements*, Kluwer Academic Publishers, Netherlands.

Patil, V, Tran, KQ & Giselrod, HR 2008, 'Towards sustainable production of biofuels from microalgae', *International Journal of Molecular Sciences*, vol. 9, pp. 1188-95.

PDM Group 2010, Environmentally sustainable recycling & process services for the food industry, viewed 14 September 2010, < http://www.pdm-group.co.uk/index.html>.

Pulz, O 2001, 'Photobioreactors: production systems for phototrophic microorganisms', *Applied Microbiology Biotechnology*, vol. 57, pp. 287-93.

Quaschning, V 2007, *Understanding renewable energy systems*, Earthscan, London.

Queensland Government 2011, Solar bonus scheme, Office of Clean Energy, viewed 27 January 2010, < http://svc196.wic512d.server-web.com/solar_bonus_scheme.cfm>

Ravelli, S, Perdichizzi, A, Barigozzi, G 2008, 'Description, applications and numerical modelling of bubbling fluidized bed combustion in waste-to-energy plants', *Progress in Energy and Combustion Science* 34 (2008) 224–253

Reijnders, L 2009, 'Acute view transport biofuels: Can they help limiting climate change without an upward impact on food prices?', *Journal of Consumer Protection and Food Safety*, vol.4, pp. 75-8.

Ricci, R 1977, 'Method of manure disposal for a beef packing operation – First interim technical report', *Office of research and Development, Environmental Protection Agency*, Cincinnati, Ohio.

Saidur, R, Islam, MR, Rahim, NA & Solangi, KH 2010, 'A review on global wind energy policy', *Renewable and Sustainable Energy Reviews*, vol. 14, pp. 1744-62.

Seeds, MA 2008, *Foundations of astronomy*, 10th edn, Thompson Brooks/Cole, Belmont, USA.

Sen, Z 2003, 'A short physical note on a new wind power formulation', *Renewable Energy*, vol. 28, pp. 2379-82.

Sheehan, J, Dunahay, T, Benemann, J & Roessler, P 1998, *A look back at the U.S. department of energy's aquatic species program – biodiesel from algae*, National Renewable Energy Laboratory, Colorado.

Shen, H & Lee, YK 1997, 'Thermotolerance induced by heat shock in *Chlorella*', *Journal of Applied Phycology*, vol. 9, pp. 471-5.

Simmons, K 2006, 'Evolution, ecology, and biodiversity', viewed 22 Febuary 2010, <kentsimmons.uwinnipeg.ca/16cm05/1116/16biomes.htm>.

Sindt, GL n.d, *Environmental issues in the rendering industry*, viewed 21 March 2012, <http://assets.nationalrenderers.org/essential_rendering_environmental_impact.pdf>.

Sorensen, B 2004, *Renewable energy. Its physics, engineering, environmental impacts & planning*, 3rd edn, Elsevier Academic Press, London.

Steenblik, R 2005, 'Liberalization of trade in renewable-energy products and associated goods: charcoal, solar photovoltaic systems, and wind pumps and turbines', *OECD Trade and Environment Working Paper*, no. 2005-07, pp. 1-40.

Sze, P 1993, *A biology of the algae*, Wm. C. Brown Publishers, USA.

Teter, N 1987, *Paddy Drying Manual*, FAO, Rome.

Train, R, Stelow, R, Cywin, A & Denit, JD 1974, 'Development document for effluent limitations guidelines and new source performance standards for the red meat processing segment of the met product and rendering processing point source category', *Office of Air and Water Programs, Environmental Protection Agency,* Washington, D.C.

Tredici, MR & Materassi, R 1992, 'From open ponds to vertical alveolar panels: the Italian experience in the development of reactors for the mass cultivation of phototrophic microorganisms', *Journal of Applied Phycology*, vol. 4, pp. 221-31.

Tredici, MR & Zittelli 1997, 'Efficiency of sunlight utilization: Tubular versus flat photobioreactors', *Biotechnology Bioengineering*, vol. 57, pp. 187-97.

Tsoutos, T, Frantzeskaki, N & Gekas, V 2005, 'Environmental impacts from the solar energy technologies', *Energy Policy*, vol. 33, pp. 289-96.

Turner, J 1999 'A realizable renewable energy future', *Science,* vol. 285, pp.687-89.

Turner, L 2007, 'Solar panel buyers guide', *ReNew*, vol. 101, pp. 48-54.

Tyree, M 2008, Derivation of wind power equation: playing with Newtonian physics, *Department of Renewable Resources*, University of Alberta, Edmonton, Canada, viewed March 2010, <http://www.ualberta.ca/>

Van der Zwaan, B & Rabl, A 2004, 'The learning potential of photovoltaics: implications for energy policy', *Energy Policy*, vol. 32, pp. 1545-54.

Varela, F 2006, Plugging the gap: A survey of world fuel resources and its impact on the development of wind energy, World Fuel Resources Ltd, United Kingdom.

Vasudevan, P & Briggs, M 2008, 'Biodiesel production- current state of the art and challenges', *Journal for Industrial Microbiology and Biotechnology*, vol. 35, pp. 421-30.

Wang, B, Li, Y, Wu, N & Lan C 2008, 'CO_2 bio-mitigation using microalgae', *Applied Microbiology Biotechnology*, vol. 79, pp. 707-18.

Weiss, W & Buchinger, J n.d, *Solar drying*, Austrian development corporation, Austria.

Witherow, JL & Scaief, JF (eds) 1976, 'Workshop on in-plant waste reduction in the meat industry', *Industrial Environmental Research laboratory, Environmental Protection Agency*, Cincinnati, Ohio.

Wright, C 2000, *The solar sprint PV panel*, Chuck Wright Consulting LLC, viewed 14 January 2010, < http://chuck-wright.com/SolarSprintPV/SolarSprintPV.html>.

APPENDIX 1 - ADR graphs for 55°C and 41°C entry air.

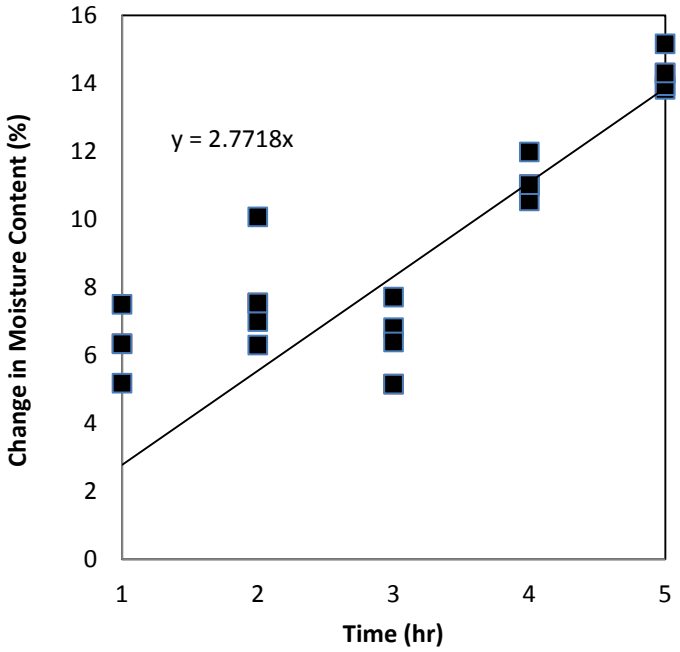

Figure 37 - Change in moisture content (wet basis) versus time for 55°C entry air temperature, paunch depth 2.5cm, time up to 5hrs. The data points have been fitted with a linear trend line.

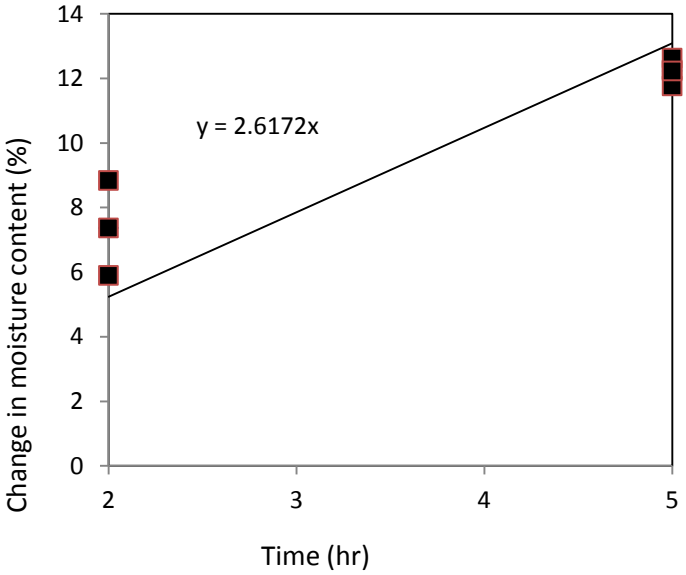

Figure 38 – Change in moisture content (wet basis) versus time for 41°C entry air temperature, paunch depth 2.5cm, time up to 5hrs.The data points have been fitted with a linear trend line.

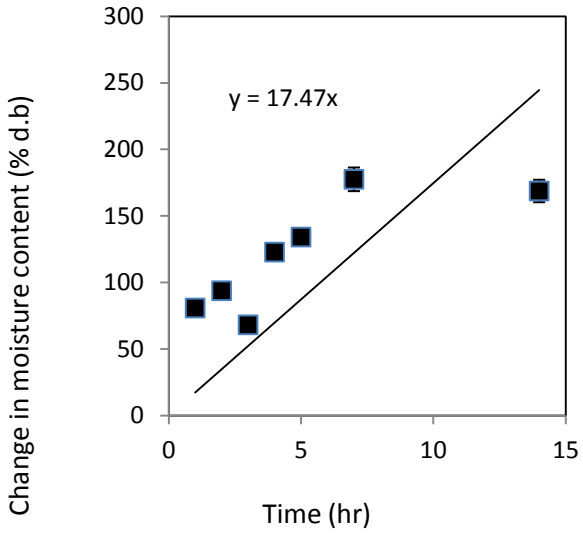

Figure 39 - Change in moisture content (dry basis) versus time for 55 °C entry air temperature, paunch depth 2.5cm, time over 5hrs. The data points have been fitted with a linear trend line.

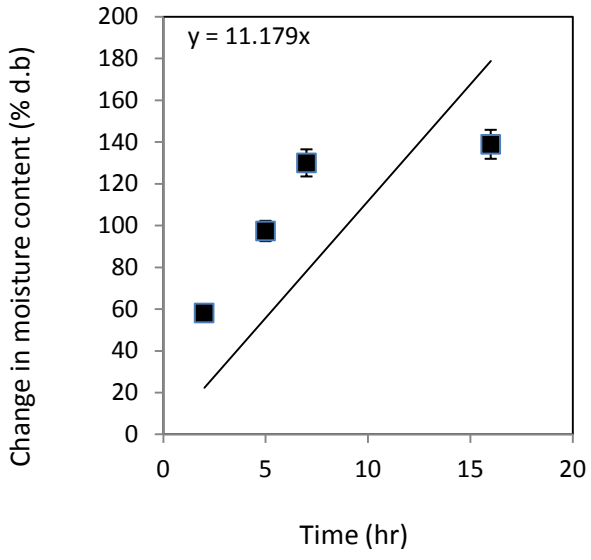

Figure 40 - Change in moisture content (dry basis) versus time for 41 °C entry air temperature, paunch depth 2.5cm, time over 5hrs. The data points have been fitted with a linear trend line.

APPENDIX 2 – Example data for tunnel dryer monitoring

Example of the operating temperature and humidity monitoring done for the tunnel dryer.

Table 13 – Example table of data collected for each run of the present experiment. T1 and T2 are the thermocouple reading for temperature, Rhi is the entry relative humidity, Rhx is exit relative humidity, Tpi is entry psychrometer temperature reading, and Tpx is exit psychrometer temperature reading.

test 1C	10.8.11	ambient	11. 5 thermometer		
high grain content		<1 day old			
				Tp psych temp	
Time	8.30am		%		°C
T1	51	**Rhi**	6.1	**Tpi**	58
T2	47	**Rhx**	8.1	**Tpx**	48.1
Time	9.00am				
T1	71	**Rhi**	4.6	**Tpi**	64.1
T2	61	**Rhx**	6.4	**Tpx**	60.1
Time	9.30am				
T1	77	**Rhi**	3.4	**Tpi**	69.2
T2	67	**Rhx**	4.8	**Tpx**	65.1
Time	10.00am				
T1	75	**Rhi**	3.5	**Tpi**	68.6
T2	66	**Rhx**	4.8	**Tpx**	64.4
Time	10.30am				
T1	79	**Rhi**	3.1	**Tpi**	70.6
T2	69	**Rhx**	4.3	**Tpx**	66.1
Time	11.00am				
T1	79	**Rhi**	3	**Tpi**	69.9
T2	69	**Rhx**	4	**Tpx**	67
Time	11.30am				
T1	77	**Rhi**	2.9	**Tpi**	70.4
T2	70	**Rhx**	3.8	**Tpx**	66.7
Time	12.00pm				
T1	78	**Rhi**	2.9	**Tpi**	70.4
T2	71	**Rhx**	3.6	**Tpx**	67.7
Time	12.30pm				
T1	80	**Rhi**	2.4	**Tpi**	73.1
T2	72	**Rhx**	3.1	**Tpx**	69.5
Time	1.00pm				
T1	77	**Rhi**	2.4	**Tpi**	73.1
T2	69	**Rhx**	3.1	**Tpx**	67.7

APPENDIX 3 – PV theory

PV's work due to the discovery of the photoelectric effect and the later development of doped semiconductor material. The photoelectric effect is where a metal ejects electrons when its surface is exposed to light. This is due to an energy transfer from a single photon to an electron in the metal. The energy of the ejected electron is independent of the light intensity. What this lead to was the idea that light was quantized (bundles of energy called photons) and that the energy, (E), of the light quanta (photon) was proportional to the frequency of its electromagnetic wave, given by:

$$E = \frac{hc}{\lambda} = hf$$

Where *h* is Planck's constant, *c* is the speed of light, λ is the wavelength, and *f* is the frequency.

The photoelectric effect can be separated into two groups: the internal and external photo electric effect (photoionisation). The internal effect applies to photons (such as visible light) without enough energy to ionize an atom but with enough energy to elevate an electron from the valence band into the conduction band. The external photo electric effect (ionisation energy) generally applies to x-rays and has enough energy to totally separate an electron from its nucleus and thus ionize the atom. The internal photoelectric effect applies to PV's as they use lower energy photons than x-rays, mainly visible, ultraviolet and infrared. The transition of the electrons from the valence band to the conduction band creates an electric current. The band gap energy is the term used to describe the energy needed to move an electron from the valence band to the conduction band. The conduction band being the band that allows

electrical conductivity. If the energy of the light is greater than or equal to the energy of the conduction band minus the energy of the valence band, $E_{light} \geq E_c - E_v$, then electrons can be photo-excited from the valence into the conduction band (Sorensen 2004).

There are three types of solids: insulators, semiconductors, and conductors (see figure 41). Insulators have empty conduction bands and require large amounts of energy due to their high band gap to jump electrons into the conduction band. Thus, insulators have high electrical resistance. Conductors have a partially filled conduction band and have low electrical resistance. Semiconductors have an empty conduction band but unlike insulators they have a low band gap energy. Thus, due to the inner photoelectric effect electrons can be elevated to the conduction band easily. PV's use semiconductor material for these reasons: they behave as insulators without the presence of radiation, and they can generate current due to the photoelectric effect (Quaschning 2007).

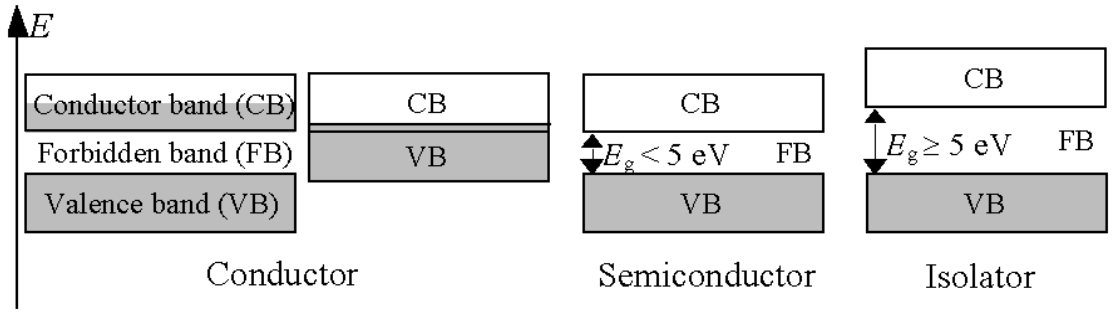

Figure 41 - Conductor, semiconductor and insulator energy bands. Insulators have a full valence band and high band gap energy which makes them have high electrical resistance. Semiconductors have a full valence band but a low band gap energy which allows them to behave as a conductor in the presence of radiation. Conductors have a full valence band and partially filled conduction band which makes them have low electrical resistance. (Quaschning 2007).

The intrinsic conduction of semiconductors is due to holes that are formed when an electron is moved into the conduction band due to radiation. There are always equal amounts of holes and electrons as shown in the equation $n = p$ where n (negative) is the electron density and p (positive) is the hole density. PV's use joined doped semiconductor material to create electrical energy differences thus removing the need for an externally applied electrical voltage. Doped semiconductors have an impurity added to them to either increase the amount of loosely bonded electrons (n-doping, donors) or to increase the amount of holes (p-doping, acceptors). The loosely bonded electrons in the n-type semiconductor require little energy to be separated from the atom and are thus free electrons. In n-doped material the electrons are the majority carriers and in p-type material the holes are the majority carriers (Quaschning 2007).

A p-n junction is created when the n and p- type material are placed together. This forms the principal concept of how PVs work. The holes and electrons diffuse from n to p and p to n type regions, due to the creation of a concentration gradient, forming positive and negative space charge regions (see figure 42). This leaves a build up of negative charge in the p-type region and a positive charge in the n-type region near the junction that form a dipole layer, (a dipole being a pair of electric charges with equal magnitude but opposite sign.), with an electrostatic potential difference. The electrostatic potential difference will hinder more electron flow until equilibrium is reached. Therefore, when PVs are in the dark with no external voltage there is no net current across the junction (Sorensen 2004). Once equilibrium

is reached a diffusion voltage (V_d) or built in voltage is produced between the n and the p regions:

$$V_d = \frac{kT}{e} \ln\left(\frac{n_a n_d}{n_i^{\,2}}\right)$$

Where $V_T = \frac{kT}{e}$ thermal voltage (PVs are temperature dependent and cannot operate at absolute zero and conductivity decreases at low and high temperatures.), k = Boltzmann constant, T = temperature in Kelvin's, e = electron charge, n_a and n_d are acceptor and donor concentrations, and n_i = intrinsic carrier density.

The space charge region width (d) is given by:

$$d = d_n + d_p = \sqrt{\frac{2\varepsilon_r \varepsilon_0 U_d}{e} \frac{n_A + n_D}{n_A n_D}}$$

Where ε_0 = permeativity of free space, ε_r = relative permativity, n_A and n_D are the donor concentrations, e= electron charge, $U_d = (V_d - V)$ diffusion voltage minus the applied bias (Quaschning 2007).

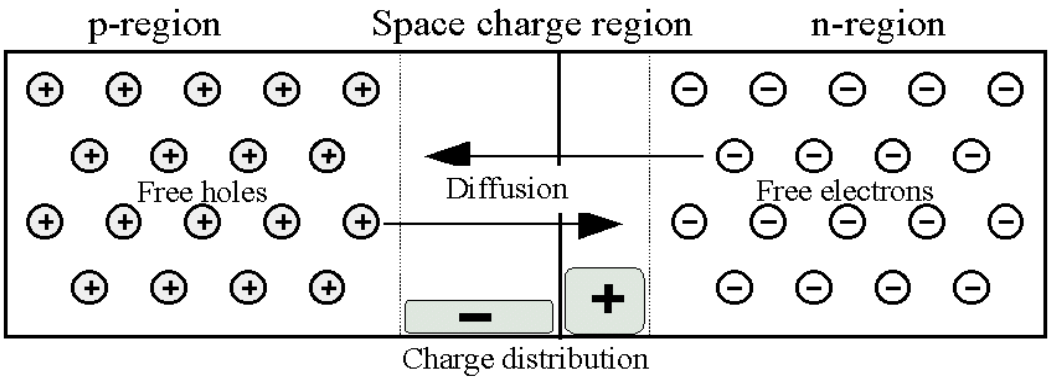

Figure 42 - P-n junction (Quaschning 2007).

APPENDIX 4 – Wind theory

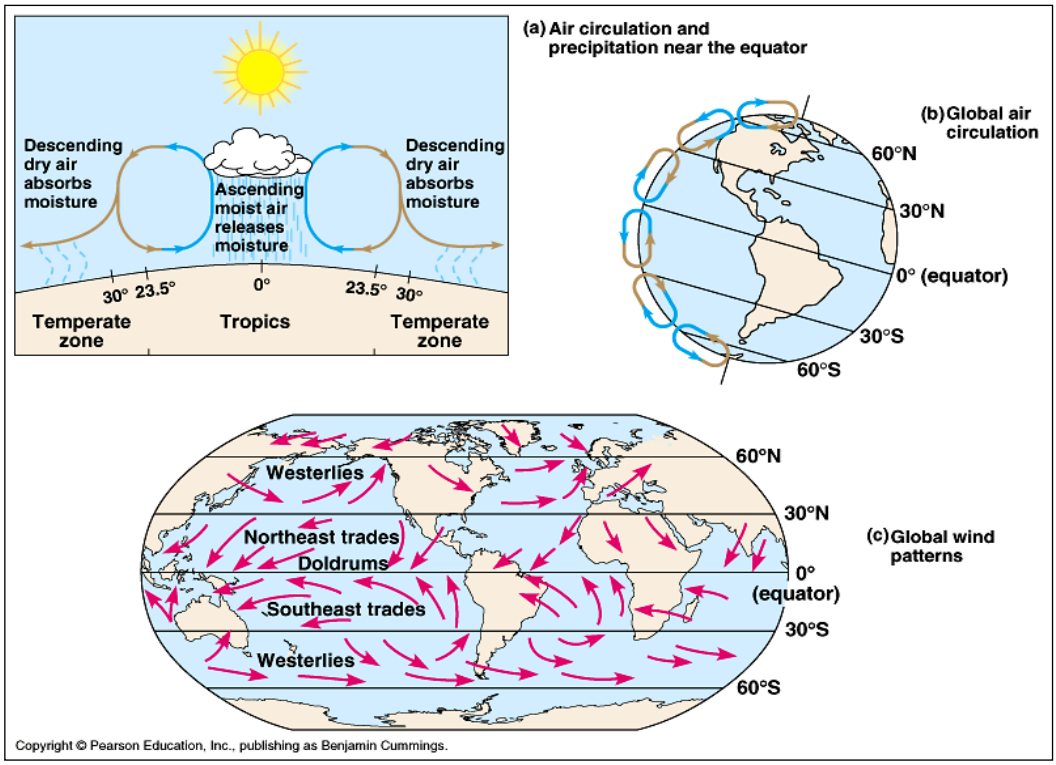

Figure 43 - The diagram shows air circulation and global wind patterns. Wind is formed due to the rising of hot air (heated by the sun) and the sinking of cool air (Simmons 2006).

Wind is caused by the movement of atmospheric air mass. This movement is due to differences in atmospheric pressure caused by the differential heating of the earth's surface. This differential heating is due to the curvature of the earth's surface which means that the suns rays have more atmosphere to travel through as the latitude increases. Therefore, the solar radiation passes through greater depth of atmosphere and thus faces more absorption and scattering. This is why the tropics are hotter than high latitude regions (Boyle 2004). As air is warmed by solar radiation it becomes less dense and rises being replaced by denser cooler air. This can also lead to localised wind forming in mountain valleys and coastal areas (Boyle 2004).

Wind turbines convert the kinetic energy contained in the wind into electrical energy by the rotation of their blades. Wind power is the term given to the kinetic energy contained in the wind and is given by:

$$P = 0.5\rho AV^3$$

Where P is the power in Watts, ρ is the density of air in kg m^{-3} (density of air at sea level is 1.2256 kg m^{-3}), A is the area in m^2, and V is the velocity in m s^{-1} (Boyle 2004). This equation is derived from the equation for kinetic energy in joules:

$$K \equiv \frac{1}{2}mv^2$$

Where K is the kinetic energy of a particle (J), m is the mass of the particle (kg), and v is the velocity (m/s).

The wind power (P) is then the mass (particles) of wind moving perpendicular to a plane of area (A). This movement is the rate of energy of the particles per unit time (J/s) which is given the term power in watts. Which can be expressed as:

$$P = \frac{dE}{dt} = 0.5\frac{dm}{dt}v^2$$

Where P is the power (W), dE/dt is the rate of energy per unit time (J/s), dm/dt is the rate of mass (particles) per unit time (kg/s), and v is the velocity (m/s).

Then the amount of air that has passed through the plane is calculated (distance through plane) for a certain amount of time. The volume of air is area times length and the mass is area times length times density or:

$$m = \rho AL$$

Where m is the mass (kg), ρ is the density of air (kg/m^3), A is the area (m^2), and L is the distance travelled by the air.

Therefore:

$$\frac{dm}{dt} = \rho A \frac{dL}{dt} = \rho A v$$

Where dL/dt is velocity.

Therefore, substituting dm/dt into the power eqn:

$$P = \frac{dE}{dt} = 0.5 \frac{dm}{dt} v^2 = 0.5 \rho A v^3$$ (Tyree 2008).

However, Sen (2003) states that this equation is not quite correct and suggests that another derivation based on first principles will supply a coefficient of $\frac{1}{3}$ instead of $\frac{1}{2}$ in the wind power equation. This difference is based on the assumption that the kinetic energy equation used in the classic version is valid for solid materials with constant mass and that the new equation bases its assumptions on air being fluid and therefore uses force and energy to derive its equation. The derivation for the new equation is as follows:

$$F = ma$$

Where Newtons second law states force = mass x acceleration.

$$F = m \frac{dv}{dt}$$

Where dv/dt is wind speed (v) during time (t).

Using $m = \rho A v t$ where m is mass, ρ is the density of air, A is area, v is velocity, and t is time in above equation then,

$$F = \rho A v t \frac{dv}{dt}$$

Using the work-energy theorem, then force times distance (dl) gives,

$$dE = Fdl = \rho Avt\frac{dvdl}{dt}$$

Where $v = \frac{dl}{dt}$, the change in length divided by the change in time is the definition of velocity gives,

$$dE = \rho Av^2tdv$$

Integrating both sides

$$\int dE = \int \rho Av^2tdv$$

$$P = \frac{1}{3}\rho Atv^3 \text{ (Sen 2003).}$$

For this thesis however, any use of the wind power equation will use the classic kinetic energy derived equation.

The wind power equation shows three important relationships. Wind power is proportional to:

1. Air density, Air density is lower at higher elevations and in tropical climates compared to cold climates.
2. Area through which the wind passes,
3. Velocity cubed has a strong influence on power output (a small rise in velocity equals a large rise in output) (Boyle 2004).

Another factor affecting the available power contained in the wind is wind shear which is the change in wind speed at different heights. Wind speed increases with height where there is less friction and turbulence. Wind shear is low when surfaces are smooth and high when there are numerous factors introducing friction and

affecting the flow of the wind (Gipe 2004). The speed loss at lower heights is due to friction at the Earths surface, caused by mountains, buildings, trees and other obstructions. As with a lot of naturally occurring effects the increase of wind speed with height is not always true and there are rare instances when the opposite happens and wind speed can decrease with height. However, it is appropriate to assume that wind increases with height and Gipe (2004) states that there are two main methods to estimate the effect of wind shear; the logarithmic model and the power law equation. Gipe (2004) states that the power law equation is the most effective as it is based on real data and is more conservative than the logarithmic model. The power law equation is given by:

$$V = \left(\frac{H}{H_o} \right)^{\alpha} V_o$$

Where V is the new wind speed, V_o is the initial wind speed, H is the new height, H_o is the initial height, and α is the wind shear exponent. The wind shear component is given by:

$$\alpha = 1/\ln\left(\frac{z}{z_o} \right)$$

Where α is the wind shear exponent, z is the reference height, z_o is the surface roughness length (Molly, cited in Gipe 2004, p. 41). Often an exponent of 1/7 is used to calculate the wind shear (Gipe 2004). However, Farrugia (2003) states that the use of the 1/7 power law could lead to underestimation of long-term mean wind speed. Farrugia (2003) found that measurements made at a Mediterranean site were 17% higher than the extrapolated value given by using the 1/7 power exponent.

Using the equation for wind power, the area swept out by the turbine blades, and the maximum energy conversion efficiency of the turbine then the maximum power output of the wind turbine (Betz limit) is given by:

$$P = 2.83 \times 10^{-4} D^2 v^3$$

Where P is the maximum power output in kW, D is the blade diameter in metres, v is the wind velocity in ms^{-1} (Hinrichs & Kleinbach 2006). Figure 44 shows the maximum theoretical output for a wind turbine based on wind speed and blade diameter. The graph demonstrates the relationship between power output and blade diameter. Increased blade diameter increases power output.

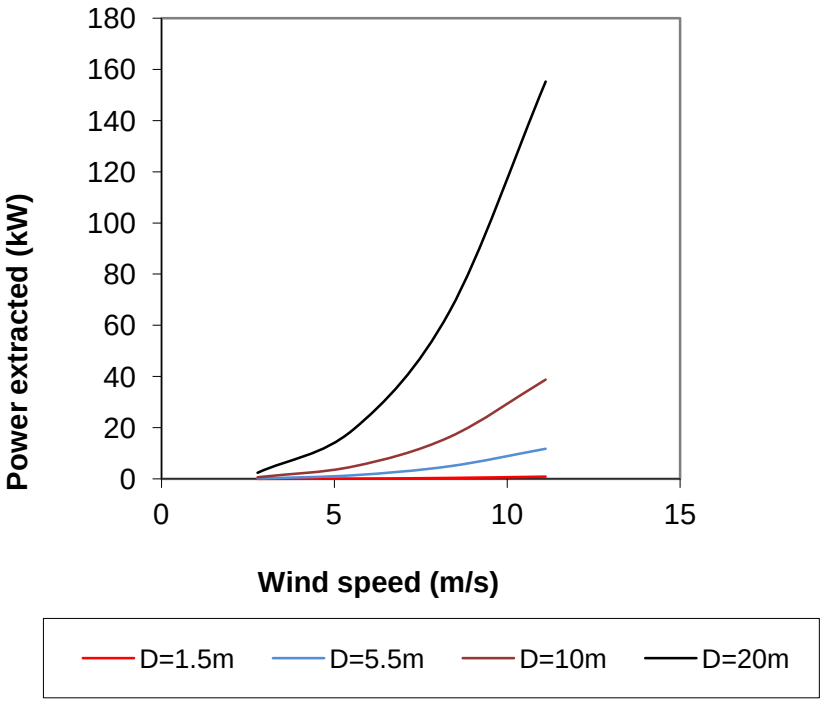

Figure 44 - The maximum theoretical output for a wind turbine based on wind speed and blade diameter using the equation: $P = 2.83 \times 10^{-4} D^2 v^3$.

Lift and drag forces

Wind turbines operate due to the transfer of force from a fluid (air) to a solid object. Lift and drag are terms used in aerodynamics to explain the force experienced by an object in an air stream. Lift and drag are two component forces that act in perpendicular directions. The magnitude of these forces is affected by the shape of the object, its orientation to the direction of the air stream, and the air stream velocity. The drag force acts in the direction of the air stream while the lift force acts perpendicular (90º) to the air stream (Boyle 2004).

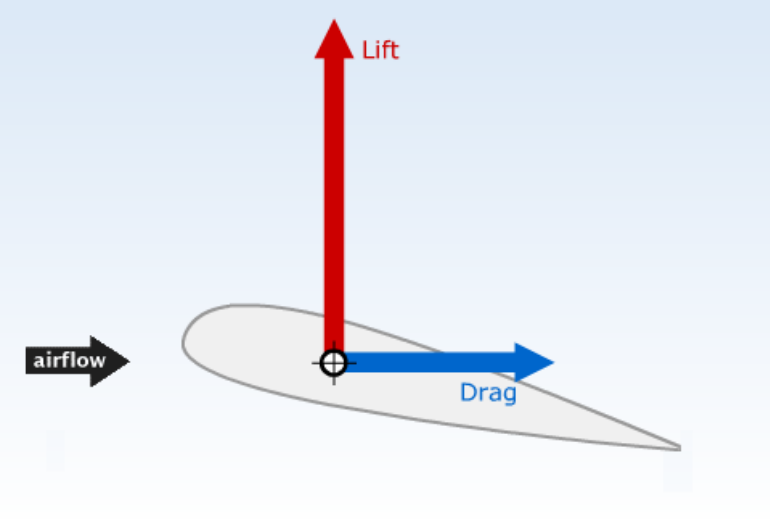

Figure 45 - The diagram demonstrates the lift and drag forces acting perpendicular to each other (First flight n.d).

The drag force is referred to as streamline when the object is designed to minimise the drag force. The drag force equation is:

$$D = \frac{1}{2} C \rho A v^2$$

Where D is the magnitude of the drag force in Newtons, C is the drag coefficient, ρ is the air density in kilograms per cubic metre, A is the cross sectional area perpendicular to the velocity in metres squared, and v (in this case) is the velocity of

the air stream in meters per second (Halliday, Resnick & Walker 1997). From the equation it is possible to see that drag depends on A and v. If an object such as a plate had its flat side perpendicular to the direction of v, it would have maximum drag. If the plate has its flat side inline with the direction of v, its drag force would be at a minimum (Boyle 2004).

Lift force is where air flows at higher speeds along the upper body of an object and lower speeds along the underside of an object which results in a lower pressure above the object and a higher pressure below. Thus, there appears to be a suction force on the object in a direction perpendicular to the direction of the velocity. The relationship between air speed and pressure is known as the Bernoulli effect (Boyle 2004, Quaschning 2007). Although the word lift is used it is also possible for the lift force to act in a sideward or downward motion depending on the application as well as in an upward motion (Boyle 2004). The lift force is given by:

$$L = \frac{1}{2} C \rho A v^2$$

Where L is the magnitude of the lift force in Newtons, C is the lift coefficient, ρ is the air density in kilograms per cubic metre, A is the projected body area in metres squared, and v is the velocity of the air stream in metres per second (Quaschning 2007). The area is found by taking the chord length times the span (which is approximately equal to the rotor radius). The chord is a reference line from which measurements are made on an aerofoil section (figure 46).

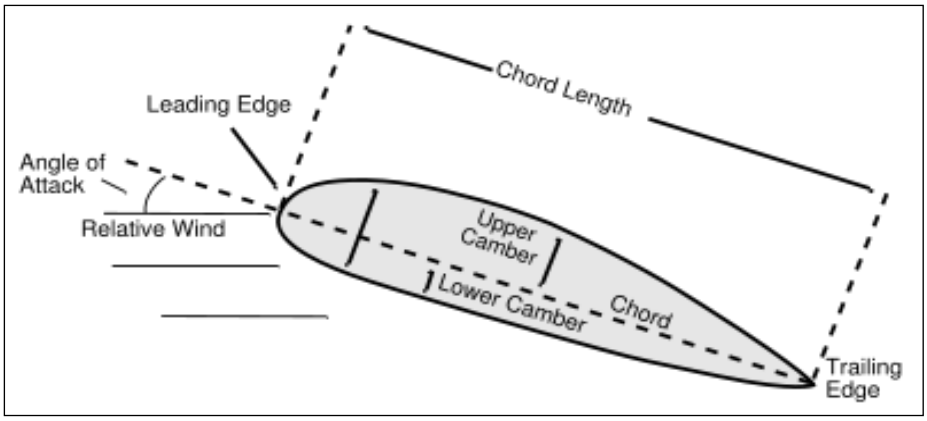

Figure 46 - The diagram shows the chord length for an object which gives the area of an object when multiplied by the span (NASA 2009).

An aerofoil is a streamlined shape that is capable of generating significantly more lift than drag. Modern wind turbines make use of aerofoil designs in order to extract as much power from the wind as possible. Therefore, factors such as number of blades, relative wind angle, and total torque can have an effect on the power output of a wind turbine (Boyle 2004).

An aerofoil is a streamlined shape that is capable of generating significantly more lift than drag. Modern wind turbines make use of aerofoil designs in order to extract as much power from the wind as possible. Therefore, factors such as number of blades, relative wind angle, and total torque can have an effect on the power output of a wind turbine (Boyle 2004).

APPENDIX 5 - Algae

Algae are from the plant kingdom and consist of both eukaryotic and prokaryotic types, with cyanobacteria and prochlorophytes being prokaryotes, and the rest eukaryotes (see note at end) (Bold & Wynne 1985). Algae range in size from the macro (>30m) to the single celled microalgae (Sze 1993). Microalgae are used for the production of oils for biodiesel as they generally produce more of the right kinds of natural oils needed for biodiesel (Sheehan et al. 1998). Therefore, for the purpose of this report, the term algae will be used to refer specifically to microalgae.

Algae are photosynthetic organisms and Sheehan et. al. (1998) suggest that the four most important categories of microalgae in terms of abundance are: The diatoms (>100 000 species), the green algae, the blue-green algae (nitrogen fixers), and the golden algae. Microalgae are the most primitive form of plants and as such are more efficient converters of solar energy, due to their simple cell structures. This means that when compared to terrestrial plants, microalgae can produce thirty times the amount of natural oil per unit area of land (Sheehan et. al. 1998). Compared to switchgrass (the fastest growing terrestrial plant) algae biomass productivity can be 50 times greater due to their high growth rates and photosynthetic efficiencies (Li et al. 2008).

Photosynthesis converts radiant energy from the sun into chemical energy. Chlorophyll contained within chloroplasts in eukaryotic cells and the thylakoid membrane in prokaryotes are the sites of photosynthesis. The chlorophyll uses light to convert carbon dioxide and water into organic compounds (carbohydrates and

water) and oxygen (Campbell & Reece 2002). This process can be described by the summary equation:

$$6\,CO_2 + 12H_2O \xrightarrow{\text{LIGHT}} 6\,(CH_2O) + 6H_2O + 6O_2$$

Carbon Dioxide — water — CHLOROPHYLL — Carbohydrate — Water — Oxygen

(Campbell & Reece 2002).

Through the process of photosynthesis, algal cells assimilate carbon and the two storage forms that carbon can take are in lipid or carbohydrate form. A higher rate of enzyme activity in lipid synthesis pathways increases the rates of oil production in algae (Sheehan et al. 1998). It was found that nitrogen (N) and silicon (Si) depletion increased oil production but slowed cell division. Sheehan et al. (1998) also found that silicon depleted cells used more incoming carbon for lipid production and less for carbohydrate production and that the cells slowly converted non-lipid cell components into lipids. It has been suggested that the reduction of cell division due to nutrient depletion may be overcome by careful control of the timing of nutrient depletion and cell harvesting (Sheehan et al. 1998). Thus, by putting the alga under stress it is possible to increase the amount of natural oils available for biodiesel production.

Algal biomass is made up of three main components: carbohydrates, protein, and natural oils. Biodiesel production uses only the natural oil component of the alga. However, when the natural oils are removed for use as biodiesel the remaining biomass can be used as a secondary product such as high protein stock feed (Sheehan

et al. 1998). While biodiesel can be produced from terrestrial oilseed crops such as soybean oil, some algal species can produce 60% of their body weight in natural oils or triacylglycerols (TAGs). This means that algae can efficiently take the place of oilseed crops for the production of biodiesel and therefore not compete with existing oilseed markets (Sheehan et al. 1998).

Photobioreactors allow manipulation of the algae to increase growth rates and oil production. A photobioreactor is a closed system that can be used to grow algae in highly selective environments. Grobbelaar (2000) states that the major factors available for manipulation in both closed and open systems for the production of mass algal cultures are: culture depth or optical cross section - culture depth over 100mm of water will absorb more and more light thus reducing light available for photosynthesis. The efficiency of this process is affected by (Figure 47) turbulence, mixing rates and patterns can be altered, nutrient content and supply (eg. CO_2), cultivation procedure, biomass concentration and areal density, and the state or potential of the photosynthetic system.

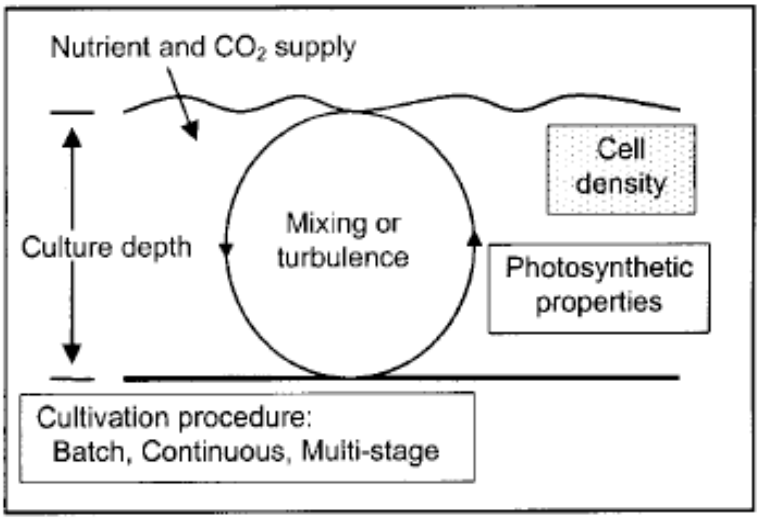

Figure 47 - The major factors available for manipulation in both closed and open systems (Grobbelaar 2000)

The main benefits of closed system bioreactors are reduced contamination risk, controllable temperature and cultivation conditions, and no CO_2 losses (Pulz 2001). Borowitzka (1999) states that there are two types of closed systems in which to grow algae: photoautotrophically and heterotrophically. In algae, heterotrophy is the ability to oxidize organic compounds in the dark for energy (Sze 1993). Heterotrophic systems use acetate or glucose as carbon sources to cultivate the algae. However, it is not possible to grow all algae heterotrophically and it often changes the algal chemical composition (Borowitzka 1999). Photoautotrophic systems use photosynthesis to create energy. Therefore, the focus of this report was on photoautotrophic systems or photobioreactors.

A number of equations can be used to aid in the measurement of inputs and outputs of photobioreactors. The equation used by Helm, Laing and Jones (1979) allows for the division rate per day of the algae to be calculated. This can be seen in the equation division rate per day (K):

$$K = \frac{1.443}{t} \times \log_e \frac{Nt}{No}$$

Where Nt number of cells at first harvest μl^{-1}, No number of cells at inoculation μl^{-1}, t is time in days to first harvest, 1.443 is factor transforming $\log_e$ to $\log_2$ in the calculation of cell division per unit time (Helm, Laing & Jones 1979).

The inoculum volume (I_v) given by Laing (1979) can be used to calculate the amount of starter culture needed to give a particular density in the culture vessel as seen in the equation: Iv = (Culture volume (L) x required inoculum density (cells/ μL^{-1})) / density of inoculating culture (cells/ μL^{-1}) (Laing 1979). For example, a 2 L culture

with a density of 10 000 cells per litre is used as an inoculum to give a density of 1 000 cells per litre in a 20 L culture (Laing 1979).

The harvesting volume (V_h) equation given by Hu, Guterman and Richmond (1996) allows for harvesting operations to be carried out and can be calculated using:

$$V_h = \frac{(X_2 - X_1)V_t}{X_2}$$

Where V_h is the harvested volume or the volume to be harvested in litres, V_t is the total culture volume in litres, X_2 and X_1 are cell densities (gL^{-1}) at daily (24hr) intervals, X_1 being any cell density desired to be established after harvesting as long as $X_1 \leq X_2$ (Hu, Guterman & Richmond 1996).

Note:
It is not actually correct to call the prokaryotic types, cyanobacteria and prochlorophytes, algae. Cyanobacteria (blue-green algae) and prochlorophytes belong to the kingdom Monera and are groups of bacteria. Algae belong to the kingdom Protista and are eukaryotic cells. Cyanobacteria and prochlorophytes are oxygenic phototrophs and resemble algae in that they have chlorophyll a, prochlorophytes also have chlorophyll b yet lack phycobilins (found on the thylakoid membranes of cyanobacteria) (Madigan et al. 2009). The prokaryotes cyanobacteria and prochlorophytes lack a nuclear region and nuclear envelope and complex oraganelles such as chloroplasts or mitochondria. They do contain thylakoids which are where the photosystems (using chlorophyll) are contained (Sze 1993). The chloroplasts in eukaryotes are related to cyanobacteria due to an endosymbiotic relationship (a cell which lives inside another cell). A heterotrophic protist may have engulfed a cyanobacteria which evolved into red and green algae (Campbell & Reece 2002).

The reason for grouping cyanobacteria and prochlorophytes with algae for this report was due to their similarities to algae and therefore many studies into biofuel group these together.

APPENDIX 6- Glossary

Augering – A drill bit with one or more blades (like a corkscrew) is used to cut away earth (or compacted material from pipes) which then feeds itself upwards inside the drill.

DAF – Water saturated with air at high pressure is added to abattoir wastewater into an open top tank. Reducing the pressure causes the air to leave the solution, bubbles form on particles within the solution, causing the particles in the wastewater to float to top. Thus, allowing the solids to be scraped from the surface of the tank and removed (Sindt n.d).

Fluidized bed incineration – like pyrolysis (see below) but in an oxygen depleted environment as opposed to in the absence of oxygen.

Gasification – The incomplete combustion of carbonaceous materials (biomass) resulting in the production of combustible gases (syngas) consisting of Carbon monoxide, Hydrogen, Carbon dioxide, and traces of Methane. Created by reacting the biomass with a controlled amount of oxygen and/or steam at high temperatures and pressures (CSIRO 2011).

Insolation – incoming solar radiation.

Paunch – partially digested grass and grains from the first stomach of ruminant animals.

Pyrolysis – Where an organic material is separated into its component parts by heat (>200°C) in the absence of oxygen.

Screw press – Machine that dewaters a high solids liquid waste stream (Doyle & Lant 2001).

Solar still – A solar dryer design that is used to distil water. In its most basic form it consists of a pit covered with a clear plastic sheet.

Syngas – The resulting gas mixture from gasification and is itself a fuel (CSIRO 2011).